Politecnico
di Torino

MSc degree in Energy and Nuclear Engineering

A.Y. 2021/2022

Purification of biogas from sulphur compounds: experimental investigation and techno-economic assessment

Supervisors:

Prof. Lanzini Andrea

Dr. Gandiglio Marta

Dr. Rozzi Elena

Candidate:

Cappai Francesca
s284708

October 2022

Table of Contents

List of Figures IV

List of Tables VI

Main acronyms and chemical formula VIII

Abstract 1

1. Biogas 3

1.1 The history 3

1.2 The production 6

1.3 The composition 8

1.4 Future trends 10

1.5 Powering fuel cells with biogas 11

1.6 Limits on biogas diffusion 13

2. Biogas impurities and purification 14

2.1 Carbon Dioxide 14

2.2 Water Vapour 15

2.3 Sulphur compounds 16

2.4 Siloxanes 17

2.5 Ammonium 18

2.6 Halogens 18

2.7 Volatile Organic Compounds 19

2.8 Nitrogen and Oxygen 19

2.9 Impurities-related main issues 19

3. The adsorption 21

3.1 The adsorption phenomena 21

3.2 Adsorption thermodynamics 23

3.3 Adsorption isotherm ... 24

3.4 Langmuir model and BET specific surface area ... 26

3.5 Factors that affect adsorption ... 27

4. Sulphur compound removal through adsorption: State of the Art ... 28

4.1 Activated carbons for H_2S removal ... 28

4.2 Zeolites for H_2S removal ... 33

4.3 Iron oxides and hydroxide for H_2S removal ... 34

4.4 Other compounds for H_2S removal ... 36

4.5 Materials for CH_4S removal ... 38

4.6 Materials for DMS removal ... 39

4.7 Materials for COS removal ... 39

4.8 Multi-component removal ... 40

5. The experimental investigation ... 41

5.1 The experimental setup ... 41

5.2 Methodology ... 44

5.3 Materials' characterization ... 45

5.4 Experiments design ... 52

6. Experimental investigation's results ... 54

6.1 Results obtained for H_2S removal (PoliTo) ... 54

6.2 Results obtained for CH_4S removal (PoliTo) ... 62

6.3 Results obtained for COS removal (ENEA) ... 63

6.4 Result obtained for DMS removal (PSI) ... 65

7. Techno-economic analysis of a multicomponent model ... 68

7.1 System configurations ... 69

7.2 Vessel sizing ... 71

7.3 Purchased equipment costs ... 74

7.4 Main costs and revenues 76

7.5 Cash flows analysis 77

8. Numerical assumptions for the techno-economic model........ 80

8.1 Assumptions for the biogas composition 80

8.2 Choice of the SOFC 81

8.3 Evaluations on the adsorption capacity........ 82

8.4 Considerations on the vessel 87

8.5 Evaluation of the purchase equipment price 88

8.6 Evaluation of costs and revenues 90

9. Scenarios 93

9.1 Monocomponent scenario 93

9.2 Multicomponent scenario........ 95

9.3 Sensitivity analysis on cost of Norit RGM-3 100

10. Conclusions 102

Acknowledgments 104

Bibliography 105

List of Figures

Figure 1.1: Total biogas installed capacity (personal elaboration from IRENA data) 5

Figure 1.2: The sustainable cycle of biogas from anaerobic digestion (personal elaboration) 8

Figure 1.3: Transformation of the energy demand in the transport sector [13] 11

Figure 1.4: Schematic representation of a SOFC powered by methane (personal elaboration) 12

Figure 3.1 - The adsorption mechanism [28] 22

Figure 3.2 - Adsorption isotherm [31] 24

Figure 3.3 - IUPAC classification for adsorption isotherms for the equilibrium between gas and solid [32] 25

Figure 5.1: The uncoated reactor 43

Figure 5.2: The coated reactor 43

Figure 5.3: The gas station 43

Figure 5.4: The bubbler 43

Figure 5.5: The bubbler 44

Figure 5.6: Gas station prototype schematic (personal elaboration) 44

Figure 5.7: Norit RGM-3 46

Figure 5.8: SulfaTrap R7H 47

Figure 5.9: Bio-Clean Gas Granular 48

Figure 5.10: Envirocarb stix 49

Figure 5.11: Airpel by Desotec 50

Figure 5.12: Adsorption isotherms of the considered materials 51

Figure 6.1: Tests on Norit RGM-3 in different conditions (500 ppm of H_2S) 55

Figure 6.2: Tests on SulfaTrap R7H in different conditions (500 ppm of H_2S)............ 59

Figure 6.3: Tests on Desotec Airpel Ultra D5, Envirocarb stix and Biocostum Gas Granular (500 ppm of H_2S, no water, no oxygen).. 61

Figure 6.4:Test on Norit RGM-3 (200 ppm of CH_4S).. 62

Figure 6.5: Test on Bioclean Gas Granular (100 ppm of CH_4S)................................... 63

Figure 6.6: ENEA tests on COS at different inlet conditions [62]................................ 64

Figure 6.7: ENEA tests on COS in dry and wet conditions (30 ppm of COS) [62]....... 65

Figure 6.8: Breakthrough curves obtained for different materials (semi-wet and wet conditions, 100 ppm DMS) [62]... 67

Figure 7.1: Purification with only one vessel (personal elaboration)............................ 69

Figure 7.2: Purification process with 2 vessels and a condenser (personal elaboration) 70

Figure 7.3: Purification process with a condenser and 1 vessel (personal elaboration). 70

Figure 8.1: Tested adsorption capacity of Norit RGM-3 on COS removal at different concentrations.. 83

Figure 8.2: Adsorption capacity of CH_4S at different concentrations........................... 85

Figure 8.3: Adsorption capacity of DMS at different concentrations 86

Figure 8.4: Purchase price of a vertical process vessel applying Turton cost functions 89

Figure 9.1: Comparison of the volume of Norit RGM-3 needed in different conditions for each component.. 95

Figure 9.2: TOC shares in each of the three plants proposed....................................... 96

Figure 9.3: OpEx shares in each of the three plants proposed 98

Figure 9.4: LCOE shares in each of the three plants proposed 100

Figure 9.5: LCOE variation depending on the purchase price of Norit RGM-3.......... 101

List of Tables

Table 1-1: Properties of a typical biogas produced through anaerobic digestion [10]..... 9

Table 2-1: Some typical sulphur compounds' concentrations inside a biogas [22] 16

Table 2-2: Some typical siloxanes' concentrations inside a biogas [22]........................ 17

Table 4-1: Activated carbons comparison.. 32

Table 4-2: Zeolites comparison.. 34

Table 4-3: Iron oxides and hydroxides comparison 36

Table 4-4: Other compounds comparison 38

Table 5-1: Useful information about the materials.. 50

Table 6-1: Test conditions with Norit RGM-3 54

Table 6-2: Test results on Norit RGM-3 56

Table 6-3: Sensitivity analysis tests conducted on Norit RGM-3 56

Table 6-4: Results of the sensitivity analysis tests conducted on Norit RGM-3............ 57

Table 6-5: Atomic percentage of the chemical elements contained inside Norit RGM-3 in the different conditions... 58

Table 6-6: Test conditions with SulfaTrap R7H 58

Table 6-7: Test results on SulfaTrap R7H.. 60

Table 6-8: Test conditions with Desotec Airpel Ultra D5, Envirocarb stix 4 mm and Biocostum Gas Granular 60

Table 6-9: Test results on other materials 61

Table 6-10: COS adsorption using Norit RGM-3 [62]... 64

Table 6-11: Performances of different materials in semi-wet conditions (4° dew point) [62].. 66

Table 6-12: Performances of different materials in wet conditions (20° dew point) [62] 66

Table 8-1: Biogas assumed composition 81

Table 8-2: SOFC main characteristics 81

Table 8-3: Resume of Norit RGM-3 adsorption capacities obtained from the experimental campaign 82

Table 8-4: Adsorption capacity of Norit RGM-3 related to the pollutant concentration 86

Table 8-5: Mass flow rate of the pollutant inside the biogas 87

Table 8-6: Main contributions to the initial investment 90

Table 8-7: Main OpEx contributions 91

Table 9-1: Most relevant data in a monocomponent scenario 94

Table 9-2: Most relevant data in a multicomponent scenario 97

Table 9-3: Comparison of economic indicators in a multicomponents scenario 99

Main acronyms and chemical formula

AC	Activated Carbon
AD	Anaerobic Digestion
BCR	Benefit to Cost Ratio
BEC	Bare Erected Cost
BET	Brunauer, Emmett and Teller
CEPCI	Chemical Engineering Plant Cost Index
CH_4	Methane
CH_4S	Methanethiol
CO_2	Carbon Dioxide
COS	Carbonyl Sulphide
DISAT	Applied Science and Technology Department (Politecnico di Torino)
DMS	Dimethyl sulphide
EDS	Energy Dispersive Spectroscopy
EPCM	Engineering, Procurement and Construction Management
GHGs	Greenhouse Gases
GHSV	Gas Hourly Space Velocity
H_2O	Water
H_2S	Hydrogen sulphide
IEA	International Energy Agency
IRENA	International Renewable Energy Agency
IRR	Internal Rate of Return
IUPAC	International Union of Pure and Applied Chemistry

LCOE	Levelized Cost of Electricity
LHV	Lower Heating Value
MCFC	Molten Carbonate Fuel Cell
N_2	Nitrogen
NH_3	Ammonia
NPV	Net Present Value
O_2	Oxygen
PBT	PayBack Time
PSA	Pressure Swing Adsorption
REmap	Renewable energy roadmap
RH	Relative Humidity
S	Sulphur
SEM	Scanning Electron Microscopy
SOFC	Solid Oxide Fuel Cell
TOC	Total Overnight Cost
TPC	Total Plant Cost
VOCs	Volatile Organic Compounds
W2W	Waste2Watts
WACC	Weighted Average Cost of Capital

Abstract

The attention toward biogas production and utilisation is consistently increasing nowadays. First of all, because wastes can be exploited to obtain it and, furthermore, because it represents an incredibly versatile renewable energy source, thanks to its ability to produce both electricity and heat.

Unfortunately, raw biogas contains different kinds of unwanted compounds that must be necessarily removed in order to be able to efficiently use it in a process. In particular, a deep purification is needed to make the biogas suitable to power a Solid Oxide Fuel Cell. In fact, this kind of device is particularly sensitive to impurities and can easily be polluted. Consequently, it is fundamental to remove almost completely every compound that can damage it. In this work the focus was set on the removal of some of the main sulphur compounds: H_2S, CH_4S, COS and DMS.

In order to efficiently obtain the biogas cleaning, adsorption processes are one of the most promising techniques applicable. Different sorbent materials claim to be suitable to obtain a good biogas purification. To find the better ones, an experimental investigation was organised, within the Waste2Watts project. The leader was PoliTo, who worked in partnership with PSI and ENEA.

Each of the research teams specifically studied the removal of a single component coupled with the materials available and considering different biogas compositions. Investigating one pollutant at a time, the goal was to determine which sorbent could have the best performance depending on the sulphur compound to be removed. At the end of the research activity only one material, Norit RGM-3, demonstrates to be a good sorbent to all four sulphur compounds.

The main limit of the experimental activity is that, in a raw biogas, all the impurities, which must be removed completely, are present at the same time. For this reason, once Norit RGM-3 was discovered as the best between the materials tested, the next step was to understand how a multicomponent adsorption could be carried out. To do so, a techno-economic model was realized, with the purpose of studying the feasibility of the whole project. The core of the model is represented on one hand by the chosen sorbent and on

the other by the clean-up system plant, for which three different designs were created. They were realized considering that the adsorption, depending on the compound, can be performed more efficiently whether or not water is present inside the biogas mixture.

Some relevant parameters were fixed, so that the techno-economic assessment could be as realistic as possible. The most relevant data for the model, which are related to the adsorption capacity, were obtained thanks to the experimental activity.

In conclusion, the different designs for the purification plant were compared, both from the energetic and economic point of view, in order to find the best compromise.

Chapter I

1. Biogas

1.1 The history

The global energy demand is currently supplied in a great percentage by fossil fuels: according to the International Energy Agency (IEA), about 80% in 2019. Fossil fuels are mainly represented by oil, which is 31% of the world energy supply, natural gas, which is 26.5%, and coal, which is 23%. These are non-renewable sources of energy that will probably be exhausted by the end of this century. Furthermore, they also have a strongly negative impact on the environment [1].

Almost every existing future Scenario underlines that the energy demand will increase consistently one year after another: energy production needs to grow accordingly to be able to match this rise. At the same time, every human action has an impact on the Earth which must be considered. One of the most urgent issues regards the necessity to reduce the greenhouse gases (GHGs) emissions in the atmosphere. A significant part of them is due to the fossil fuels' combustion. A relevant strategy to minimise the impact of climate change and global warming on the planet is currently strictly needed. Moreover, fossil fuels are not always convenient from the point of view of supply. In fact, many regions of the world that export fossil fuels are politically unstable, as a result they may be unpredictable in terms of energy security. Furthermore, the impact of price rise includes a significant negative effect on the lower income consumers, generating social problems to deal with. Alternative sources of energy must be developed as soon as possible, but for being applicable efficiently they must be not only environmentally friendly, but also attractive from an economic point of view, technically feasible and secure. Currently, the electricity sector requests can be supplied by renewables already in a satisfying way. The main contributors are principally solar, hydro or wind energy. The biggest concerns are instead related to the heat and cooling market. This sector is critical because it is difficult to reach full independence without fossil fuels intensive utilisation. In this context, the exploitation of biomass finalised to biogas production represents, despite being challenging, a viable alternative. [2].

The first biogas utilisation may be dated as long ago as the 10th century B.C., when its purpose could have been to heat up water for heating baths in Assyria. Also, in Ancient China there is the possibility for a rudimental process for anaerobic digestion of solid wastes to be realised. Anyhow, the first documented attempt of biogas production and exploitation was only performed during the mid-nineteenth century: anaerobic digesters were first constructed in New Zealand and then in India. After that, in China, the first installation was built in 1921 and used to treat household wastes, while in Germany the first large agricultural biogas plant began to operate in 1950. However, the interest related to biogas was limited until the ‘70s, especially because oil price was low enough to make biogas related technologies not competitive at all. The attention towards biogas has had the chance to rise after the oil crisis of 1973-74 and 1979. The sudden increase of oil prices forced the governments to find energy sources in alternative to fossil fuels with some urgency. Biogas then had a growth till the second half of the ‘80s, which was significantly faster in the rural areas of Asia, Africa and South America. The diffusion of biogas technologies experienced a reduction in these regions, but at the same time new applications were found in the industrial and urban waste treatment contexts. Since 2000, another rapid increase concerning the number of plants has occurred, thanks to a more diffused environmental awareness and technological development [3].

The total biogas installed capacity experienced an increase of more than 8 times in the last 20 years, going from a global value of 2.5 GW in 2000 to 20.2 GW in 2020. Europe is by far the leader in this field, where it owns almost 70% of the total installed capacity, with 13.8 GW in 2020. At the same time, values are increasing consistently also in North America and in Asia, reaching respectively 2.6 GW and 2.0 GW in 2020. All the other regions are still far from a significant exploitation of biogas, even though the development of this technology occurring worldwide is not negligible [4], [5].

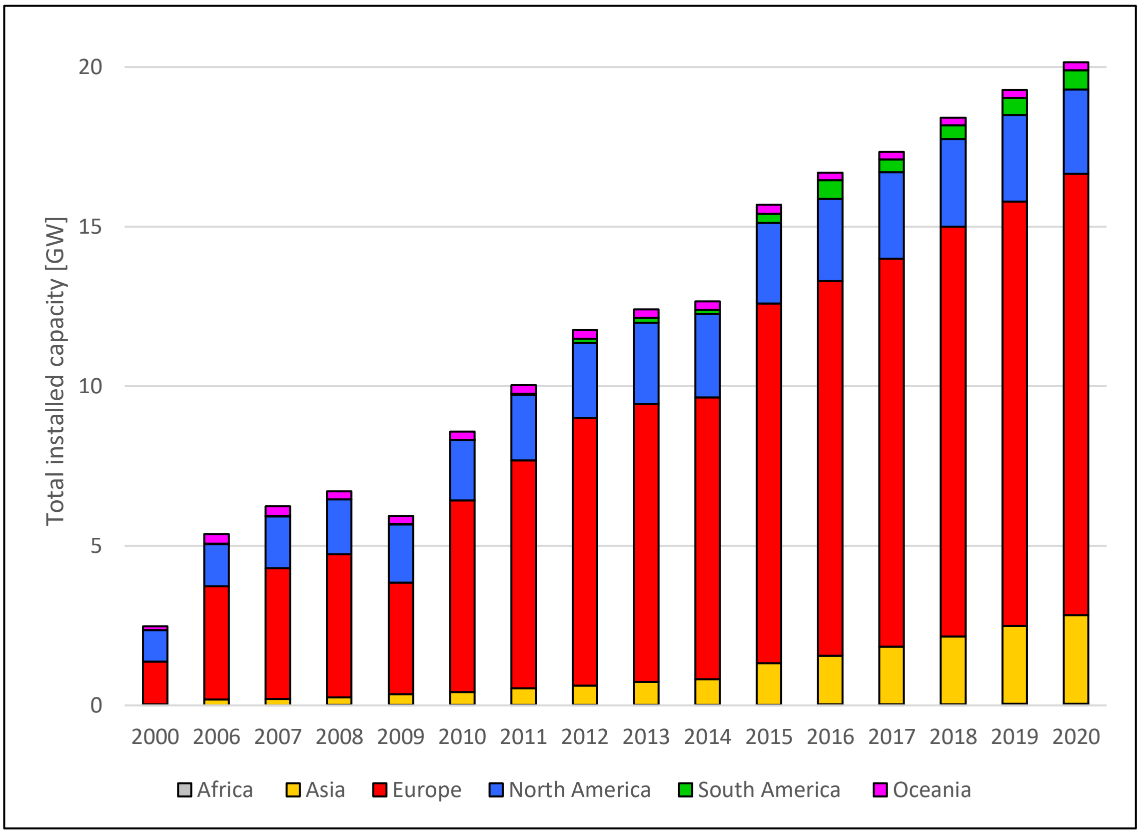

Figure 1.1: Total biogas installed capacity (personal elaboration from IRENA data)

In Italy, in 2020 there were 2201 plants powered by biogas, for an overall power equal to 1452 MW. Biogas is mainly used in the thermal sector, where its exploitation reached a value of 13000 TJ, and it comes mainly from wastes, sludges, agricultural activities and forestry activities. On average, Italian biogas plants have a power lower than 1 MW [6].

This constant increase is representative of a promising technology, which will probably be interesting to invest in, hence it is dutiful to underline that it still has a long way to go in order to become relevant in the energy mix. The 20.2 GW produced globally is a tiny value if related to the totality of renewables: it represents only 0.7% of the 2799 GW of renewables produced worldwide in 2020. As a comparison, in 2020 hydropower produced 1211 GW, wind energy 733 GW and solar energy 714 GW [5].

Today biogas represents an important energy source for developing countries. It can be commonly used to power refrigerators, lamps, engines and most importantly for cookers and stoves. As an example, the efficiency of a stove is strongly affected by the kind of alimentation. If traditional fuels are used, the efficiency is in a range of only 5-15%.

Switching to biogas can consistently improve this situation: depending on the conditions of utilisation and the design of the stove, a minimum of 20% and a maximum of 56% can be reached. Moreover, this change in the used fuels can lead to an increase of health for people living in underdeveloped countries that currently use solid fuels or open fires to cook. In fact, these methods increase internal air pollution, due to the production of small particles and carbon monoxide, with a consequent increase of burden diseases [3].

Despite its limited diffusion, the interest toward biogas remains high also in the developed countries, mainly because of its environmental benefits. The most promising application fields are the treatments of domestic wastewaters, household solid wastes, industrial wastes and agricultural residues [7].

1.2 The production

Biogas is a fuel produced thanks to the anaerobic digestion (AD), a microbial mediated process that decomposes the organic matter in absence of oxygen (O_2). The AD takes place in a reactor called anaerobic digester, in which, after a series of redox reactions, the carbon is converted into carbon dioxide (CO_2) and methane (CH_4). Carbon dioxide is the most oxidised form of carbon, while methane is its most reduced one. These reactions can be catalysed thanks to many different microorganisms, which act in synergy inside the reactor. The organic matter used to perform the process can come from many different sources: the most common are food wastes, wastewaters, livestock wastes or crops. This latter option is only likeable, from a sustainability point of view, if regards residues instead of dedicated agricultural land. Therefore, a key aspect of this process is the possibility of recycling wastes, because it leads to a consequent valorisation of organic residues in an energy productive process. The products obtained are basically three: biogas, fertilizer and livestock bedding. The biogas represents the energy extracted from the biowastes, the fertilizer is an output that can be useful in agriculture as soil conditioner, while the residual part can be used as livestock bedding. The output of the anaerobic process is particularly interesting because it generates a versatile energy carrier, guaranteeing at the same time a good exploitation of an organic matter mainly composed of residues. Furthermore, it could be a starting point for a circular economy concept: on one hand there is the generation of renewable energy and, on the other, all the other components of the process can be recycled or reused [7].

The AD process is influenced by various crucial parameters that can be analysed and controlled to optimise the overall process. The chemical composition of the substrate, for example, depends directly on the source of the organic matter used. Knowing its characteristics may allow one to choose the better technology to treat it, as well as relevant information about its biodegradability, bioaccessibility and bioavailability. Some typical organic materials are:

- Carbohydrate rich organic materials: they are contained in any substrate. If their concentration is too high, they can be responsible of a pH decrease, then it is convenient to mix them with wastes that have a lower content of components which are easily degradable;
- Protein rich organic materials: they are present in all organic substrates, but in variable concentrations; a protein rich substrate is also rich in energy, thus can generate a considerable amount of biogas. However, the amine group ($-NH_2$) of proteins amino acids can react generating ammonia, that at high concentrations inhibits bacteria action;
- Fat rich organic materials: the presence of fats in considerable amounts can cause problems related to blocking, microbial inhibition or adsorption of the biomass, for these reasons it is convenient to mix them with carbohydrate-rich materials to balance the AD process.

The pH value is probably one of the most affecting factors. Most of the microorganisms that take part in an AD process prefers a neutral pH range, usually the best values for biogas production are between 6.8 and 7.2. In addition, also temperature is fundamental for the survival of microorganisms: the process can be psychrophilic, if the temperature is around 25 °C, mesophilic, if it is at about 35 °C or thermophilic, if it reaches 55 °C. The best microorganisms growth occurs at mesophilic or thermophilic temperatures, however the latter is more difficult to control and more energy intensive, while the former is more stable and then preferable [8].

Biogas production through anaerobic digestion is currently a well-established technology, normally used to generate heat, but also for the combined generation of heat and power.

There is also the possibility to upgrade the biogas to biomethane, which is usable as vehicle fuel or can be injected directly in the natural gas grid (if compliant with the national requirements). The whole process, in addition to the exploitation of renewable sources, is carbon-neutral too. In fact, the combustion of biogas produces water and carbon dioxide, which are useful for the crops growth, while crops produces oxygen for the combustion in turn. As a consequence, it represents a good alternative option for what concerns both energy efficiency and environmental impact [9].

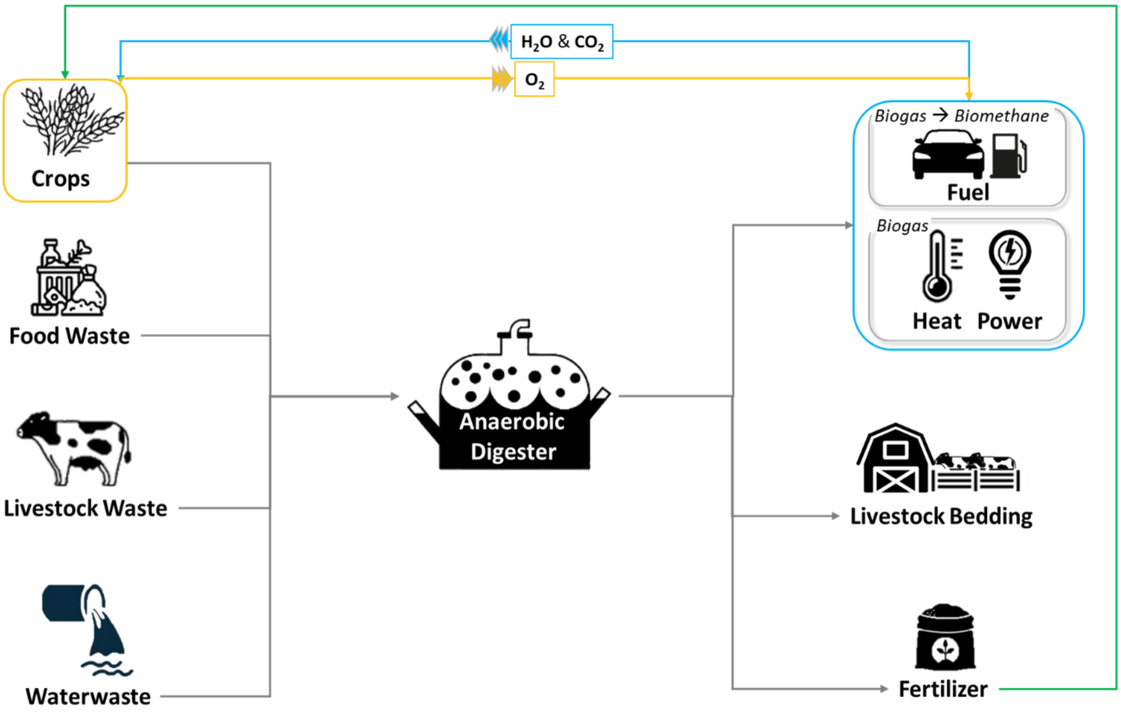

Figure 1.2: The sustainable cycle of biogas from anaerobic digestion (personal elaboration)

1.3 The composition

Biogas is composed mainly of CH_4, in a percentage between 55 and 70%, and CO_2, in a percentage that goes from 30 to 45%. Various other components can be found inside the biogas in traces. What chemical compounds are produced and their quantity depends on many variables, such as the kind or raw biomass used, the conditions of the AD and so on. Some of the most common impurities are hydrogen sulphide (H_2S), which is usually present as a 0.005-2%, ammonia (NH_3), in a quantity lower than 1% and water (H_2O), which instead can represent a significant portion of 5-10%. It is also possible to find traces of oxygen (O_2) and nitrogen (N_2) from 0 to 2% each, as well as hydrogen (H_2), from 0 to 4%, and siloxanes, which go from 0 to 0.02% [10].

These impurities can be dangerous for combustion engines; thus, it is usually necessary to remove them partially or totally, in order to avoid any risk of damage or corrosion. Another characteristic of the biogas is that it can burn easily thanks to the presence of CH_4, but it is necessary an amount of methane greater than 45% for the biogas to become flammable. The percentage of CO_2 instead makes its calorific value lower, also limiting the energy content and the Wobbe index. From this point of view, the carbon dioxide acts as a diluent of the mixture, so it can be necessary to remove it in order to make the biogas suitable for certain applications, for example as fuel. The main characteristics of a biogas obtained from anaerobic digestion are resumed in the table below [10].

Table 1-1: Properties of a typical biogas produced through anaerobic digestion [10]

Property	Value
Composition	55-70% CH_4
	30-45% CO_2
	Traces of other compounds
Energy content [kWh/m^3]	6.0-6.5
Wobbe index [MJ/m^3]	19.5
Ignition temperature [°C]	650-750
Normal density [kg/m^3]	1.2
Molar mass [kg/kmol]	16.043
Flame speed [cm/s]	25
Lower heating value [MJ/kg]	17
Critical pressure [bar]	75-89
Critical temperature [°C]	-82.5

1.4 Future trends

The European Union (EU) is one of the leaders in renewable energy development and environmental awareness. The seventh of its Sustainable Development Goals, to be reached till 2030, is specifically about "Affordable and Clean Energy". The target, which is really challenging, is to provide energy focusing not only on the technical aspects, but also on the economic and environmental ones. In this context, biogas represents a really versatile source of energy, being able to provide electricity, heat and fuels. Biogas production is strongly dependent on natural resources, then a heavy capital of investment will be needed for its production and distribution, to avoid the risk of ecosystem disruption and to guarantee socio-economic rights for the locals [11].

One of the most significant aspects related to biogas production in Europe is the creation of new supply chains for the feedstock of biomass. Furthermore, it represents a possibility of development for rural areas. In 2015, 50% of the global quantity of biogas, which corresponds to 18 billion m^3, was produced in the EU. Anaerobic digestion plants represent the major contributor to this growth. The produced biogas has an efficiency of about 35-40% in a traditional gas engine. Half of the biogas produced is currently dedicated to heat production, but the installed electricity biogas plant capacity is rapidly increasing worldwide, reaching 16 GW in 2016. Depending on the country, it is also really different the sources from whom biogas is produced: the most common are anaerobic digestion (74% of the total production in Europe), landfill gas (17%), sewage sludges and thermochemical processes (9%) [12].

The most interesting sector for biogas development is the transport one, because it is the one that lags the most behind energy transition. In the transport sector, in 2015 only 4% of the energy needed was supplied by renewables. According to the REmap Case (a renewable energy roadmap proposed by IRENA, the International Renewable Energy Agency), by 2050 the use of oil will drop by about 70% with respect to 2015, thanks to the combined action of biofuels utilisation and electrification of the transport sector. As a result, the share of renewables in 2050 will be estimated at 58% of the total. The share of biofuels could possibly reach alone 22%. A scenario like the one proposed would need a global investment of 14 trillion dollars, 3.4 of them dedicated specifically to the development of biofuels [13].

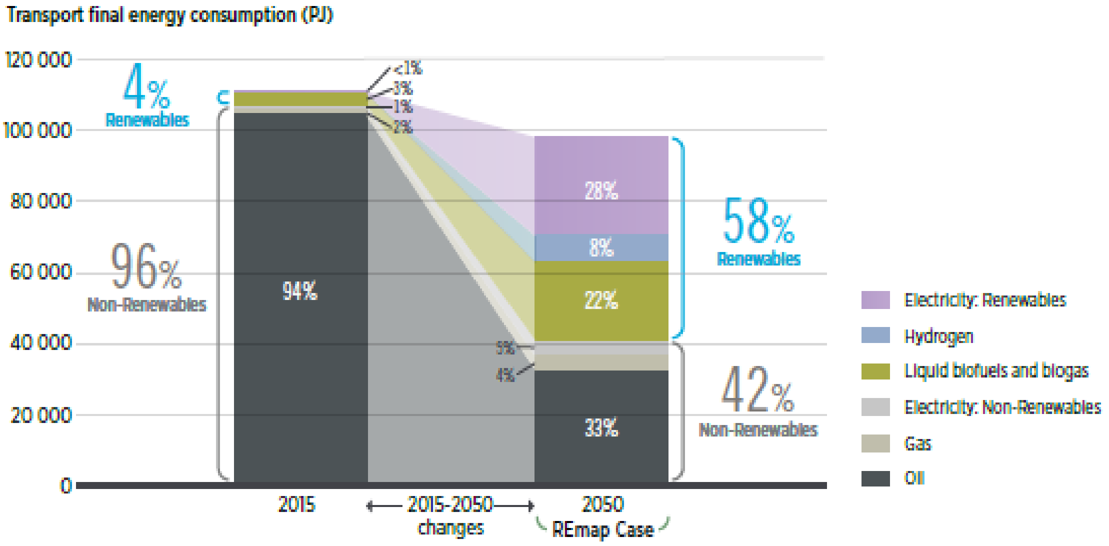

Figure 1.3: Transformation of the energy demand in the transport sector [13]

1.5 Powering fuel cells with biogas

Fuel cells can convert, through electrochemical reactions, chemical energy into electrical energy. They are made by an anode and a cathode, separated by an electrolyte. The process is organised in two different steps: at the anode side an oxidation occurs, while at the cathode side there is a reduction. The anode and the cathode are connected by a wire, in order to create a pathway for electrons.

The ideal fuel to use into a fuel cell is hydrogen. Unfortunately, H_2 is complicated to produce and is also difficult to store in a safe and economic way. That’s why a huge interest was put in finding other fuels which can be used in substitution. Biogas can be a good alternative fuel to power some kind of fuel cells. In particular, its methane content can be effectively used to power Solid Oxide Fuel Cells (SOFC) or Molten-Carbonate Fuel Cells (MCFC). Usually, the former is preferred, because the latter have a corrosive electrolyte layer: therefore, an additional CO_2 flow, which is not always easy to make available, would be required at the cathode side. The SOFC operates at high temperature (500-1000 °C) with an efficiency that can reach 60-62% [14].

At the anode side, the chemical reaction of oxidation occurs:

$$CH_4 + 2O_2^- \rightarrow 2H_2O + CO_2 + 4e^- \tag{1.1}$$

While at the cathode side the reaction of reduction occurs:

$$\frac{1}{2}O_2 + 2e^- \rightarrow O^{2-} \tag{1.2}$$

The overall reaction is then:

$$CH_4 + 2O_2 \rightarrow 2H_2O + CO_2 \tag{1.3}$$

Which has an enthalpy (ΔH) of -803.3 kJ/mol.

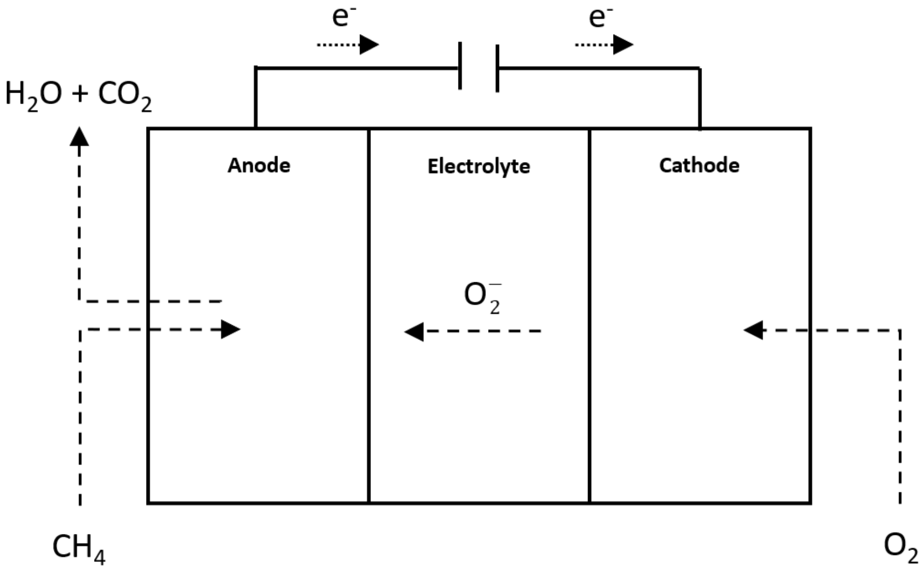

Figure 1.4: Schematic representation of a SOFC powered by methane (personal elaboration)

One of the main limits of this system is related to the carbon deposition risk. This phenomenon reduces performances and durability of the fuel cell and in the worst cases can lead to the cell cracks and delamination. To avoid this problem, the methane flow can be diluted with oxygen, carbon dioxide or water. From an energetic point of view, the best option is the latter, where water produced at anode can be directly recirculated and added to the CH_4 flow (anode recirculation). The same procedure could be possible with the produced CO_2, but in this case the carbon ratio becomes worse (with water it is equal to 3, while with carbon dioxide is 1), as a consequence the quality of the fuel decreases. In both cases the reaction is endothermic [14].

1.6 Limits on biogas diffusion

Despite its many advantages, some considerations on the limits of biogas must be taken into account to have a complete overview on the related applications.

Firstly, methane is a gas that, although its shorter atmospheric life, has a greenhouse effect much stronger than CO_2: it was calculated that its impact could be 28-36 times greater in a 100-years horizon, but even 84-87 times greater in a 20-years horizon. This means that biogas, being mainly constituted by CH_4, has a limited contribution in reducing the global carbon emissions, in particular if compared with other renewables, like solar or wind, which can be considered almost zero emissions energy sources [15].

It must also be considered that biogas can be prone to explosion if it comes in contact with oxygen, this makes it possibly unstable. Moreover, the biogas technologies currently available are not so efficient and are not simple nor low cost. This latter factor is particularly relevant: economic competitiveness is not negligible in the development and applicability of a certain process with respect to others. In addition, supplying a large population through biogas is currently not possible because large-scale production is not practicable right now, both from the economic and the technological point of view. A big limitation is related to the little new technologies introduced to make the process more efficient and affordable, consequently a limited number of investors is currently interested in putting capital on biogas. Anaerobic digestion is also a process which is strictly connected to the weather conditions: bacteria's optimal life temperature is indeed at about 37 °C, as a result they must consume heat energy to be able to survive in colder climates. Finally, the limitation of biggest concern is related to the impurities contained in the biogas, even after a process of refining. The presence of unwanted chemical species is a problem that has the need to be further analysed, because it is the main focus of this work [16], [17].

Chapter II

2. Biogas impurities and purification

The most important component of a biogas is the CH_4, while the presence of all the other compounds is usually undesirable, because the vast majority of them negatively affect biogas exploitation. Because of that, these impurities and trace compounds are known as biogas pollutants. The purification process consists in the removal of contaminants. This is beneficial because it consistently reduces the effects of corrosion on engines and it is also positive because it minimises the effects on the environment and human health of harmful components. Eventually the biogas can be upgraded to biomethane, as a result the calorific value is increased in order to be compliant with the fuel standards [18].

Technologies related to the purification and upgrading of the biogas are of recent interest. The main techniques currently investigated are the water scrubbing, the cryogenic separation, the membrane separation and, most of all, the adsorption [19].

2.1 Carbon Dioxide

The greatest non-combustible part of the biogas is made by CO_2, which consistently limits the biogas utilisation. Its percentage depends on pressure, temperature and liquid content inside the digester. The energy content of the biogas decreases with the increase of the CO_2: if the biogas is used for power or heat generation its presence can be tolerated, while if it is used as a fuel it is necessary to eliminate it as an impurity [10].

Carbon dioxide removal allows to increase the calorific value and density of the gas. To separate CO_2 from the biogas many solutions are possible: the most practiced takes advantage of the different solubility of CO_2 and CH_4 into water. This process is called water scrubbing and results in a biogas with 95-99% in volume of methane. Separation of carbon dioxide can be also carried with an adsorption of gas molecules to a solid surface. The process is known as Pressure Swing Adsorption (PSA). The adsorbents which are used are materials with a high specific surface area, like titanosilicates, zeolites, silica gels, activated carbon and carbon molecular sieves. In this kind of process, the water vapour needs to be separated before the adsorption, to avoid the risk of poisoning the adsorbent material. Together with the CO_2, in this step also N_2 and O_2 can be removed. The CH_4 recovery of this process is in a range between 96 and 98%, with a 2-4% of methane losses. A main disadvantage of this plant is that adsorption sites are blocked by NH_3 and H_2S, that's why also a desulphurization step is needed [10], [19].

Other techniques take advantage of membranes of hollow fiber modules or spiral wound modules. The separation can be at high pressure or a gas-liquid adsorption membrane. This technology is low cost and highly efficient, but its applicability largely depends on the material selected. Biological techniques are another interesting option because they are environmentally and economically suitable. To upgrade the biogas, heterotrophic, chemotrophic and autotrophic bacteria can be used. The last possibility is a cryogenic separation that exploits the different pressure and temperature ranges in which gases liquefy. By cooling and compressing biogas it is then possible to obtain biomethane, because the carbon dioxide liquefies at a higher temperature than methane [20].

2.2 Water Vapour

An AD can be a wet process, if the moisture content is between 85 and 99.5%, or a dry process, if the humidity is in a range of 60-85%. A certain amount of water, accordingly to the temperature and pressure, can evaporate during the whole process, becoming part of the biogas. H_2O is likely to be a problem due to its corrosive effect on equipment and because it can produce acidic solution reacting with other components like H_2S, NH_3 or CO_2. Furthermore, the presence of water negatively affects the heat value [10].

The removal of water can be performed changing the pressure and temperature conditions in such a way that a physical separation becomes possible, because the H_2O condensates. Adsorption separation is a possibility too: it uses activated charcoal, molecular sieves or silica. To allow the continuous operation two columns of packed bed operate in parallel.

Siloxane and other particles, which can dissolve in water, can be removed at the same time [10], [19].

2.3 Sulphur compounds

Sulphur compounds are probably the most problematic impurities in biogas. The most common one is the hydrogen sulphide (H_2S), but it is possible to also find mercaptans, like methanethiol (CH_4S), carbonyl sulphide (COS) and disulphides. If the H_2S content is high, acidification and oil lubricity reduction occur. Moreover, hydrogen sulphide is highly toxic, inflammable and dangerous for human health [10], [21].

The concentration of sulphur compounds inside a biogas can be strongly variable, but some typical values are provided by Papadias et al. [22]. In particular, the highest amount is due to hydrogen sulphide, while all the other molecules are usually present in significantly lower quantities.

Table 2-1: Some typical sulphur compounds' concentrations inside a biogas [22]

Molecule	Typical concentration [ppm]
Hydrogen sulphide	400-2897
Methanethiol	0.08-1.07
Carbon sulphide	0.05
Dimethyl sulphide	0.04

One of the most promising techniques for H_2S removal is based on adsorption processes, both chemical or physical, which makes use of activated carbons, zeolites, iron oxides/hydroxides or other adsorbent materials. Its main advantages are a limited cost and a low energy consumption, as well as limited maintenance requirements. It is also possible to perform absorption techniques, which have a high removal efficiency and use regenerable materials but are expensive and energy intensive. Membrane technology can represent an improvement of the purification process, because of the low energy consumption and easy process, coupled with a high H_2S removal efficiency. Also in this case costs are high, furthermore there is a low methane yield [23].

It is also possible to perform desulfurization processes directly inside the digester, making use of micro-organisms or iron-based salt solutions. The former can convert H_2S into elemental sulphur deposits, while the latter allow the precipitation of iron sulphide. This process can also make use of air or oxygen injection ("micro-aeration"). These techniques are effective for the hydrogen sulphide removal, while their effect on the other sulphur compounds is currently not fully understood [24].

2.4 Siloxanes

Siloxanes are organic silicon compounds (Si). Gaseous siloxanes have a negative effect on the production process because they turn into abrasive and hard silica, which damages the combustion chamber, while into fuel cells they can cause a degradation due to deposition. Volatile siloxanes may cause technical problems as well [21].

Table 2-2: Some typical siloxanes' concentrations inside a biogas [22]

Molecule	Typical concentration [ppm]
Octamethylcyclotetrasiloxane (D4)	0.83-20.14
Ecamethylcyclopentasiloxane (D5)	1.69-18.13
Hexamethyldisiloxane (L2)	0.12-2.26
Octamethyltrisiloxane (L3)	0.06-0.47

Conventional methods for siloxanes removals are based on adsorption processes that use activated carbon, molecular sieves or silica gel as adsorbent materials. Refrigeration, and subsequently condensation, techniques are another simple way for siloxane removal. Moreover, they allow water separation at the same time. Its main problem regards high costs of operation. A separation that makes use of polymeric or inorganic membranes is also an option. Their main characteristic is to be permeable and selective toward a certain molecule. The main issue is about the need of a pre-clean of the biogas of any particle that can damage the membrane. It is also possible to perform a gas-liquid absorption. This procedure, called scrubbing, transfers the contaminants from the gas phase to the liquid phase. In this case, polar organic solvents are the best material for siloxane removal [25].

2.5 Ammonium

Ammonium is generated by a feed that contains a significant quantity of nitrogen or by thermophilic digestion. During the combustion process, ammonium reaction with oxygen produces nitric oxide (NO), that can further react if released in the atmosphere. Ammonium concentration in a biogas is normally limited (a few ppm), but this value can increase if the process is carried on at high pH (more than 8.3, this is quite common in thermophilic processes, where the temperature is higher) or if the mixing is too fast [21].

It is currently difficult to eliminate ammonium alone: the main technologies coupled its removal at the same time of other substances. NH_3 can be removed together with H_2S, using activated carbons that perform an adsorption, but with the risk of ammonium sulphate, $(NH_4)_2SO_4$, accumulation. It is also possible to remove NH_3 and H_2O using a PSA system [10].

2.6 Halogens

Halogens are substances containing chlorine, bromine and fluorite. Their main problem is that during combustion in an engine they break down, forming hydrogen chloride (HCl), hydrogen bromide (HBr) and hydrogen fluorite (HF), which are all acidic and corrosive [21].

Halogens can be usually removed applying the purification options described for CO_2, H_2O and H_2S. If further purification is needed, biological methods are the most promising option [26].

2.7 Volatile Organic Compounds

VOCs can belong to different chemical families, such as aromatics, alcohols, alkanes and so on. Their quantity in the biogas depends on the organic matter from which the biogas come from. The measured VOCs amount comes from the direct volatilization of compounds at the beginning of the process, while from the substrate biodegradation rate after a certain time. The main concerns related to VOCs regards the fact that they lead to equipment problems and have a negative impact on the environment [10].

VOCs can be usually removed, as said for halogens too, applying the purification options described for CO_2, H_2O and H_2S. Also in this case, if a further purification is needed, biological methods are the most promising option [26].

2.8 Nitrogen and Oxygen

N_2 and O_2 are not usually present inside a biogas, thanks to the anaerobic conditions of the production process. If nitrogen is present, that means a strong denitrification or an air leakage are occurring. However, a small amount of O_2 can be present in the raw biomass: it can be dangerous because it can cause an explosion if, at about 25°C, the methane content is higher than 60% and the air range is between 8.5 and 20.7%. Furthermore, N_2 and O_2 presence dilute the gas, making methane percentage decrease. They can be removed with an adsorption method that uses molecular sieve or activated carbon [10].

2.9 Impurities-related main issues

The biggest concerns about using biogas in traditional energy applications (as, for example, gas boilers and internal combustion engines) are related to the quantity of methane and hydrogen sulphides in the biogas. It is recommended a quantity of H_2S lower than 1000 ppm: if the value is higher, it is necessary to treat the biogas before being able to use it. Considering that any biological material contains sulphur, in particular if it has a high concentration of proteins, the removal of H_2S becomes vital to obtain a good quality biogas. Considering instead more advanced technologies there are even stricter requirements, for what concerns both quality and quantity of trace compounds. For fuel vehicles and grid injection the quantity of CO_2 must be below 2-6%, while hydrogen sulphides must be below the value of 5-23 mg/m^3. The quantity of dust and particles must be of maximum 5 mg/m^3. For fuel cells the limitations are not necessarily on CO_2, but the other trace compounds must be limited in a stronger way. For example, in a Molten-Carbonate Fuel Cell, the quantity of H_2S must be below 0.1 ppm and, in addition, other sulphur compounds like CH_4S must be removed [9].

Chapter III

3. The adsorption

Adsorption is one of the most promising and applied technologies in biogas purification. Understanding this process better is fundamental to clarify the purpose of this work. The main goal is indeed the removal of sulphur compounds with adsorbent materials. Starting from the raw biogas, an adsorbent material can remove the unwanted chemical compounds, resulting in a biogas composed quite totally by methane. Only at this point is it possible to use it in the wanted process or application [18].

3.1 The adsorption phenomena

Adsorption phenomena are processes that happen at the level of the surface. They are made by:

- Adsorbent (or substrate): it is a solid and porous material and it is the active site where the adsorption occurs;
- Adsorbate: it is a chemical species that is adsorbed by the adsorbent.

The concentration of the adsorbate occurs at the level of pores [27].

It is possible to individuate two main categories: the chemisorption, which is a chemical adsorption where there is the generation of chemical bonds, and the physisorption, a physical adsorption, where the link is provided by electrostatic forces like the London-Van der Waals. It is not always easy to distinguish between these two groups, because intermediate cases frequently occur. However, this differentiation is reported because it is useful conceptually. In a physical adsorption there is no share of transfer electrons: therefore, all the species that interact maintain their individuality. This process is not site specific, meaning that the particles of the adsorbed material can cover any point of the surface freely. Contrariwise, in a chemical adsorption the chemical bonding forces the process to be site specific because it fixes adsorbed particles to a certain location. Furthermore, a chemisorption process leads to larger interaction potentials [29].

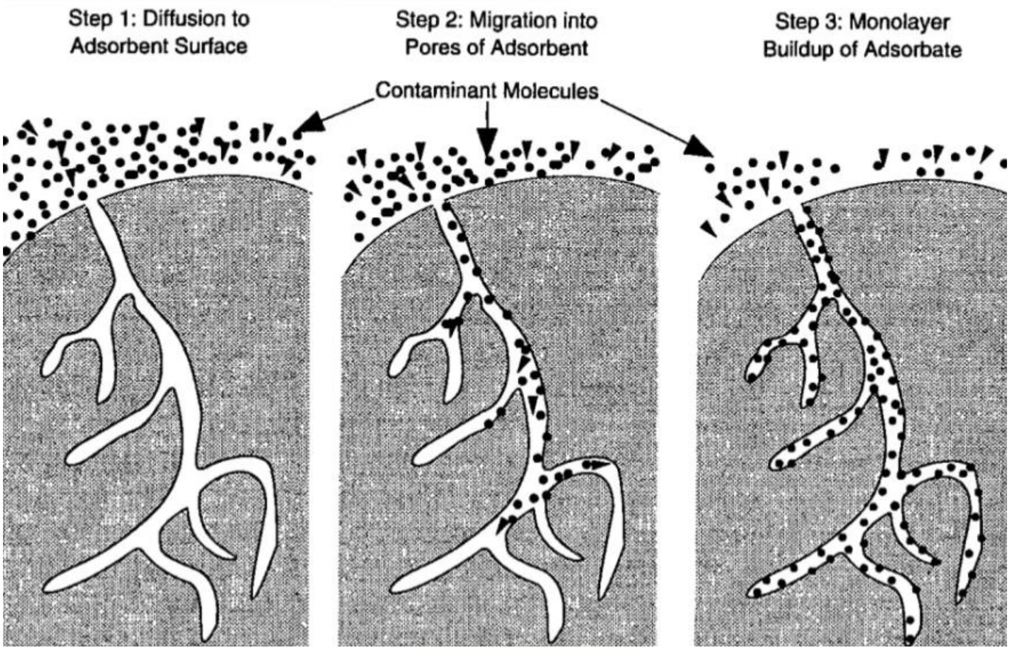

Figure 3.1 - The adsorption mechanism [28]

There is a proportionality between the quantity of gas or vapour which is adsorbed and the mass of the solid material. With few exceptions, the surface of most solids is not homogeneous, therefore the adsorption sites can have a variable energy. The most affecting factors for the entire process are the surface area and the porosity. Consequently, a good adsorbent material must have these two parameters as big as possible. The porous structure can be divided in three categories:

- Macropores: very large pores, with a minimum size of 100-200 nm;
- Intermediate pores: their dimension is between 1.5 and 200 nm, which is greatly bigger than the size of the adsorbate molecules;
- Micropores: their dimension is between 1 and 1.5 nm, which is comparable with the size of the adsorbate molecules [30].

3.2 Adsorption thermodynamics

In order to have a spontaneous process, from a thermodynamic point of view, it is necessary to have a Gibbs free energy value lower than zero. The formula is the following:

$$\Delta G = \Delta H - T \cdot \Delta S < 0 \tag{3.1}$$

Where ΔG is the Gibbs free energy, ΔH is the enthalpy change, T is the absolute temperature and ΔS is the entropy change.

Considering that the adsorption process causes a reduction of the molecular motion's freedom, these processes always experience a reduction of the system entropy. Accordingly, the ΔS has in any case a negative value. Consequently, the enthalpy variance is forced to be negative and to be greater in magnitude with respect to the T·ΔS value in order to obtain a spontaneous process. A negative value of ΔH means then that adsorption is an exothermic phenomenon [27].

The most important effects of the equation (3.1) are related to the temperature of the process and its reversibility. For chemisorption, the enthalpy change is usually higher, then it has a higher probability to occur even if the temperature is high. On the other hand, a chemisorption process is more difficult to reverse, because the desorption occurs at higher temperature. For physisorption the contrary is true: it is effective only at low temperature, but it is easier to reverse because lower temperatures are sufficient.

Gibbs free energy can be also related to the equilibrium constant K_c, which represents the ratio of the equilibrium concentration of the adsorbate on the adsorbent to the equilibrium concentration of the adsorbate in the solution, through the following formulation:

$$\Delta G = -R \cdot T \cdot \ln(K_c) \tag{3.2}$$

where R is the universal gas constant and T is the absolute temperature.

Combining the equations (3.1) and (3.2), it is possible to obtain the van't Hoff equation:

$$\ln(K_c) = -\frac{\Delta S}{R} - \frac{\Delta H}{R \cdot T} \tag{3.3}$$

Which condense in a single expression the relation between the equilibrium constant, the entropy change and the enthalpy change [31].

3.3 Adsorption isotherm

Adsorption isotherm represents a quite simple technique to investigate the feasibility of a specific sorbent in a particular application. The process can be favourable, unfavourable, linear or irreversible [31].

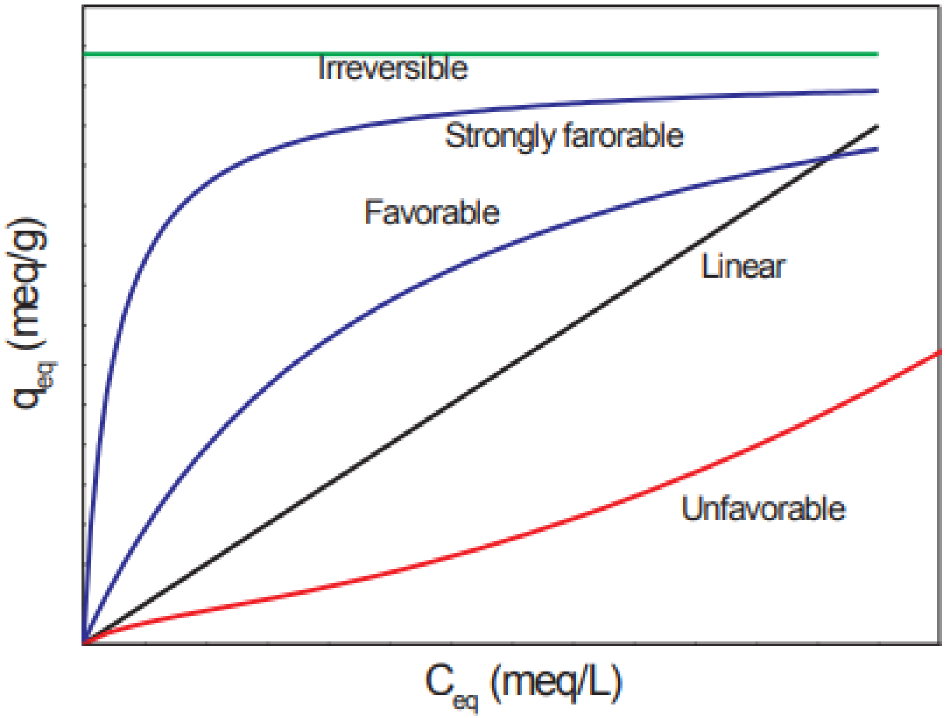

Figure 3.2 - Adsorption isotherm [31]

The shape of an adsorption isotherm is particularly useful to obtain qualitative information about the overall process. According to IUPAC, a classification of the different kinds of adsorption isotherms is available. Currently, there are six types of isotherms for the equilibrium between gas and solid. This classification is an extension of the Brunauer's: while the modern classification considers six types of isotherms, the Brunauer classification considers instead all the others but the VI. Each type has its specific characteristics:

- Type I isotherm: it is commonly used for the adsorption of microporous adsorbents;

- Type II isotherm: adsorption on microporous adsorbent with strong interaction between adsorbate and adsorbent;
- Type III isotherm: adsorption on microporous adsorbent with weak interaction between adsorbate and adsorbent;
- Type IV isotherm: mono adsorption and capillary condensation;
- Type V isotherm: multilayer adsorption and capillary condensation;
- Type VI isotherm: describes the fact that adsorption isotherms can have more than one step; as said this type wasn't included in Brunauer classification [32].

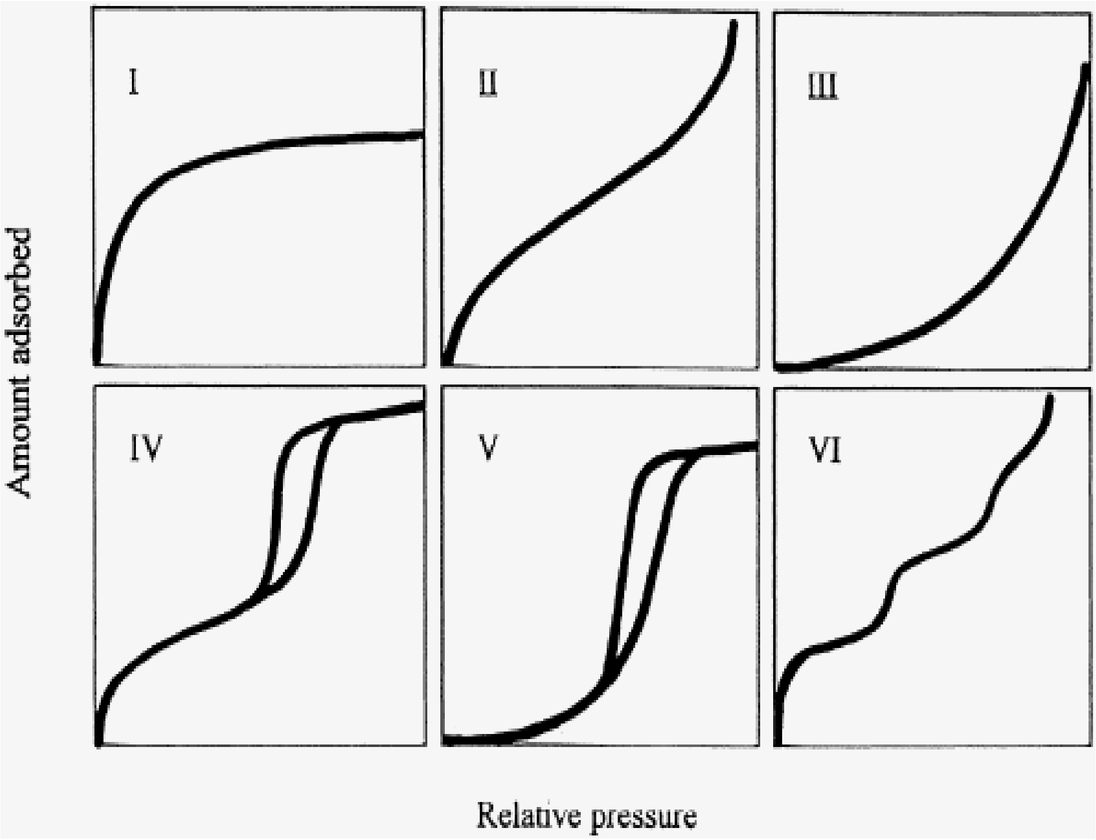

Figure 3.3 - IUPAC classification for adsorption isotherms for the equilibrium between gas and solid [32]

3.4 Langmuir model and BET specific surface area

Langmuir isotherm is a two-parameter empirical isotherm that describes microporous materials which exhibit Type I isotherms. Its main assumption is to consider the adsorption as limited to one monolayer. It considers a dynamic equilibrium, which is a balance between adsorption and desorption relative rates. The adsorption is proportional to the part of the adsorbent's surface which is open, the desorption is proportional to the one which is closed. The equation that describes the model is:

$$\frac{C_e}{q_e} = \frac{1}{q_m \cdot K_l} + \frac{C_e}{q_m} \tag{3.4}$$

Where C_e is the equilibrium concentration of adsorbate in the adsorbent, q_e is the quantity of adsorbate, q_m is the maximum loading capacity, K_L is the Langmuir constant.

The most important characteristics of this model can be condensed in the separation factor R_L, a dimensionless constant expressed as follow:

$$R_L = \frac{1}{1 + K_L \cdot C_o} \tag{3.5}$$

Where C_o is the initial concentration of the adsorbate.

The value of R_L indicates if the adsorption is either irreversible (R_L =0), favourable (0< R_L <1), linear (R_L =1) or unfavourable (R_L >1) [33], [34].

BET (Brunauer-Emmett-Teller) theory is an expansion of the Langmuir model, which considers a multilayer adsorption. It is a useful method that allows to calculate the specific surface area of any material, but it is particularly indicated for materials that exhibit Type II and Type IV isotherms. Its expression is the following:

$$\frac{1}{W \cdot (\frac{p_0}{p} - 1)} = \frac{1}{W_m \cdot C} + \frac{C - 1}{W_m \cdot C} \cdot \frac{p}{p_0} \tag{3.6}$$

Where W is the weight of gas adsorbed, p/p_0 is the relative pressure, W_m is the weight of adsorbate as a monolayer and C is the BET constant.

The specific surface area can then be defined as:

$$S = \frac{W_m \cdot N \cdot A_{cs}}{M \cdot w} \tag{3.7}$$

Where N is the Avogadro's number ($6.023 \cdot 10^{23}$), M is the molecular weight of the adsorbate, A_{cs} is the adsorbate cross sectional area and w is the sample weight [35].

3.5 Factors that affect adsorption

The adsorption phenomena can be affected by many factors. The first fundamental difference depends on the nature of adsorbate and adsorbent: different kinds of materials can behave in a completely different way even if the conditions are similar. For example, an easier liquefiable and higher water solubility gas is adsorbed more efficiently thanks to the greater van der Waals forces. One of the most important factors is surely the surface area of the adsorbent: clearly if there is a bigger amount of available surface the adsorption phenomena can significantly increase. Subsequently, a rough and porous surface is the best for an adsorption process, because these two characteristics make the overall surface increase. The concentration of adsorbate is another significant factor: the greater it is, the greater the adsorption. According to Le Chatelier's principle, a low temperature guarantees a better adsorption, because the adsorption process is exothermic. That means that decreasing the temperature the extent of adsorption increases, while increasing the temperature the extent of adsorption decreases. Moreover, at a constant temperature the extent of adsorption is proportional to the pressure, in a certain range of values [36].

Chapter IV

4. Sulphur compound removal through adsorption: State of the Art

Sulphur compounds are the components of main interest in this study. In particular, the focus is on hydrogen sulphide (H_2S), methanethiol (CH_4S), dimethyl sulphide (DMS, $(CH_3)_2S$) and carbonyl sulphide (COS). The most problematic one is H_2S, due to its negative effect on the environment and human health. For these reasons, it must be carefully removed. It is normally present in a quantity between 100 and 10 000 ppm, depending on the substrate combination: the value is higher if the quantity of proteins is consistent. Moreover, H_2S has a corrosive behaviour, which is a problem in combustion engines [19].

There are many studies concerning the best materials for H_2S removal. The goal is mainly to obtain a good adsorption, but economic and environmental considerations play a significant role as well. Currently, the most promising technology regards activated carbons, zeolites and iron oxides and hydroxides, but also other options are studied and tested.

4.1 Activated carbons for H_2S removal

Activated carbons (AC) are a wide range of carbonised materials, whose main characteristic is the high porosity and surface area. Their unique characteristics concerning adsorption processes depend on the presence of different functional groups, such as carbonyl, phenol, carboxyl, quinone and lactone, but also O_2, H_2 and N_2. From a theoretical point of view, any carbon-rich organic material can be used to produce an activated carbon, but the most common sources are wood, lignite, charcoal and peat shells. One of the determinant steps in AC synthetization is the selection of a suitable chemical activator agent, because it consistently influences the performances of the material. Activated carbons are one of the most promising materials for what concerns H_2S adsorption [37].

Micoli et al. [38] proposed, as possible adsorbents, AC impregnated with KOH, NaOH or Na_2CO_3 solutions. Accordingly, in their work these materials were named as AC-NaOH, AC-KOH and AC-Na_2CO_3, and compared to a non-impregnated AC. The test was conducted in an innovative laboratory scale plant, where a gas stream of He which contains 8 ppm of H_2S was sent, at 0.1 L/min, in a fixed bed reactor, which was immersed in a 40° water bath. Firstly, the results obtained indicate that impregnation in general makes the adsorption capacity better. Furthermore, while AC-NaOH and AC-KOH breakthrough curves are similar, AC-Na_2CO_3 presents a significantly longer breakthrough point after which the concentration increase of H_2S is low. Of all the materials tested in the study, the AC-Na_2CO_3 is then by far the most promising.

Cimino et al. [39] investigated the effect of water and oxygen of H_2S adsorption on CuO-ZnO onto AC. The total metal loading was of 10%wt. in three different combinations: only Cu (Cu/AC), 50% of Cu and 50% of Zn ($Cu_{0.5}Zn_{0.5}$/AC), only Zn (Zn/AC). The test was conducted at a temperature of 30°C and atmospheric pressure. The inlet concentration of H_2S was 100 ppm_v, while the feed gas was composed of nitrogen, in addition to oxygen (2500 ppm_v), water (50% relative humidity) or a mixture of oxygen and water (2500 ppm, 50% relative humidity). Results showed that Zn/AC adsorbed worse than Cu/AC, but the best combination is $Cu_{0.5}Zn_{0.5}$/AC. The presence of oxygen seems to increase the adsorption capacity, in particular if copper is present: this means it can be a good catalyser. Moreover, the presence of water makes the adsorption even better. In conclusion, these tests show that coupling oxygen and water in the feed, results obtained are incredibly positive for H_2S removal.

Sawalha et al. [40] proposed a H_2S removal carried on synthetizing activated carbons prepared by different biomass wastes available in the region of their study, Palestine. The chosen biomasses were almond shells (ALM), eucalyptus (EUC) and coffee grains (COF), which were impregnated with potassium hydroxide (KOH) or zinc chloride ($ZnCl_2$). The test was performed in a fixed bed filter filled with ACs. The biogas steam had an average H_2S concentration of 970 ppm and was flowing at 1.5 L/min. Considering the non-impregnated material, EUC is the one with the highest adsorption potential, while the one of COF was so limited to be almost negligible. The subsequent test with impregnation, done only on EUC, shows a rapid increase of the breakthrough time. EUC-KOH reached high performances (more than EUC-$ZnCl_2$), thanks to the increase of chemical affinity. This test was particularly interesting because it demonstrated that easily available primary sources can be suitable for H_2S removal. In developing countries, this can be an important asset to allow biogas diffusion.

Tuerhong et al. [41] investigated activated carbons prepared in a dairy cattle manure, because of their economic and environmental benefits coupled with a high efficiency in H_2S removal. To obtain a suitable material, they were pyrolyzed at different temperatures (450°, 650° or 850°C) for one hour and then brought to the activation temperature of 850°C. After this process, streams of H_2O or CO_2 were purged directly for activation. The CO_2 flow rate was 100 ml/min for one sample and 1000 ml/min for another. The steam activated ACs were named as AC1(450/850 H_2O), AC2(850/850 H_2O), AC3(650/850 H_2O), AC4 (650/850CO_2/1000) and AC5(650/850CO_2/100). The first number represents the pyrolyzing temperature, the second the activation temperature, then the stream (water or carbon dioxide) is indicated. In the CO_2 case, also the flow rate is reported. The gas was made of N_2, H_2S and O_2. At inlet the H_2S concentration was 1200 ppm. The adsorption was then conducted at room temperature and atmospheric pressure. Differences between AC1 and AC2 breakthrough curves were consistent, even though their surface area is similar. An analogous consideration is true for AC3 and AC5. AC4 resulted as the material with the longest breakthrough point, while AC5 has the shortest. The strong differences in adsorption may be due to the different adsorption kinetics at the level of surface.

Cepollaro et al. [42] used a series of monometallic and bimetallic Cu/Mg oxide-based structured catalytic sorbents, obtained synthesising activated carbons by impregnation. The impregnation was conducted with a technique that uses aqueous solutions of $Cu(NO_3)_2\cdot\frac{2}{5}H_2O$ or $Mg(NO_3)_2\cdot 6H_2O$; catalytic sorbents with 5%wt. nominal metal loading of Cu or Mg where used. The test was at 30°C and 1 atm. The gas stream was of N_2, with an additional H_2S concentration of 200 ppm. Subsequent impregnation of Cu and Mg was at 2.5%wt. The parent AC (Helsa AC), used as a comparison parameter, showed poor behaviour: it reached the breakthrough soon after the starting of the test. The presence of Cu increases the adsorption, but the most significant effect is obtained with the presence of Mg, which increases the situation strongly. $Mg_{5.0}$ and $CU_{2.5}Mg_{2.5}$ have a high removal efficiency, being by far the most efficient in this study.

Choudhury et al. [43] carried out the first test on iron-impregnation of biochar, using as substrate corn stover biochar (CSB) and maple wood biochar (MB). Results obtained were compared with the Fe-unimpregnated materials. The iron-impregnated maple wood biochar (MB-Fe) had the highest H_2S adsorption capacity, about 4 times higher with respect to the unimpregnated version. The impregnated version is better also for corn stover biochar (CSB-Fe), but the overall performance is worse with respect to Mb-Fe.

Monteleone et al. [44] performed tests on Norit RGM-3 and Airpel Ultra DS, which are also two of the materials tested during the PoliTo laboratory activity. They demonstrated that the adsorption capacity of Norit RGM-3 strongly depends on the conditions in which the various experiments are performed. The best results were obtained in presence of oxygen inside the biogas, in particular at higher temperature, and with a lower GHSV value. For what concerns Airpel Ultra DS, it was confirmed that it must be used at ambient conditions and with a relative humidity of 70% in order to work properly (with a dry gas results are incredibly poor). The adsorption capacity appears to be another fundamental parameter: a lower velocity exponentially increases the removal efficiency.

Table 4-1: Activated carbons comparison

	Initial H_2S ppm	BET surface area [m^2/g]	t_{br} [min]	Adsorbed H_2S at t_{br} [mg/g]	Adsorbed H_2S at t_{sat} [mg/g]	Ref.
AC	8	1110	725	49.8	-	[38]
AC-Na_2CO_2	8	1106	1222	83.9	-	[38]
$Cu_{0.5}Zn_{0.5}$/AC + N_2 + 2500 ppm_v O_2 + 50% RH water	100	570	7	25	118	[39]
Eucalyptus	970	-	90	-	690	[40]
AC4 (650/850 CO_2/1000)	1200	408	2030	-	868	[41]
$Cu_{2.5}Mg_{2.5}$	200	640	366	63.1	178	[42]
$Mg_{5.0}$	200	670	559.8	82.9	242	[42]
MB-Fe	500	59.8	300	15.2	23.9	[43]
CSB-Fe	500	34.9	30	1.5	8.2	[43]
Norit RGM-3 + 0.1% O_2 (T=120°C, GHSV=3800 h^{-1})	400	671.3	-	-	123	[44]
Norit RGM-3 + 0.125% O_2 (T=120°C, GHSV=3800 h^{-1})	375	-	-	-	320	[44]
Airpel Ultra DS + 0.1% O_2 + 74% RH GHSV= 2000 h^{-1}	400		-	-	110	[44]
Airpel Ultra DS + 0.1% O_2 + 74% RH GHSV= 10000 h^{-1}	400		250	-	50	[44]

4.2 Zeolites for H_2S removal

Zeolites are crystalline aluminosilicate. They are made of SiO_2 frameworks, but in some places the Si^{4+} (silicon) ion is substituted by Al^{3+} (aluminium), thus in these locations a negative charge is carried. The structure is a three-dimensional framework that forms pores with a uniform size of molecular dimension. When a zeolite contains an equal number of Al and Si atoms, the density of exchangeable cations is maximum, thus they become interesting for adsorption processes [45].

Alonso-Vicario et al. [46] studied the behaviour of synthetic molecular sieves (5A and 13X), as well as a natural zeolite called Clinoptilolite. Zeolites were activated prior to utilization with a proper method based on washing and calcination. The inlet concentration of H_2S was 5 ppm. Clinoptilolite was the material with better performances: activation methods were further investigated, changing the washing and drying temperature, in order to choose the optimized option. The most promising activation method was the one with a washing at 40°C followed by a drying at 220°C. With this process, the adsorption capacity of the material increases by 14 times with respect to the non-activated zeolites. It was also demonstrated that a lower diameter (1-3 mm) was beneficial from the point of view of performances.

Micoli et al. [38] proposed Cu and Zn modified 13X zeolites as possible materials. For the test, 1.6 mm of diameter spheres were used. The biogas was made of He and H_2S (8 ppm), which flowed through a fixed bed, immersed in a 40°C water bath. Modified 13X zeolites were prepared by ion exchange or impregnation of $Cu(NO_3)_2$ and water or $Zn(NO_3)_2$ and water. The four materials obtained are accordingly named as: 13X-Ex-Cu, 13X-Ex-Zn, 13X-In-Cu, 13X-In-Zn. All modified zeolites behave better, from the point of view of breakthrough time, with respect to the parent zeolite. The best result is obtained using 13X-Ex-Cu: it presents a larger breakthrough time and the increase of H_2S concentration after this point is slow. The results obtained for the other three materials show instead similar results between each other. The use of Cu instead of Zn is preferable in both ion exchange and impregnation cases.

Bahraminia et al. [47] tested NaA nano zeolite, synthesised hydrothermally and modified by Ag^+ ions through an ion-exchange process (named AgNaA). The test was conducted at atmospheric pressure and ambient temperature. The inlet H_2S concentration was 15

ppm_v. Results were compared with commercial 4A, which shows breakthrough points much lower than the ones of NaA nano zeolite. Ag^+ exchanged nano zeolite has the best overall performance. This is probably due to the highest surface area of nano zeolite with respect to commercial 4A. Furthermore, AgNaA nano zeolite can be regenerated with no significant change in the adsorption capacity.

Table 4-2: Zeolites comparison

	Initial H_2S ppm	**BET surface area [m^2/g]**	**t_{br} [min]**	**Adsorbed H_2S at t_{br} [mg/g]**	**Adsorbed H_2S at t_{sat} [mg/g]**	**Ref.**
Clinoptilolite (activated, 40°C washing, 220° drying)	5	34.2	260	1.4	-	[46]
13X	8	582	47	3.06	-	[38]
13X-Im-Cu	8	575	580	6.8	-	[38]
AgNaA nano-zeolite	15	-	310	33.24	-	[47]

4.3 Iron oxides and hydroxide for H_2S removal

Iron oxides are chemical compounds composed by iron (Fe) and oxygen. The most common are wüstite (FeO), iron peroxide (FeO_2), magnetite (Fe_3O_4) and hematite (αFe_2O_3). Iron hydroxides also contain hydrogen. The most common are $Fe(OH)_2$ and $Fe(OH)_3$ [48].

Iron compounds are particularly interesting if they are in nanostructures. Nanoparticles represent indeed a great option because they guarantee a great surface area, as well as a reduced generation of wastes thanks to the long adsorbent bed life [49].

Djema et al. [49] proposed as a possible material the NIO (nanostructured iron oxide). NIO was tested in a vertical fixed-bed continuous flow reactor, at room temperature and atmospheric pressure. The material was obtained from mining residues, and it is made of cylindrical pellets of 2 mm in diameter and 4-10 in length. Coming from waste, this material is particularly interesting because it has clear advantages both from the economic and environmental point of view. Together with its relatively low cost, it can possibly be regenerated. The gas mixture used was a synthetic gas made only of N_2 and H_2S, which was tested in different operative conditions. The most important results regard the GHSV, the concentration of H_2S and the presence of moisture. A decrease of GHSV was beneficial for the purification process because it leads to an increase of the breakthrough time. In comparison with some of the most common activated carbons tested in the same conditions, results obtained are good. The decreasing of H_2S concentration led to a reduction of breakthrough capacity as well, as expected due to the higher mass transfer coefficient. The presence of moisture in the gas was another negatively affecting factor. At the same operating conditions, a water-saturated gas reaches the breakthrough time considerably faster than the dry gas. In conclusion, operating conditions strongly affect the adsorption capacity of NIO, which is anyway a suitable material, in particular if the H_2S concentration is low. Furthermore, its cost-effectiveness makes this material a good alternative for desulfurization of a biogas.

Raabe et al. [50] investigated 35 different Fe-based adsorbents. Four different industrial iron oxides were used as reference. The feed was composed of 500 H_2S ppm_v in N_2. Globally, the iron oxides, αFeO2, had a worse performance with respect to iron hydroxides, $Fe(OH)_3$ and iron oxyhydroxides, FeOOH. In fact, iron oxides show a low breakthrough time, as well as the lowest adsorption capacity. With $Fe(OH)_3$ the best results were obtained, also because the surface area is the greatest.

Costa et al. [51] studied hematite, obtained by the precipitation of iron hydroxide, activated with copper oxide. A concentration of 200 ppm in N_2 was provided. The test was conducted at atmospheric pressure and the temperature was kept below 50°C, in order to minimize running costs. As expected, increasing the bed length and decreasing the concentration of H_2S in the flow, the breakthrough time increases. Fe_2O_3-based pellets show a better behaviour increasing the temperature. This material, at 50°C, was the one with the best performance, in comparison with commercial ZnO and SulfaTreat 410 HP at any temperature in the range 25-80°C.

Wang et al. [52] tested both SulfaTrap R7 and SulfaTrap R8, two commercial materials that were also tested by PoliTo. Their performances were compared with the ones of SulfaTreat. The experiments were conducted at ambient pressure, with a gas made of CH_4 (50 v%), CO_2 (40 v%) and N_2 (10 v%), and a H_2S concentration of 200 ppm. The GHSV was equal to about 1500 h^{-1}. The results obtained show that both materials have significantly better performances with respect to SulfaTreat. In particular, SulfaTrap R7 demonstrates to be the best material of the three at room temperature, with a breakthrough of about 3 days and a good adsorption capacity.

Table 4-3: Iron oxides and hydroxides comparison

	Initial H_2S ppm	**BET surface area [m^2/g]**	**t_{br} [min]**	**Adsorbed H_2S at t_{br} [mg/g]**	**Adsorbed H_2S at t_{sat} [mg/g]**	**Ref.**
Nanostructured iron oxide (GHSV= 1250 h^{-1})	200	73	424	2.5	-	[49]
Nanostructured iron oxide (GHSV= 1750 h^{-1})	200	73	244	2.0	-	[49]
$Fe(OH)_3$	500	258-301	37	-	103	[50]
Fe_2O_3	200	54	610	9.1	-	[51]
SulfaTrap R7	200	-	4000	38.9	-	[52]
SulfaTrap R8	200	-	1700	22.3	-	[52]

4.4 Other compounds for H_2S removal

Even though activated carbons, iron oxides and hydroxides and zeolites are the most diffused and studied materials for H_2S removal by adsorption, many other materials were tested, in order to find new suitable adsorbents.

Kawase et al. [53] consider molten carbonate at high temperature for H_2S removal. The initial H_2S concentration was 200 ppm. Using molten carbonate is not a good option if the CO_2 concentration is relevant, while a high H_2O concentration is beneficial. The desulfurization effect depends on the temperature. The best temperature range is between 800 and 1000 °C. Over all the materials tested, molten salts containing Li_2CO_3 or K_2CO_3 have the shortest breakthrough times, while the ones containing $BaCO_3$ have the longest. Adding metal alloy powders, made of Cu, Ni_2B and FeB, to the molten salt was tested as a possible catalyst. Despite the results showing a higher breakthrough time, the overall effect of adding powders was found to be insignificant.

Abdullah et al. [54] propose kaolin as adsorbent. The natural kaolin tested was sieved to obtain a powder and the kaolinite adsorbent was calcined in a muffle furnace to remove any VOC. The experiment was conducted in a fixed bed column. The biogas was made of N_2 and 200 ppm of H_2S. The most important result obtained is the increase of breakthrough points decreasing the gas flow rate. This confirms the fact that contact time between the adsorbent and the gas is a key factor for the adsorption capacity. Also the temperature is particularly relevant. Increasing the temperature, the material behaves better, and an increased adsorption capacity is experienced. Unfortunately, the results show that adsorption capacity of kaolin is really low, if compared to commercial zeolite, AC and zinc oxide. In conclusion, kaolin cannot be effective as adsorbent material for H_2S removal.

Ahn et al. [55] tested iron-exchanged sand (IES), obtained from tetraethylorthosilicate, Acid mine drainage sludge (AMDS), obtained from mining, silica blue, sand and iron-exchanged zeolite (IEZ), prepared form commercial 13X zeolite through an ion-exchange method. AMDS is particularly interesting for its high specific surface density, furthermore it has the best performance over the other materials. Its adsorption capacity is even better than zeolite 13X, while IES and sand had the worst performances. The test was conducted with a mixture of H_2S (110-126 ppm_v) and N_2.

Table 4-4: Other compounds comparison

	Initial H_2S ppm	BET surface area [m^2/g]	t_{br} [min]	Adsorbed H_2S at t_{br} [mg/g]	Adsorbed H_2S at t_{sat} [mg/g]	Ref.
Na_2CO_3/K_2CO_3/ $BaCO_3$ (64/16/20)	2000	-	174	-	-	[53]
NaCl/Na_2CO_3 (57/43)	2000	-	144	-	-	[53]
Kaolin (flow rate 20 ml/min)	200	-	6	5.4	8.7	[54]
Kaolin (reactor T=85°C)	200	-	22	20.2	26	[54]
Acid Mine Drainage Sludge	110-126	156	2500	-	8.4	[55]
Iron-Exchanged Sand	110-126	3	52	-	33.7	[55]

4.5 Materials for CH_4S removal

Methanethiol (CH_4S) is formed inside the biogas through degradation of amino-acids that contain sulphur. CH_4S reduction later forms methane, carbon dioxide and hydrogen sulphide. CH_4S removal from a biogas is less studied with respect to H_2S. The main reason is that CH_4S doesn’t negatively affect the biogas utilization into traditional operations, like combustion engines. Therefore, it wasn't necessary in the shortest time to find a way to remove it. The situation changes with fuel cells, in which the limits on trace compounds are much stricter than the ones for vehicle applications. Then, in a fuel cell, CH_4S must be limited, because it can pollute the cells. As an example, in a molten carbonate fuel cell (MCFC), the tolerance limit for methanethiol is below 1 ppm [9].

CH_4S removal represents a new challenge in the biogas purification field because there are quite no studies on its removal from biogas. The test campaign of PoliTo will be dedicated to the study of this molecule, as well as hydrogen sulphide.

4.6 Materials for DMS removal

Dimethyl sulphide (DMS) is one of the most resistant sulphur compounds to purification processes. Usually, its concentration inside a biogas is several ppm. DMS presence strongly affects fuel cells, usually causing a significant long-term performance degradation but sometimes also determining an immediate negative effect. For this reason, it is fundamental to lower to 1 ppm (or even less, if possible) the dimethyl concentration. The literature concerning the removal of this molecule, even though is currently limited, evidences the difficulty of a satisfying purification process. The most suitable technology could be the adsorption because the process is simple, can be conducted at ambient temperature and is highly efficient. The most promising materials for adsorption purification are activated carbons, zeolites, sepiolite and metal oxides [56].

On this compound, PSI conducted its research activity.

4.7 Materials for COS removal

Carbonyl sulphide (COS) is formed naturally from H_2S, following a hydrolysis reaction:

$$H_2S + CO_2 \rightarrow COS + H_2O \tag{4.1}$$

About 3-10% of the sulphur content in a gas can become COS. Due to its pollutant effect on a fuel cell, it is necessary to remove it till the part per billion (ppb) level [57].

The removal of COS is typically performed through a high temperature (greater than 100° C) hydrolysis, which reconvert COS to H_2S. The most performant materials are based on alumina and titania, doped with different promoters to improve the effectiveness. For what concerns COS adsorption procedure, they have been much less studied. The main problem is that COS has a low polarity, which makes the adsorption process difficult for the vast majority of materials. The only sorbents that can be suitable for the process are activated carbons, rhodium and layered double hydroxides. This leads to the need of a better understanding of the capture and elimination of this contaminant from a biogas flow [58].

ENEA studied this sulphur compound in its experimental investigation.

4.8 Multi-component removal

Multi-stage adsorption processes can be used to remove all major impurities at a time. The main advantages of this kind of procedure are the possibility to operate at room temperature and the fact that it is suitable also for small-scale applications. In addition, the process is quite simple, which means it could become the most practicable and cheap purification method. Most studies performed on biogas unwanted compounds were conducted with a single adsorbent-loaded reactor. The limit of this approach is that a single material which can remove all the impurities simultaneously and with a good efficiency doesn't exist. Furthermore, the same material could require different conditions, as for example, the percentage of relative humidity, to better remove different molecules. Another possibility is making use of more reactors connected in series. However, using many reactors doesn't necessarily guarantee an improvement of the overall performance. Furthermore, it is not always feasible from an economic point of view [59].

An optimized multi-component removal model, both from the energetic and economic point of view, will be the goal of this work.

Chapter V

5. The experimental investigation

The following work is part of the European Waste2Watts (W2W) project. The purpose of the research activity is the design, the construction and the testing of a solid oxide fuel cell (SOFC) fed by an agricultural biogas. To implement a system of this kind, one of the most relevant steps is the purification of the biogas from the impurities that it can contain. Once the key contaminants to be removed are identified, the main goal is to find flexible and low-cost materials for the removal of biogas impurities, suitable both for small (<100 kW) and large-to-medium scale (>100 kW). The research team is led by PoliTo, which activity is mainly focused on H_2S and CH_4S removal, and includes as partner ENEA, which investigate carbonyl sulphide (COS), and PSI, which work on dimethyl sulphide (DMS). Furthermore, ENEA and PSI are also studying multi-contaminants [60].

5.1 The experimental setup

The PoliTo gas station prototype is designed in order to offer a flexible system, in which different gas mixtures and humidity levels can be set. It is composed of six inlet pipes, which allow the gas injection. Two of them can be used to inject, through a rotameter, a flow of N_2 and air respectively. These two streams must be set manually and can't be remotely controlled. Furthermore, they are used at the end of every test, in order to clean the line and the sensor from the impurities. On the contrary, the other four can be adjusted through a Mass Flow Controller (MFC) produced by Bronkhorst and can be also set remotely using Flow View, a dedicated PC software. These four streams are used for the injection of CH_4, O_2, CO_2 and for the gas mixture that contains a gas with a precise concentration of H_2S (or CH_4S). This gas, in the experiments performed by PoliTo, is a synthetic biogas made of CH_4 and CO_2, with a known quantity of H_2S, equal to 1000 ppm, or CH_4S, equal to 460 ppm. The feed of the gas plant can be regulated accordingly with the kind of test to perform. The concentration of H_2S or CH_4S which flows in the plant can also be adjusted as wanted. The six gas pipes are connected with a valve for the regulation of inlet flows into the gas station. Each pipe is then connected to two valves in parallel. One of them leads directly to the reactor (dry path), while the other is connected with a bubbler instead (wet path). These two valves can be independently open or closed, depending on the relative humidity percentage wanted for the gas flow during the experiment. The bubbler makes possible the humidification of the gas flow and can be controlled also from the point of view of temperature. It is convenient to only humidify the CH_4 stream, while letting the CO_2, O_2 and CH_4+H_2S or CH_4+CH_4S flow in the dry line. In parallel with the bubbler a humidity sensor measures the humidity level of the mixture. This sensor is sensitive to H_2S and CH_4S, therefore it is only used at the beginning of the test, to verify the relative humidity level.

The gas mixture is then sent to the reactor, which is the core of the whole process. The reactor is loaded with a defined quantity of adsorbent material, which is weighted with a precision balance before starting the test. The material is in pellet shape: due to the reactor conformation it is indeed not possible to use powders. The reactor has a cylindrical shape, which dimensions are:

- 115 mm overall length;
- 22 mm diameter (D).

The reactor is loaded with the adsorbent material, so that the adsorption bed has a length (L) equal to 66 mm. In this way, the ratio between the adsorption bed and the diameter of the reactor (L/D) is equal to 3. This value was chosen because it is the minimum suitable to avoid the formation of preferential pathways. To limit the thermal losses during the operation of the gas station, the reactor is covered with an insulating coating. Dedicated valves allow bypassing the reactor if needed, for example to calibrate the mass spectrometer.

Four thermoregulators are present. One is connected with the reactor and exhibits its temperature, while the remaining three are coupled with heating cables and can be regulated according to the conditions wanted. Security valves and security thermostats guarantee that the limits of the gas station are not overcome. To detect the concentration of H_2S an electrochemical sensor by Siegrist is available at the end of the whole cycle.

This sensor can detect hydrogen sulphide concentration in a range of 0-1000 ppm. Instead, to detect the concentration of CH_4S the procedure is slightly more complicated because it makes use of a mass spectrometer by Hidden Analytical, which must be calibrated every time before the experiment starts. The mass spectrometer can be possibly used to detect H_2S concentration as well when a higher precision is needed. All the tests were performed at a temperature which was between the ambient one and 50 °C. The results obtained during the experiment are registered thanks to FlexLogger, a dedicated software. Lately, the values of interest (typically, the most important one is the ppm quantity registered) is analysed using an Excel datasheet [61], [62].

Figure 5.1: The uncoated reactor

Figure 5.2: The coated reactor

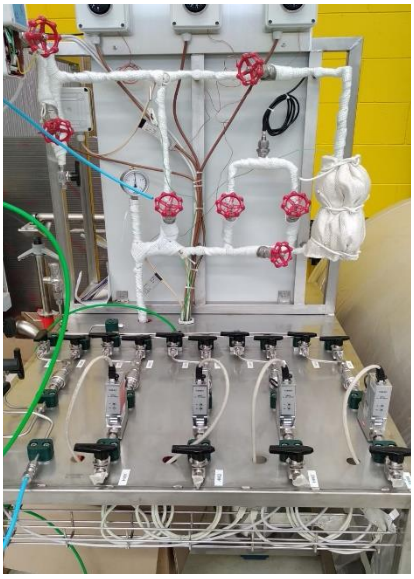

Figure 5.3: The gas station

Figure 5.4: The bubbler

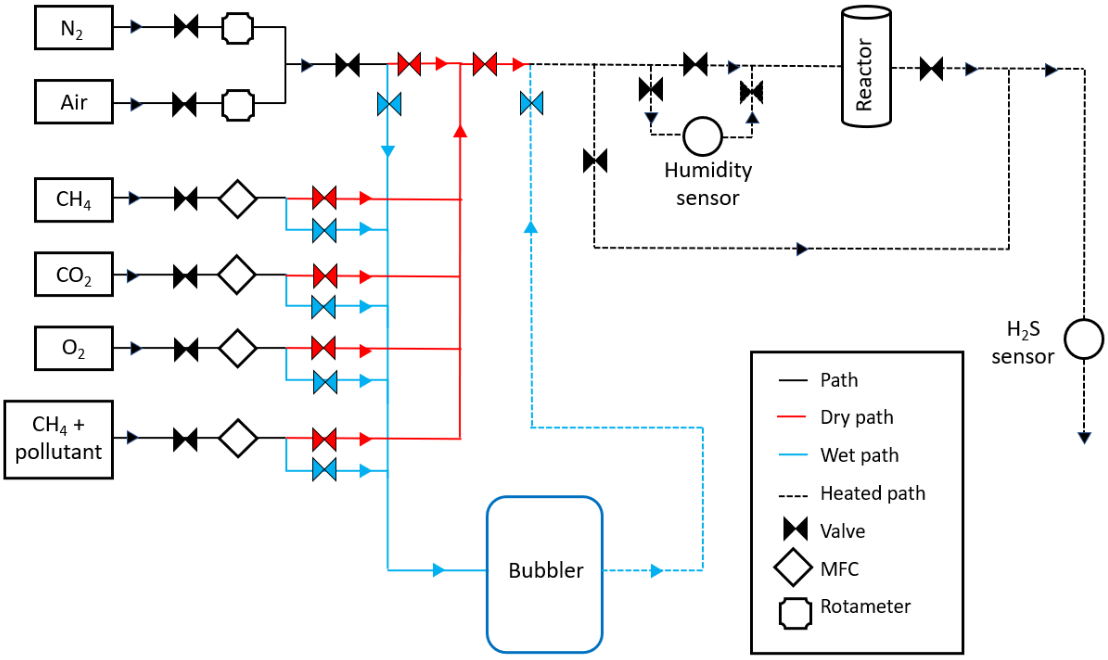

Figure 5.6: Gas station prototype schematic (personal elaboration)

5.2 Methodology

After the tests are performed, the concentration of H_2S or CH_4S in ppm is known at any time. These values are likely to be affected by instrumental errors if a spectrometer is used, generating peaks which must be eliminated, so that the graphical representation becomes clearer. To obtain a tendency indicator, the moving average method was used. By applying this procedure, the average value of 100 subsequent points was considered. The main goals of the experiment are to calculate the breakthrough point and the adsorption capacity in [$g_{H2S}/g_{adsorbent}$] or [$g_{CH4S}/g_{adsorbent}$] of the adsorbent material tested. The breakthrough point is defined as the time in which, for the first time, a value above the threshold is registered. In the Waste2Watts project, this threshold value was set as the time instant when 5 ppm of pollutant are detected as the outlet concentration value. The adsorption capacity is the quantity of adsorbate captured by the adsorbent material per unit of volume or mass.

The adsorption capacity C_{ads}, was calculated as:

$$C_{ads} = \frac{\sum G_{tot} \cdot (PPM_{inlet} - PPM_{outlet}) \cdot \Delta t}{M_{sorbent}} \cdot 100 \quad [\%] \tag{5.1}$$

Where G_{tot} is the mass flow rate, PPM_{inlet} is the inlet concentration of H_2S or CH_4S, PPM_{outlet} is the outlet concentration of H_2S or CH_4S, Δt is the time interval between two subsequent time measurements and $M_{sorbent}$ is the mass of the adsorbent material.

The cumulative of these expressions from the starting point to the breakthrough time give the adsorption capacity at breakthrough, while the cumulative from the start to the saturation give the adsorption capacity at saturation. In the next steps of this work, the adsorption capacity at breakthrough will be the parameter of greatest importance.

The total mass flow is known because it is set as an input. The concentration of H_2S or CH_4S is known as well, both at inlet and at outlet: the inlet quantity is set as an input value, while the output one is detected by the dedicated sensors. Consequently, the difference between these two values obviously gives the amount of ppm adsorbed by the material. The mass of the adsorbent material can be found using a precision balance, before putting the material inside the reactor. At this point is sufficient to apply the given formula to obtain a value of H_2S or CH_4S adsorbed in the wanted unit of measurement.

5.3 Materials' characterization

A consistent number of materials was tested in the W2W project. These are not only commercially available materials, but also innovative materials obtained directly from suppliers. The ones in which the focus is on, are the most promising tested by PoliTo, whose characteristics are briefly resumed for a better understanding of their properties.

Norit RGM-3

Norit RGM-3 is an activated carbon produced by Cabot Corporation. It is composed for more than 90% by activated carbon and for about 10% by copper carbonate and copper hydroxide. One of its main applications is the purification of liquid and gaseous substrates. It is important to store Norit RGM-3 properly, in order to avoid dust deposits on the surface, which can lead to an explosive mix. Furthermore, it is convenient to avoid contact with volatile chemical compounds and strong oxidizing agents. Unfortunately, this material is not regenerable nor biodegradable and it must be correctly disposed of at end life, because it is strongly toxic if dispersed in water [63].

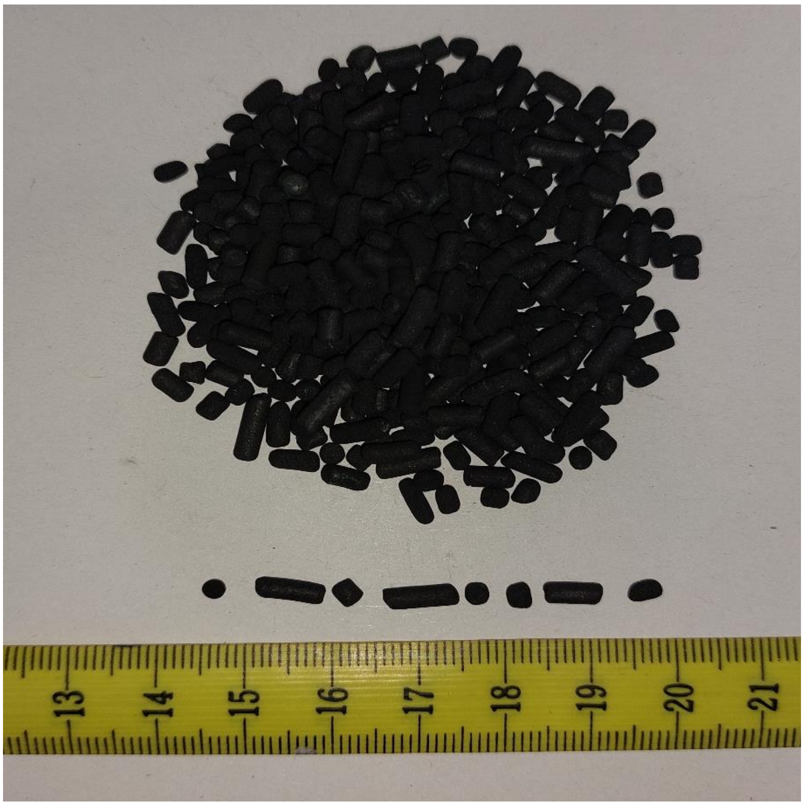

Figure 5.7: Norit RGM-3

SulfaTrap R7H and SulfaTrap R8

SulfaTrap R7 is a family of materials for the ultra-purification of biogas, made of inexpensive metal oxides and ceramic binders. They can remove to a very low concentration any organic sulphur compound, such as H_2S, sulphides and mercaptans. They can remove unwanted compounds both in dry and wet conditions: in the former case, the concentration should be better between 10 and 100 ppm_v, while in the latter fully saturated conditions are suggested. These materials are safe to handle, easy to dispose of and relatively cheap. During the experiments performed by Polito, in particular SulfaTrap R7H is used [64].

Another important family of materials is the SulfaTrap R8, which is composed of activated carbons with surface modification that allow the physical adsorption of sulphur compounds. These materials have a significant removal efficiency. The most used during the experiments of the Waste2Watt project was SulfaTrap R8C, which is particularly indicated for COS removal [65].

Figure 5.8: SulfaTrap R7H

Bio-Clean Gas Granular

Bio-Clean Gas Granular is a material produced by Biocostum S.r.l., an Italian company specialized in biogas and biomethane plant optimization. Bio-Clean Gas Granular is an iron hydroxide composed of $Fe(OH)_3$ for 98% and constituted by pellets with a dimension of 2-8 mm. It is particularly indicated for H_2S removal. Furthermore, it is not dangerous at all, so it can be stored without any specific limitation. This material is interesting because it can be fully regenerated or recycled into a digester. The regeneration can be carried on simply with the exposition at air: the sulphur compounds adsorbed by the material become indeed S_2, detaching from the pellet spontaneously. The regeneration process takes about fifteen days to be completed. Bio-Clean Gas Granular is then totally biodegradable [66].

Figure 5.9: Bio-Clean Gas Granular

Envirocarb stix

Envirocarb stix is an impregnated coal-based pellet, produced by Chemviron (Calgon Carbon Corporation). This material originated from bituminous coal and suitable binders activated with an alkaline solution which enhance the adsorption phenomena. Envirocarb stix is primarily designed to remove odour compounds and acid gases from air, but it can also efficiently remove H_2S, mercaptans, chlorine, sulphur dioxide and hydrogen chloride from a biogas stream. The pellet dimension is 4 mm of diameter and 9 mm of length: these dimensions could be good to help reduce pressure drops. It can work both in low or high relative humidity conditions and has a good durability (with better results if the water content is higher). Furthermore, it has excellent filling characteristics and can perform a rapid adsorption [67].

Figure 5.10: Envirocarb stix

Airpel Ultra D5

Airpel Ultra D5 is an extruded impregnated activated carbon produced by Desotec. It is particularly indicated for gas phase applications. Airpel Ultra D5 derives from selected grades of anthracite coal, which guarantee a high hardness, and is impregnated with specific chemicals that improve the chemisorption capacity. It has enhanced adsorption capacity for H_2S and mercaptans and a fast adsorption kinetics [68].

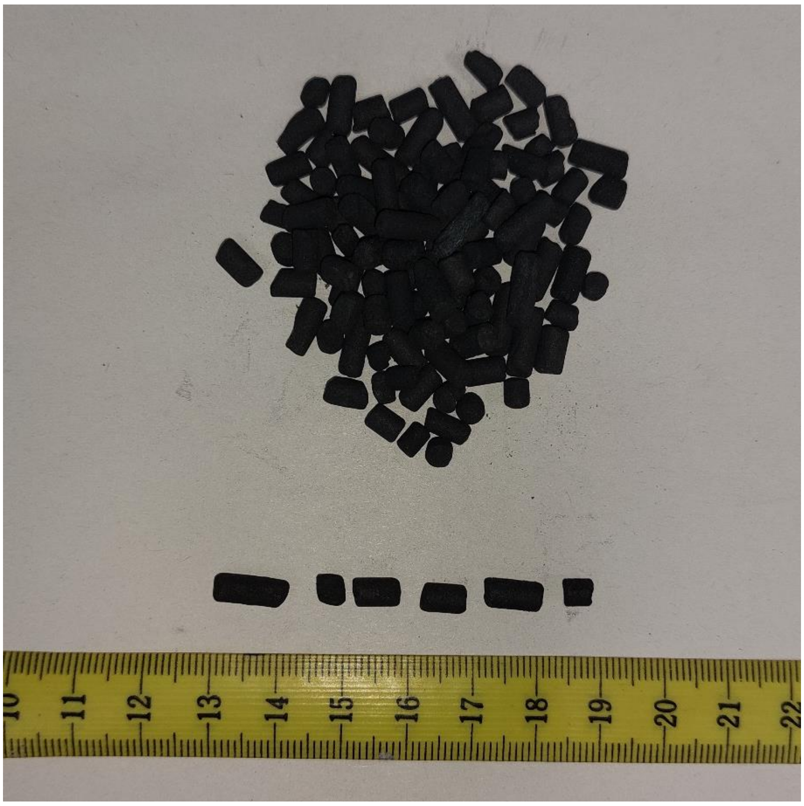

Figure 5.11: Airpel by Desotec

Some useful information about the materials were summarized in the table. The results were obtained by the tests performed by the DISAT (the Applied Science and Technology Department) at Politecnico di Torino and by ENEA.

Table 5-1: Useful information about the materials

Material	Type of material	BET surface area [m^2/g]	Average pore width [4V/A nm]	Bulk density [kg/m^3]
Norit RGM-3	Impregnated AC	1031	3	420
SulfaTrap R7H	Metal-based	30	8	920
SulfaTrap R8C	Impregnated AC	687	3	631
Bioclean Gas Granular	Metal-based	131	8	756
Envirocarb stix	Impregnated AC	622	3	536
Desotec Airpel Ultra D5	Impregnated AC	697	3	530

The BET analyses conducted by the DISAT also allow the comparison of the adsorption isotherms of each material. The investigation conducted on these curves allows to schedule the tests: it was decided to start with the materials which were expected to have the worst performances and then the ones which could possibly work better. This strategy was chosen to exploit the brief test duration in case of low performances materials, so that it was possible to increase the expertise in using the gas station prototype before starting the investigation on more promising materials, for whom tests were longer.

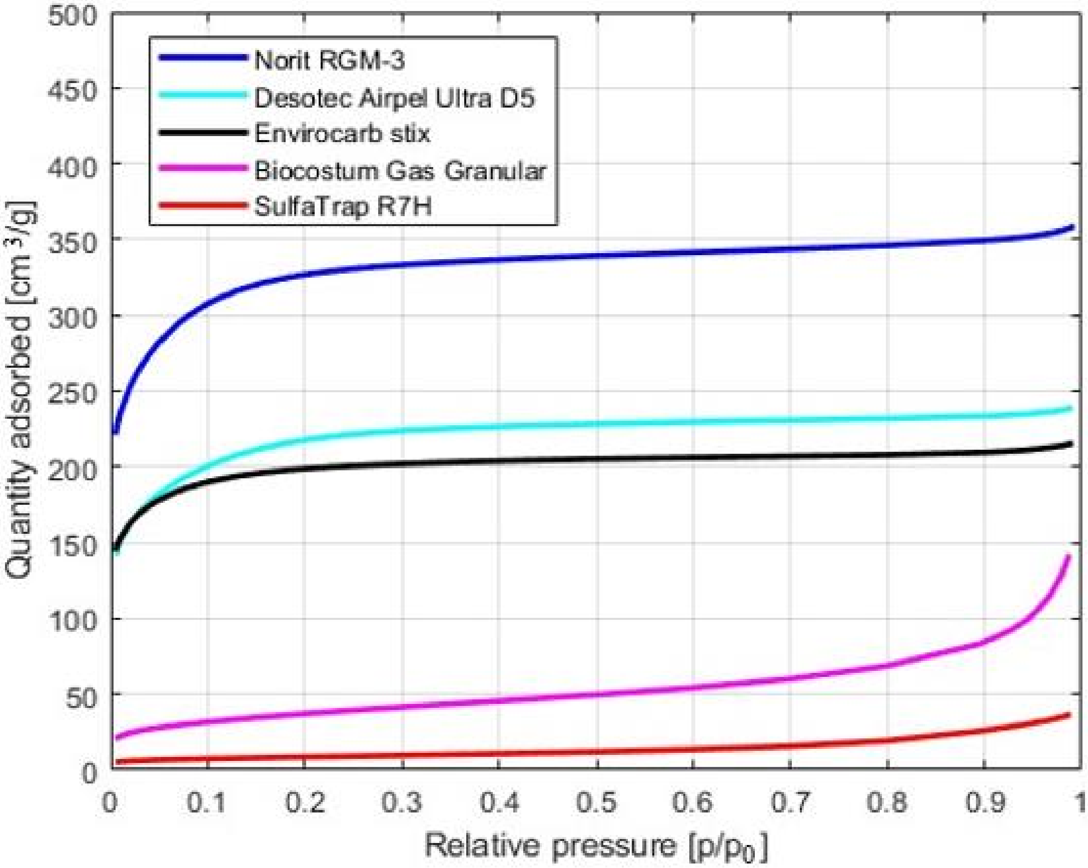

Figure 5.12: Adsorption isotherms of the considered materials

5.4 Experiments design

The tests were conducted by PoliTo for H_2S and CH_4S, while experiments on COS and DMS were conducted by ENEA and PSI respectively.

Tests on H_2S

The tests conducted by PoliTo investigated mainly Norit RGM-3, SulfaTrap R7H, BioClean Gas Granular, Envirocarb stix and Airpel Ultra D5. These adsorbents were studied relatedly to their loading capacity of hydrogen sulphide. Every test was initially performed with a biogas mixture made of methane, carbon dioxide and H_2S. Only the most promising materials were further investigated in presence of oxygen and in presence of both oxygen and water, in order to understand which are the better conditions for the process.

Some parameters were kept constant in all the experiments performed. In particular, the fixed values were:

- The initial concentration of H_2S, at 500 ppm;
- The overall mass flow rate, at 610.3 Nml/min;
- The GHSV, at 1500 h^{-1};
- The macro-composition for the tests in dry conditions, which was 50% CH_4 and 50% CO_2;
- The macro-composition for the tests in presence of oxygen, which was 50% CO_2, 0.5% O_2 and 49.5% CO_2;
- The macro-composition for the tests in wet conditions, which was 60% CH_4, 39.5% CO_2 and 0.5% O_2, with a relative humidity equal to 50%.

On H_2S concentration a post-mortem and a sensitivity analysis (250-500 and 750 ppm) were performed, using Norit RGM-3 as sorbent material.

Considering that the final target is the utilization of the purified biogas in a SOFC, the most relevant results concern the adsorption capacity at breakthrough, because a fully purified biogas during the whole operation time is the only option to avoid the fuel cell pollution. For this reason, many tests were stopped before the saturation was reached.

Tests on CH_4S

The tests conducted by PoliTo for methanethiol removal are approximately performed in the same way as the ones for hydrogen sulphide.

The parameters that were kept constant were:

- The mass flow rate, at 610.3 Nml/min;
- The GHSV at 1500 h^{-1}.

Unfortunately, the research of PoliTo on this pollutant is not at the same stage of advancements of H_2S. Results obtained are currently partial and not all the materials have been tested. This lack of data is partially minimized because at least Norit RGM-3, which appears to be promising also for the removal of the other sulphur compounds investigated, was satisfyingly tested with good results. Further research will be dedicated to the study of Norit RGM-3 in different conditions: in particular it will be relevant to understand if it's better to work in absence of water or if a certain relative humidity has a beneficial effect on the overall process. Also, SulfaTrap materials (R7H and 8C mainly) require a deeper investigation, in order to understand if they can be competitive with Norit RGM-3. The other materials were temporarily neglected due to their low performances with hydrogen sulphide, although a more complete study on them is needed as well.

Tests on COS and DMS

ENEA tests on COS [62] were performed with a GHSV= 1500 h^{-1}, an inlet concentration of COS of 30 ppm and a RH= 50%. The biogas composition was 50% CH_4 and 50% CO_2 and the temperature was 30 °C. Furthermore, a sensitivity analysis on COS concentration was conducted, considering 5, 15 and 30 ppm.

The experiments conducted by PSI on DMS [62] were instead performed with a mixture made by 55% of CH_4 and 45% CO_2 (in volume). Initially, the concentration of DMS was 100 ppm.

Chapter VI

6. Experimental investigation's results

The tests on H_2S and CH_4S removal are reported in a more extended form because they are performed by the Politecnico di Torino team. Contrariwise, for what concerns COS and DMS experiments, being performed respectively by ENEA and PSI, only the most significant results for the purposes of this work will be reported.

6.1 Results obtained for H_2S removal (PoliTo)

Results with Norit RGM-3

Norit RGM-3 was by far the most promising material for H_2S removal between the ones tested. The experiments were performed in a slightly different way depending on the conditions. The main differences regard the partial mass flow rates and the quantity of material used.

Table 6-1: Test conditions with Norit RGM-3

Test conditions	CH_4+H_2S [Nml/min]	CH_4 [Nml/min]	CO_2 [Nml/min]	O_2 [Nml/min]	Sorbent mass [g]
No Water **No Oxygen**	152.6	152.6	305.1	0.0	14.05
No Water **With Oxygen**	152.6	152.6	302.1	3.1	14.20
With Water **With Oxygen**	152.6	213.6	241.1	3.1	14.20

The test with neither water nor oxygen was conducted for about 29 h, at the end of this time it was stopped because the saturation point was reached. The test with oxygen and without water lasted for 124 h, and was stopped before the saturation point, but well after the breakthrough time. The test with water and oxygen was stopped after 116 h, shortly after it reached the breakthrough.

The test conducted with both water and oxygen is by far the one with the better performances. The presence of oxygen demonstrates to be a strong factor of increase in terms of adsorption (as also shown by the experiment with oxygen and without water), but the presence of water makes the loading capacity increase enormously. These tests clearly show how the H_2S removal using Norit RGM-3 should be conducted, if possible, in presence of both water and oxygen, which are quite common conditions in a real biogas.

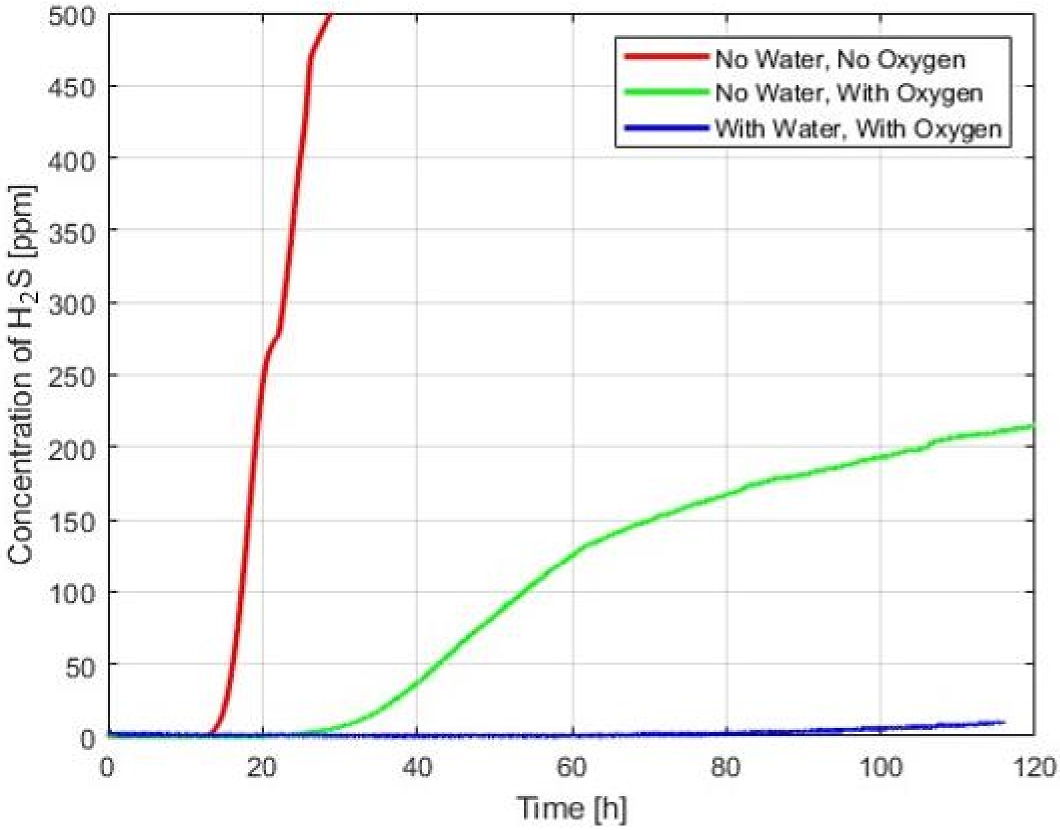

Figure 6.1: Tests on Norit RGM-3 in different conditions (500 ppm of H_2S)

The numerical results obtained are reported in the table.

Table 6-2: Test results on Norit RGM-3

Test conditions	t_{br} [h]	Adsorbed H_2S at t_{br} [%]	Adsorbed H_2S at t_{sat} [%]
No Water No Oxygen	13.83	2.74	4.16
No Water With Oxygen	28.33	5.55	-
With Water With Oxygen	94.68	18.53	-

Sensitivity analysis on H_2S concentration

Once it was understood that the best removal conditions for hydrogen sulphide are obtained if water and oxygen are present, some sensitivity analysis on the inlet concentrations were performed. Considering the theory of the adsorption phenomena, the expected result is a change in terms of adsorption capacity with a variation of the pollutant content inside the biogas. In particular, the assumed outcome is that the greater the inlet concentration, the greater the adsorption capacity.

Table 6-3: Sensitivity analysis tests conducted on Norit RGM-3

H_2S concentration [ppm]	CH_4+H_2S [Nml/min]	CH_4 [Nml/min]	CO_2 [Nml/min]	O_2 [Nml/min]	Sorbent mass [g]
250	76.3	228.9	302.1	3.1	14.20
500	152.6	213.6	241.1	3.1	14.20
750	228.9	228.9	149.5	3.1	14.20

The tests were performed considering the same mass flow (610.3 Nml/min) and GHSV (1500 h^{-1}) as previously but changing the compositions so that the relative humidity is equal to the 50% in each case. The amount of material used was kept fixed as well, at a value of 14.20 g. The inlet concentrations were respectively equal to 250, 500 and 750 ppm.

None of the tests was conducted till saturation. As expected, increasing the concentration of hydrogen sulphide at the inlet, the adsorption capacity consistently increases. On the other end, the breakthrough time is reached faster if the pollutant concentration is higher.

The numerical results obtained are reported in the table.

Table 6-4: Results of the sensitivity analysis tests conducted on Norit RGM-3

H_2S inlet concentration [ppm]	t_{br} [h]	Adsorbed H_2S at t_{br} [%]	Adsorbed H_2S at t_{sat} [%]
250	176.00	17.25	-
500	94.68	18.53	-
750	79.71	23.43	-

Norit RGM-3 post-mortem analysis

The DISAT of Politecnico di Torino performed a Scanning Electron Microscopy-Energy Dispersive Spectroscopy (SEM-EDS) analysis on Norit RGM-3 in order to evaluate its capacity to adsorb H_2S. To do so, samples in different conditions were considered:

- Blank sample of Norit RGM-3, which was used as a reference (Norit);
- Norit RGM-3 after being tested with a stream of 50% CH_4, 50% CO_2 and 500 ppm of H_2S (Norit_H_2S sample);
- Norit RGM-3 after being tested with a stream of 50% CH_4, 49.5% CO_2, 0.5% O_2 and 500 ppm of H_2S (Norit_H_2S_O_2 sample);
- Norit RGM-3 after being tested with a stream of 60% CH_4, 39.5% CO_2, 0.5% O_2, 35-40% RH and 500 ppm of H_2S (Norit_H_2S_O_2_H_2O sample).

The EDS analysis reveals a significantly increased quantity of sulphur (S) in the Norit_H_2S_O_2_H_2O. This quantity is greater than the one of the Norit_H_2S_O_2 sample. Moreover, both of them have a sulphur content bigger than the one of the Norit_H_2S

sample. All the three samples show a significantly increased anatomic percentage of S with respect to the reference one.

Table 6-5: Atomic percentage of the chemical elements contained inside Norit RGM-3 in the different conditions

Element [%]	Norit	Norit_H_2S	Norit_H_2S_O_2	Norit_H_2S_O_2_H_2O
C	43	42	34	36
O	28	22	32	20
Cu	16	18	9	9
Si	2	1	1	2
K	3	2	1	1
Ca	2	1	1	3
S	3	14	23	29

Therefore, this post-mortem analysis clearly demonstrates that Norit RGM-3 has the ability to adsorb hydrogen sulphide, in particular if it comes in contact with oxygen.

Results with SulfaTrap R7H

SulfaTrap R7H appears to be a suitable material for H_2S adsorption.

Table 6-6: Test conditions with SulfaTrap R7H

Test conditions	CH_4+H_2S [Nml/min]	CH_4 [Nml/min]	CO_2 [Nml/min]	O_2 [Nml/min]	Sorbent mass [g]
No Water No Oxygen	152.3	152.6	305.1	0.0	37.25
No Water With Oxygen	152.3	152.6	302.1	3.1	37.25
With Water With Oxygen	152.6	213.6	241.1	3.1	34.80

The test conducted without water and without oxygen lasted 124 h. The test with oxygen and without water was stopped after 91 h. The test with both water and oxygen lasted for 46 h. All the three tests were stopped before the saturation point was reached.

Contrariwise to what happened testing Norit RGM-3, in the case of SulfaTrap R7H the presence of water and oxygen appears to be significantly negative for the adsorption capacity of the material. The best conditions are obtained considering a biogas that doesn't contain water and oxygen. These two compounds are likely to be present in a real biogas, consequently in order to efficiently use SulfaTrap R7H the biogas probably needs a pre-clean step, where at least water is removed. This can be done simply using a condenser. On the other hand, the removal of O_2 could be slightly more complicated.

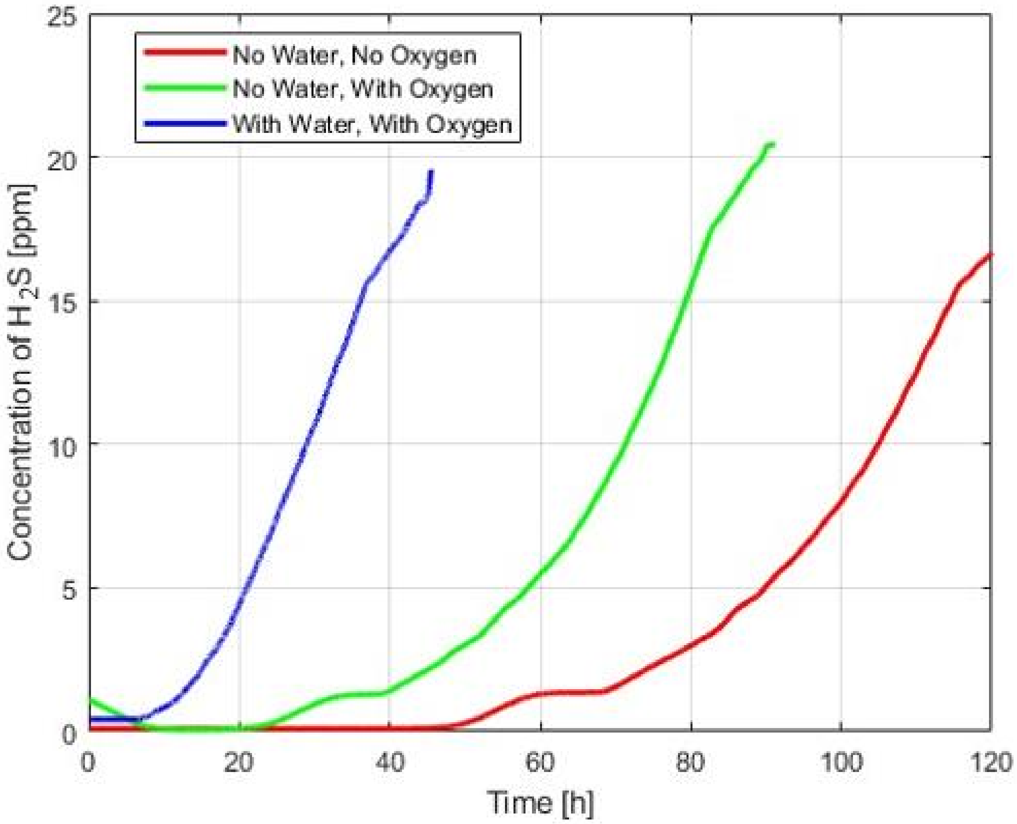

Figure 6.2: Tests on SulfaTrap R7H in different conditions (500 ppm of H_2S)

The numerical results obtained are reported in the table.

Table 6-7: Test results on SulfaTrap R7H

Test conditions	t_{br} [h]	adsorbed H_2S at t_{br} [%]	adsorbed H_2S at t_{sat} [%]
No Water **No Oxygen**	90.86	6.78	-
No Water **With Oxygen**	59.69	4.45	-
With Water **With Oxygen**	25.15	2.01	-

Results with other materials

For what concerns Desotec Airpel Ultra D5, Envirocarb and Biocostum Gas Granular, the experiments were significantly worse with respect to what obtained with Norit RGM-3 and SulfaTrap R7H. For this reason, they were only tested in absence of water and oxygen, but for this work they were not further analysed in other conditions.

Table 6-8: Test conditions with Desotec Airpel Ultra D5, Envirocarb stix 4 mm and Biocostum Gas Granular

Test conditions	CH_4+H_2S [Nml/min]	CH_4 [Nml/min]	CO_2 [Nml/min]	O_2 [Nml/min]	Sorbent mass [g]
Desotec Airpel Ultra D5	152.6	152.6	305.1	0.0	15.82
Envirocarb stix 4 mm	152.6	152.6	305.1	0.0	17.81
Biocostum Gas Granular	152.6	152.6	305.1	0.0	16.96

The test with Desotec Airpel Ultra D5 lasted for 6 h. The experiment with Envirocarb stix was stopped after 22 h. The experiment with Biocostum Gas Granular was 29 h long. All of them were stopped when the saturation point was reached.

From the results obtained, it is clear to see that the adsorption capacity of these three materials is not competitive with what tested for Norit RGM-3 and SulfaTrap R7H.

Realistically, they are not convenient for the purification goals that are the target of this work. For this reason, it was decided to temporarily focus the attention on some most promising material, postponing further studies on Desotec Airpel Ultra D5, Envirocarb stix and Biocostum Gas Granular.

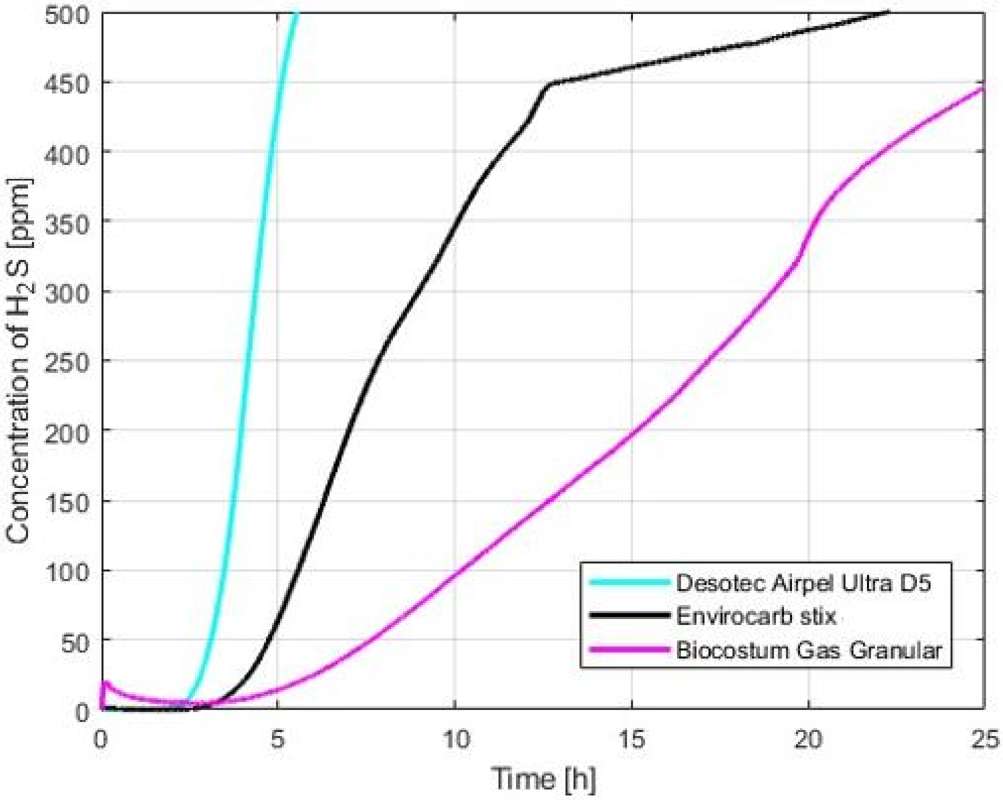

Figure 6.3: Tests on Desotec Airpel Ultra D5, Envirocarb stix and Biocostum Gas Granular (500 ppm of H_2S, no water, no oxygen)

The numerical results obtained are reported in the table.

Table 6-9: Test results on other materials

Material	t_{br} [h]	Adsorbed H_2S at t_{br} [%]	Adsorbed H_2S at t_{sat} [%]
Desotec Airpel Ultra D5	2.35	0.41	0.73
Envirocarb stix	3.19	0.50	1.37
Biocostum Gas Granular	0.02	0.00	2.71

6.2 Results obtained for CH_4S removal (PoliTo)

Results with Norit RGM-3

The first material investigated, because of its great performances in H_2S removal, was Norit RGM-3. The goal was to discover if also for methanethiol removal this component could have a significant adsorption capacity. The tests were conducted in absence of water and oxygen, but of course the further research activity will also investigate other conditions. The concentration of CH_4S was equal to 200 ppm at inlet.

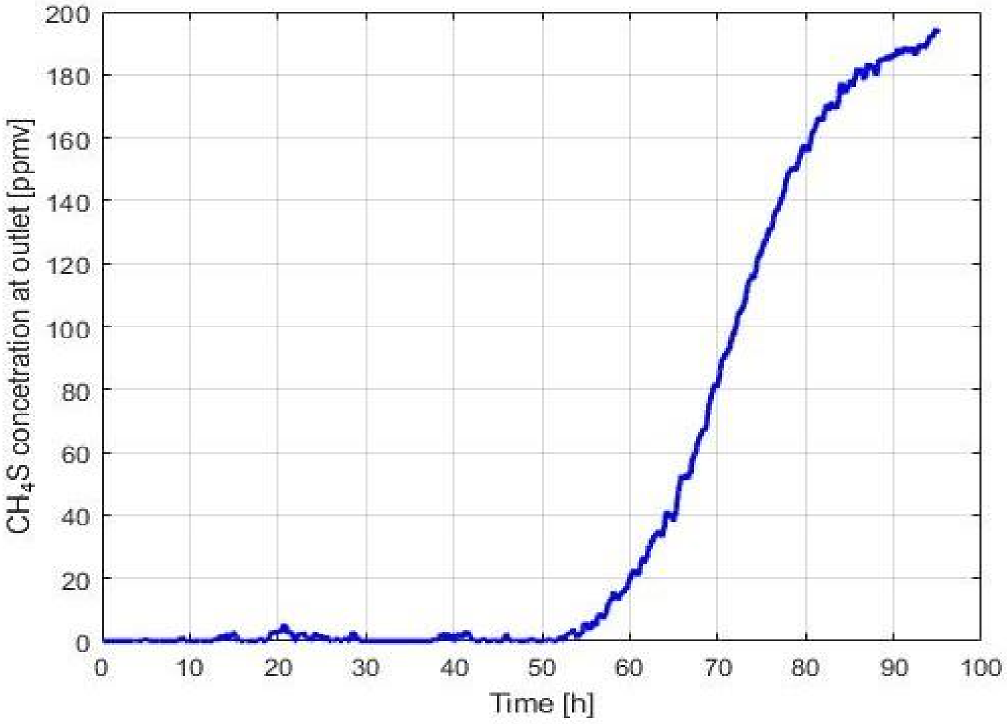

Figure 6.4:Test on Norit RGM-3 (200 ppm of CH_4S)

The adsorption capacity at breakthrough is equal to 8.33%, with a breakthrough time equal to 59.9 h. This result confirms the suitability of Norit RGM-3 also for the purification from CH_4S.

Results with Bio-Clean Gas Granular

For what concerns Bio-Clean Gas Granular, it wasn't a good material for the purification from hydrogen sulphides. Results obtained show that it is not efficient for CH_4S either. The test was conducted at 100 ppm of concentration. The adsorption capacity at breakthrough is equal to zero, while the one at saturation is 0.06%. Due to the poor results obtained, no more tests were performed on this material.

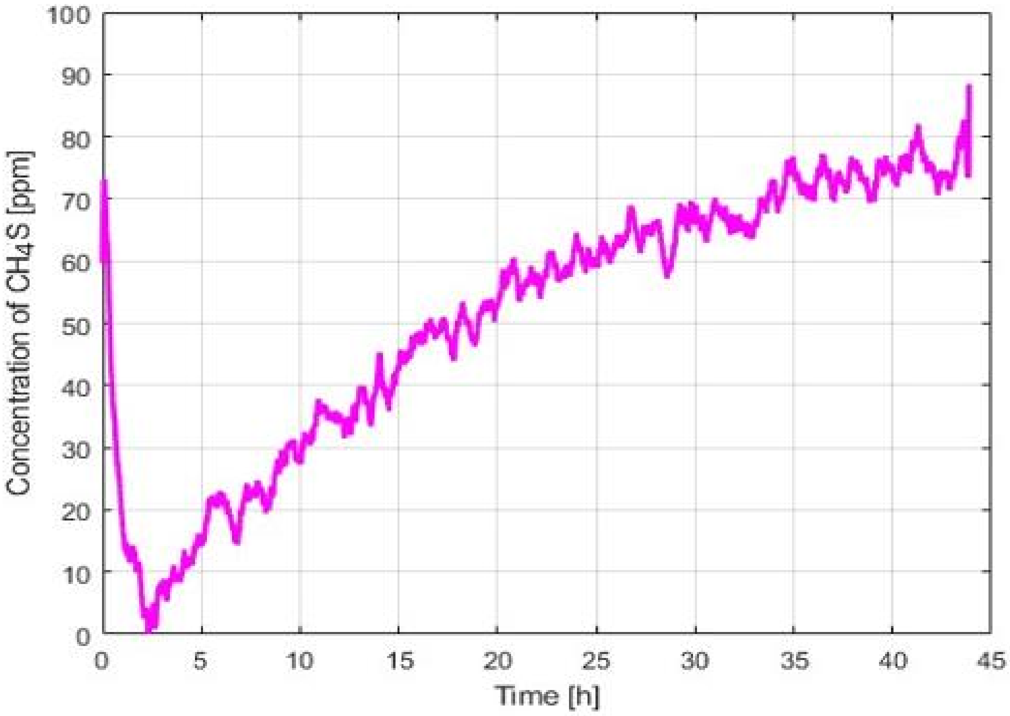

Figure 6.5: Test on Bioclean Gas Granular (100 ppm of CH_4S*)*

6.3 Results obtained for COS removal (ENEA)

ENEA experiments [62] on COS show that Sulfatrap R7H and BioClean Gas Granular are utterly inadequate for the removal of this pollutant. In fact, they appear to be completely transparent to this compound. For this reason, their adsorption capacity is approximately zero and they were eliminated from the study.

The most promising results were obtained with Norit RGM-3, even though also with this material the adsorption capacity is extremely limited. With respect to the performances of this material in removing H_2S (which reached an adsorption capacity of 18.53%), the COS removal is considerably lower (only 0.083%). This suggests that no chemical process occurs, but only weak intermolecular Van der Waals forces make adsorption possible. Eventually, also Airpel Ultra DS 6 can be considered as a possibility, but with significantly lower performances.

Norit RGM-3 was also chosen in order to perform a sensitivity analysis on the inlet COS quantity. To do so, two more tests were performed at 15 ppm and 5 ppm. All the other conditions were kept fixed. The tests show that the differences due to the initial COS concentration are consistent: the adsorption capacity of the material decreases with the decrease of COS concentration. This is probably due to the reduced interaction between sorbent and contaminant.

The results obtained are resumed in the table.

Table 6-10: COS adsorption using Norit RGM-3 [62]

Inlet concentration [ppm]	**t_{br} [h]**	**Adsorbed COS at t_{br} [%]**	**Adsorbed COS at t_{sat} [%]**
5	4.5	0.020	0.08
15	2.21	0.031	0.40
30	2.95	0.083	0.69

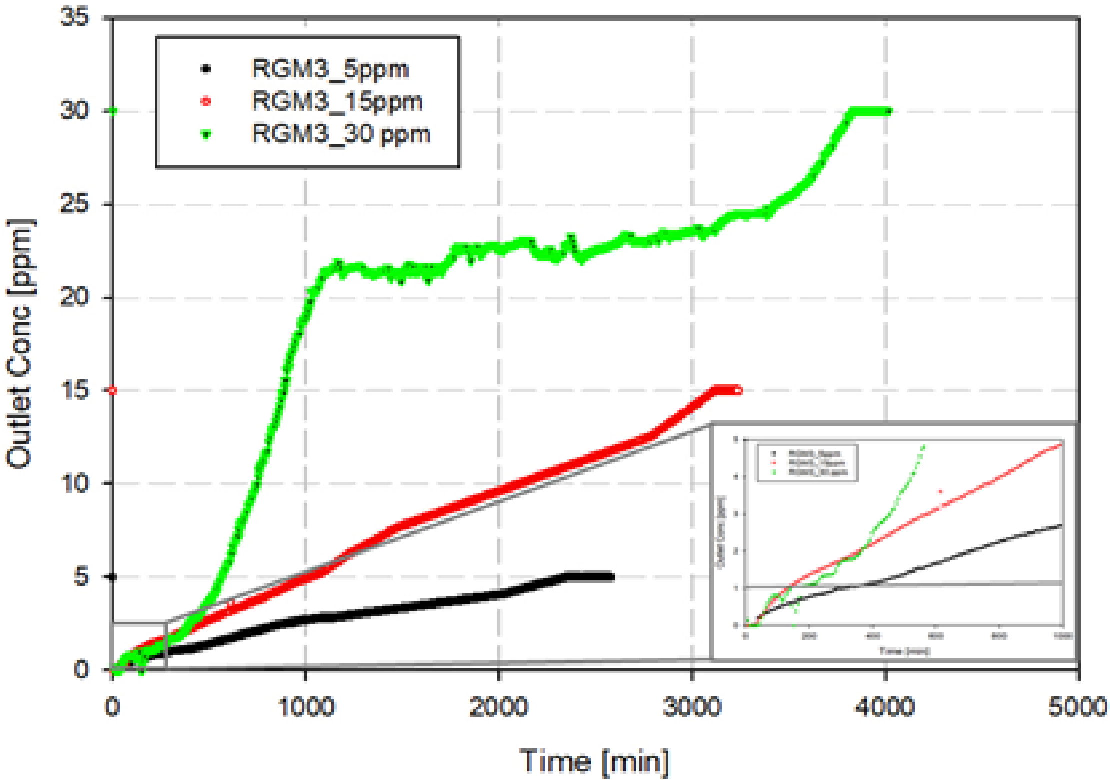

Figure 6.6: ENEA tests on COS at different inlet conditions [62]

Being the most promising between all the materials tested, Norit RGM-3 was further investigated in order to discover in which conditions it can operate better. Another test was performed, this time with a dry flow (RH=0%) and an inlet concentration of 30 ppm. All the other parameters were fixed at the conditions previously declared. The test demonstrates that adsorption capacity in absence of water significantly increases. Therefore, if possible, a dry biogas guarantees to obtain better performances.

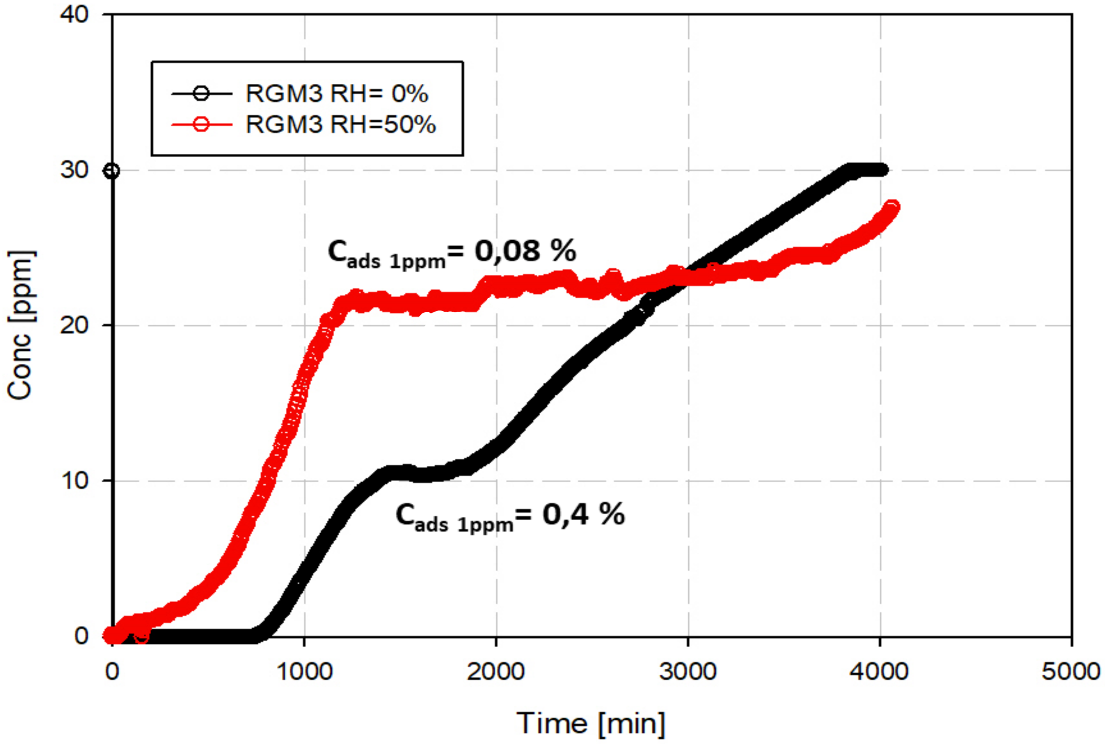

Figure 6.7: ENEA tests on COS in dry and wet conditions (30 ppm of COS) [62]

6.4 Result obtained for DMS removal (PSI)

PSI lab activity was focused on DMS removal [62]. Some of the tested materials were eliminated after a few tests due to their breakthrough time close to zero. The other materials tested, which were Norit RGM-3, SulfaTrap R8 and SulfaTrap R2, Biosorb Composite, showed nearly the same breakthrough time. In dry conditions, the most promising material appears to be SulfaTrap R2. The evolution of SulfaTrap R8 and Norit RGM-3 show quite similar behaviour, with also good performances. This is probably due to their composition, because they both are copper-based activated carbons.

After the first set of tests, other experiments were conducted in presence of water at saturation value and keeping fixed all the other conditions. The presence of water demonstrates a strong effect on all the materials. With water, Norit RGM-3 outperforms all the other materials, becoming the most suitable one. Furthermore, its breakthrough time was the one less influenced by the presence or absence of H_2O. SulfaTrap R2 performances strongly decreased with water, probably because of its zeolite structure.

Table 6-11: Performances of different materials in semi-wet conditions (4° dew point) [62]

Material	t_{br} [h]	Adsorbed DMS at t_{br} [%]	Adsorbed DMS at t_{sat} [%]
Biosorb Composite	~11	1.3	-
SulfaTrap R8	~10	1.1	-
Norit RGM-3	~10	1.4	-
SulfaTrap R2	~9	0.8	-

Table 6-12: Performances of different materials in wet conditions (20° dew point) [62]

Material	t_{br} [h]	Adsorbed DMS at t_{br} [%]	Adsorbed DMS at t_{sat} [%]
Biosorb Composite	~6.0	0.7	-
SulfaTrap R8	~2.2	0.3	-
Norit RGM-3	~9.0	1.1	-
SulfaTrap R2	~0.5	0.2	-

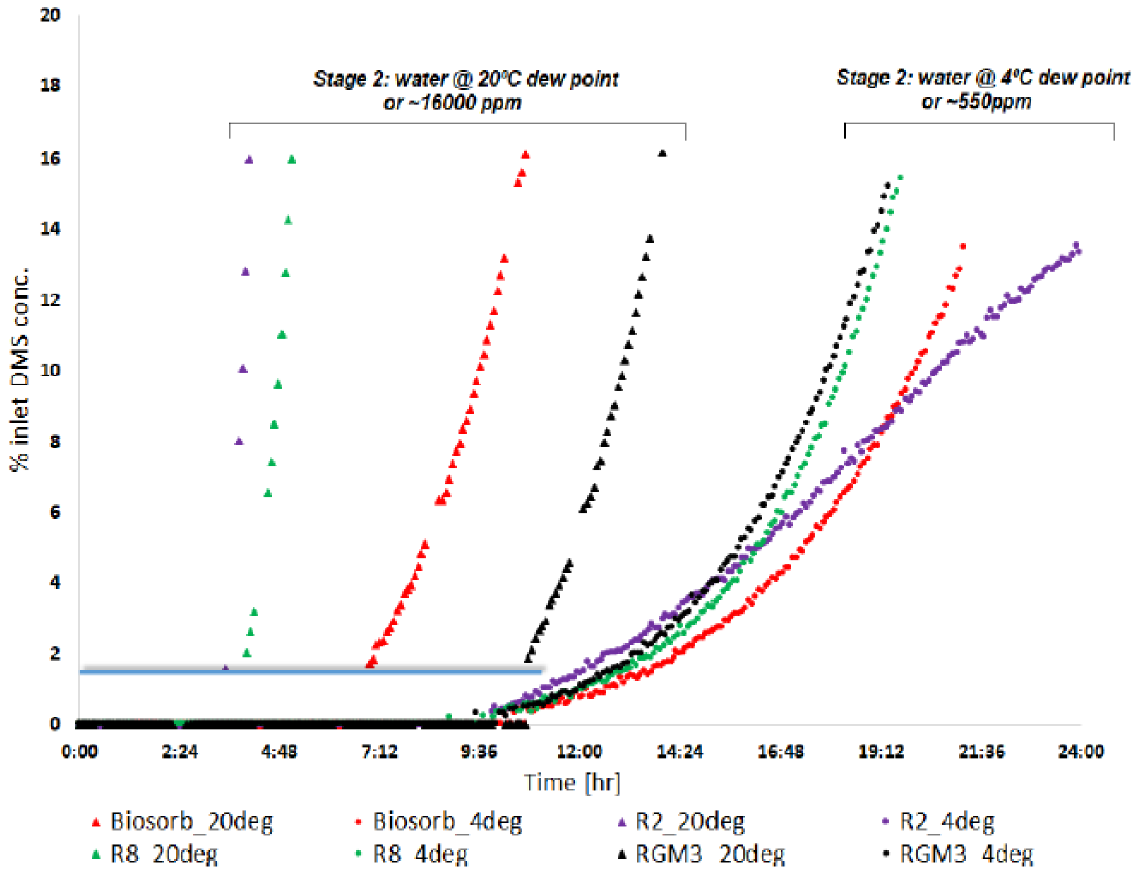

Figure 6.8: Breakthrough curves obtained for different materials (semi-wet and wet conditions, 100 ppm DMS) [62]

Chapter VII

7. Techno-economic analysis of a multicomponent model

In a real case scenario, biogas purification processes are much more complicated with respect to what is tested in a laboratory. The greatest part of the experiments conducted during the Waste2Watts project regards a synthetic biogas which contains only one pollutant at a time. This is useful to investigate accurately the effect of an adsorbent material on a specific compound because the adsorption potential of a single material can abruptly change based on the component that it has to remove. Moreover, the adsorption efficiency can be influenced also by the presence of oxygen and/or water in the mixture, with different effects depending on the compound.

The problem of this approach is that inside a real biogas there is not a single pollutant, but many of them at the same time. The scope of this part of the work is to propose a multicomponent adsorption model, which considers both technical and economic aspects, based on the tests performed by PoliTo, ENEA and PSI. The multicomponent adsorption model will consider the four compounds studied by these three research teams: H_2S, CH_4S, COS and DMS. This model can anyhow be extended to other chemical species if data on these compounds becomes available.

The goal is to calculate not only the amount of adsorbent material needed for the purification, but also to perform an economic evaluation of the overall process. It was supposed that the purified biogas is used to power a Solid Oxide Fuel Cell (SOFC), whose energy produced can be sold or auto consumed. To verify the economic feasibility some economic indicators will be considered.

7.1 System configurations

The starting point of the techno-economic model is a schematisation of a plant whose purpose is the purification of the raw biogas inside a dedicated reactor, and subsequently its use inside a SOFC to produce energy.

To do so, the simplest way is to consider a single vessel, in which the raw biogas is cleaned using an adsorbent material. At this point, the purified biogas is directly used to fuel the SOFC. This plant is cheap because it needs only one component but is not optimised from the energetic point of view: it removes all the sulphur compounds in presence of water and oxygen because the biogas is not treated in any way.

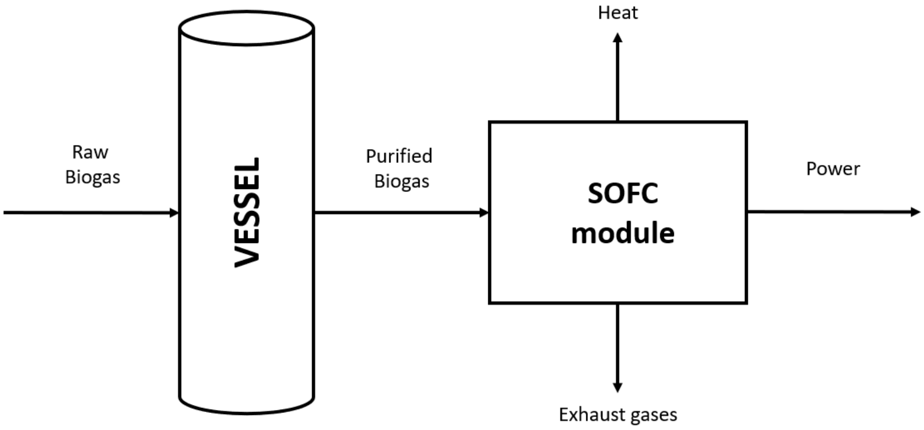

Figure 7.1: Purification with only one vessel (personal elaboration)

Another approach is also possible. From the experimental tests it is in fact known that the adsorption capacity of a material can abruptly change if water is present or not. For some pollutants, H_2O has a beneficial effect, while others can experience a better removal if water is not present. To optimise the adsorbent material utilisation, and consequently to reduce the costs connected to the material purchase, it is then possible to consider the presence of 2 different vessels. On the other hand, a plant of this kind has higher investment costs. In the first vessel, the biogas contains an amount of water while the pollutants are removed, while in the second one a purification in absence of water is carried on. To obtain an adsorption with no water, a condenser is put between the first and the second vessel. The volume of the two vessels is again obtained as the sum of the amounts of material needed for the purification with and without water.

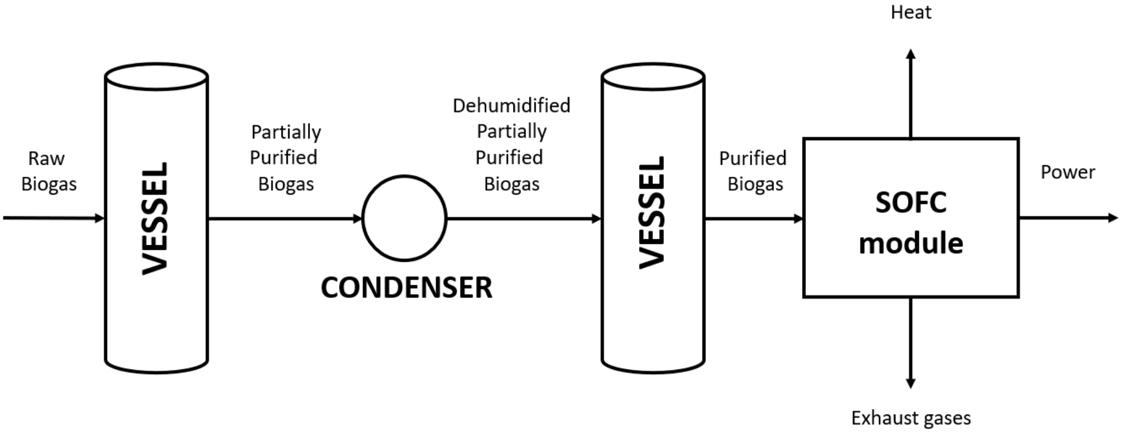

Figure 7.2: Purification process with 2 vessels and a condenser (personal elaboration)

Possibly, a third option can be considered. Assuming that the adsorbent material of interest guarantees a good adsorption for the pollutants in absence of water, a model composed by a condenser before a vessel can be proposed. In a plant of this kind, the raw biogas is dehumidified, and then cleaned. This option is cheaper than the one with two vessels, but on the other hand it is not convenient with respect to the option with only one vessel.

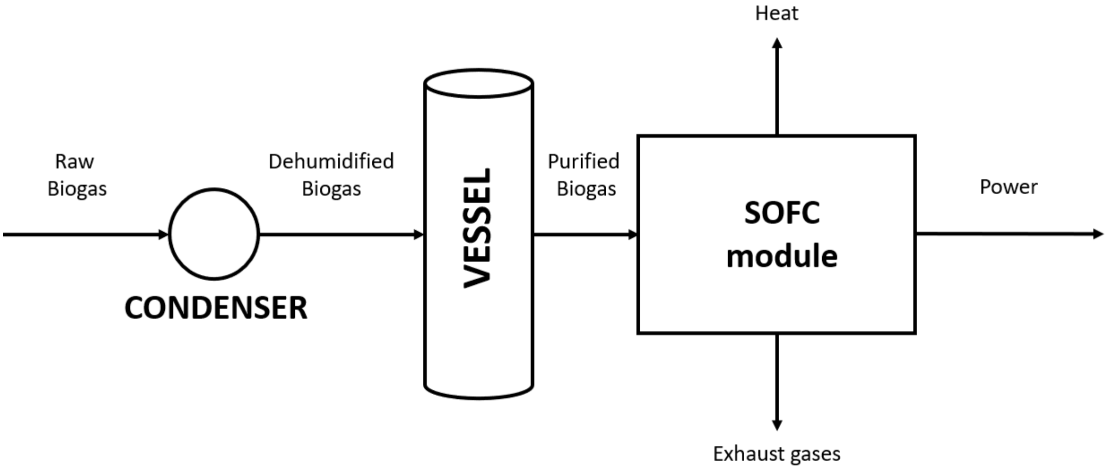

Figure 7.3: Purification process with a condenser and 1 vessel (personal elaboration)

7.2 Vessel sizing

Once the plant options are defined, the process needs the calculation of the amount of adsorbent material needed for the biogas purification. The purification process takes place in dedicated vessel(s), which must be dimensioned according to the quantity of sorbent needed.

The proposed model considers the biogas composition as known. The main components of the mixture are methane, carbon dioxide, oxygen, nitrogen and water. The percentage of CH_4 and CO_2 are the most relevant, while there is only a little amount of O_2 and N_2. The quantity of water is well under the saturation limit. The percentage of methane is particularly relevant, because it is used to calculate the Lower Heating Value (LHV) of the mixture, and consequently the inlet flow.

The biogas also contains pollutants, in variable quantities (expressed in ppm) which were assumed to be known. The amount of these compounds can be realistically set starting from values obtained for real biogas. The compounds of interest for the model are H_2S, DMS, COS and CH_4S.

The loading capacity of the material with respect to the specific pollutant that is necessary to remove is the most important parameter that is necessary to know. Its value depends not only on the kind of component, but also on its quantity in the mixture and on the conditions in which the adsorption is conducted. It is particularly difficult to set proper values for this parameter in a multicomponent case.

The proposed methodology considers the adsorption capacity of each pollutant as it was the only one inside the biogas. The adsorption capacity numerical value is considered equal to the one at breakthrough: that’s because the outcoming biogas must contain as little as possible impurities. With this assumption it is possible to exploit the data obtained during the experimental activity dedicated to mono components. Clearly, the biggest limit of this kind of hypothesis is that it doesn’t consider the chemical interaction between the different pollutants.

The adsorbent material density is known from the analysis performed by the DISAT department of Politecnico di Torino and by ENEA. The purified biogas powers a SOFC, for which the efficiency, capacity factor and electric power are assumed as known.

At this point, some fundamental parameters can be calculated.

The inlet flow (Q_{in}) of biogas can be obtained as:

$$Q_{in} = \frac{Wel_{SOFC}}{LHV \cdot \eta_{SOFC}} \quad [\frac{Nm^3}{h}] \tag{7.1}$$

Where Wel_{SOFC} is the electric power of the SOFC, LHV is the lower heating value of the biogas and η_{SOFC} is the efficiency of the SOFC.

The concentration of each pollutant is given by:

$$CC_{pollutant} = \frac{PPM_{pollutant} \cdot MW_{pollutant}}{22.4} \quad [\frac{g}{Nm^3}] \tag{7.2}$$

Where $PPM_{pollutant}$ is the amount of pollutant inside the mixture, $MW_{pollutant}$ is the molar weight of the pollutant and 22.4 is the number of litres that contains a mole of gas.

The flow rate of each pollutant can then be obtained as:

$$Q_{pollutant} = Q_{in} \cdot CC_{pollutant} \quad [\frac{g}{h}] \tag{7.3}$$

The mass of contaminant which is removed strongly depends on the breakthrough time BT:

$$M_{pollutant} = Q_{pollutant} \cdot BT \quad [g] \tag{7.4}$$

Then, the mass of sorbent needed for the removal can be found as:

$$M_{sorbent} = M_{pollutant} \cdot LC_{pollutant} \quad [g] \tag{7.5}$$

Where $LC_{pollutant}$ is the loading capacity of the adsorbent material with respect to the considered pollutant.

This value can be easily converted into a volume, because the density of the material ($\rho_{sorbent}$) is known:

$$V_{sorbent} = \frac{M_{sorbent}}{\rho_{sorbent}} \quad [m^3] \tag{7.6}$$

The procedure described exploits the data obtained experimentally for the monocomponent case. To extend this model to the multicomponent case it was assumed that the total quantity of sorbent needed for the multicomponent case is equal to the sum of the amounts necessary in the monocomponent ones. By this way, the quantity of material needed is probably overestimated, making the hypothesis strongly conservative. This translates to:

$$V_{total} = V_{H_2S} + V_{DMS} + V_{COS} + V_{CH_4S} \quad [m^3] \tag{7.7}$$

Where V_{H2S}, V_{DMS}, V_{COS} and V_{CH4S} are the sorbent volumes calculated individually with the procedure previously described.

Once the overall volume of sorbent needed is known, it is possible to suppose that the adsorption process takes place in a vessel with exactly that volume. Consequently:

$$V_{vessel} = V_{total} \quad [m^3] \tag{7.8}$$

The vessel is supposed to have a cylindrical shape, whose dimensions are set in such a way that the ratio between length and diameter is equal to 3, so that the formation of preferential pathways is avoided. To do so, also a sufficient superficial gas velocity must be guaranteed.

Then, the area of the vessel will be:

$$A = \frac{Q_{in}}{SGV} \quad [m^2] \tag{7.9}$$

Where SGV is the superficial gas velocity.

The diameter of the vessel consequently is:

$$D = \sqrt{\frac{4 \cdot A}{\pi}} \quad [m] \tag{7.10}$$

And the length of the vessel is:

$$L = \frac{V_{vessel}}{A} \quad [m] \tag{7.11}$$

7.3 Purchased equipment costs

Economically, clearly buying only one vessel costs much less than buying more components. Consequently, the one vessel option guarantees to reduce the initial investment cost. On the other hand, the option with two vessels and a condenser represents an optimised process, which reduces the amount of adsorbent material needed for the operations of purification. This translates into the possibility to reduce the costs related to the adsorbent material purchase during the life of the plant. The two options have both pros and cons and will be analysed so that the best option will be discovered. The plant with a condenser and a vessel is halfway from the point of view of costs, while it is difficult to determine in advance if it can be more efficient than the others energetically.

To calculate the costs of the vessels and the condenser, Turton cost functions were applied [69] . The costs obtained (C_{BEC}) from the literature refers to the period between May and September 2001. A simple proportion can be applied to convert the cost into an actualized value, that takes into account the inflation. To do so, the Chemical Engineering Plant Cost Index (CEPCI) values in 2001 and 2022 must be considered. The formulation will be:

$$C_{BEC}(2022) = C_{BEC}(2001) \cdot \frac{CEPCI(2022)}{CEPCI(2001)} \tag{7.12}$$

In general, the purchase cost of an equipment can be calculated as:

$$C_{BEC} = C_p^0 \cdot F_P \cdot F_M \quad [€] \tag{7.13}$$

C_p^0 is the purchased costs of an equipment made of carbon steel and operating at ambient pressure. Its value fits the following equation:

$$C_p^0 = 10^{(K_1 + K_2 \log_{10} A + K_3 (\log_{10} A)^2)} \quad [€] \tag{7.14}$$

Where the values for K_1, K_2 and K_3 can be obtained from dedicated tables, while A is the capacity or size parameter for the equipment considered. The correlation between K_1, K_2, K_3 and A is only true in a certain range of the A parameter.

For what concerns the vessels, the size parameter is the volume, whose value is calculated with the procedure previously described. For the condenser, the size parameter is the area. To obtain its value, the following steps can be followed.

The mass flow of biogas was previously calculated, while it is possible to assume for the biogas a temperature (approximately ambient temperature) at the inlet of the condenser and a lower temperature at the outlet. The heat flux exchanged is then given by:

$$\Phi = G_{biogas} \cdot cp \cdot \left(T_{outlet,biogas} - T_{inlet,biogas}\right) \quad [kW] \tag{7.15}$$

Where G_{biogas} is the biogas mass flow, and cp is calculated considering the composition of the biogas, which is made of methane, carbon dioxide, oxygen and nitrogen:

$$cp = cp_{CH_4} \cdot \%CH_4 + cp_{CO_2} \cdot \%CO_2 + cp_{O_2} \cdot \%O_2 + cp_{N_2} \cdot \%N_2 \quad [\frac{kJ}{kgK}] \tag{7.16}$$

The cold stream is represented by water, which inlet and outlet temperatures can be assumed as well. The heat exchange is between a gas and water, as a consequence it is possible to set a realistic value for the heat transfer coefficient (U) from literature.

$$A = \frac{\Phi}{\Delta T_{ml} \cdot U} \quad [m^2] \tag{7.17}$$

Where:

$$\Delta T_{ml} = \frac{\Delta T_1 - \Delta T_2}{ln\left(\frac{\Delta T_1}{\Delta T_2}\right)} \quad [°C] \tag{7.18}$$

With $\Delta T_1 = T_{inlet,biogas} - T_{outlet,water}$ and $\Delta T_2 = T_{outlet,biogas} - T_{inlet,water}$.

Considering that, as calculated, the mass flow of biogas stays constant, so does the area of the condenser.

The cost of an equipment increases with the increase of its operating pressure. The effect of pressure on costs is considered by the pressure factor F_p, which can be calculated as follow:

$$F_P = 10^{(C_1 + C_2 \log_{10} P + C_3 (\log_{10} P)^2)} \quad [-] \tag{7.19}$$

Where the values for C_1, C_2 and C_3 can be obtained from dedicated tables, while P is the pressure.

The cost of the equipment also changes depending on the material used for its construction. The material factor F_m covers the differences between the costs of different materials. Its value can again be obtained from proper tables.

At the end of this procedure the clean-up system cost is known. The cost of the condenser, if the inlet flow is assumed constant, is constant as well. The vessel's purchase cost varies instead with the volume.

7.4 Main costs and revenues

To run an energy plant, different kinds of costs must be considered.

First of all, there are the costs related to the process equipment, the supporting facilities and the direct and indirect labour. The main contributions to this portion of costs, named BEC (Bare Erected Cost) are in this project:

- The SOFC, which purchase price directly depends on its electric power;
- The infrastructures;
- The electrical and control system;
- The clean-up system for the biogas.

At this point, it's necessary to take into account all the costs related to EPC contractor services. Adding these costs, the engineering, procurement and construction management (EPCM) costs are considered. Then, all the unknown costs that can be unforeseen or omitted due to lack of experience on a project must be estimated. To do so, all the process and project contingencies must be summed up to the EPCM value, so that the Total Plant

Cost (TPC) is obtained. The last factors that affect the price are related to the pre-production costs, the inventory capital, the financing cost and other owner's costs. Adding these values to TPC, the Total Overnight Cost (TOC) is obtained [70].

Another significant cost is related to all the expenses that occur during the operation and maintenance of the system and is called OpEx (Operational Expenditure). The main contribution to OpEx are:

- The substitution of the reformer catalyst;
- The substitution of the SOFC stack;
- The labour cost;
- The general maintenance;
- The substitution of the clean-up adsorbent.

The costs related to the clean-up of the system are the main goal of this part of the work, so they will be investigated with particular attention in a dedicated part of this work.

It is also possible to analyse the revenues of this kind of system. They are divided in two main categories: incomes and savings. Incomes depend on the earning from the electric energy produced which is sold to the national grid. The value for which it is possible to sell the produced electricity can depend on specific incentives. In Italy, a minimum guaranteed price is defined for the electric energy produced from any kind of renewable source. The savings represents instead the cost reduction of electric bills for the user of the system. All the energy which is not purchased from the national grid but auto consumed represents an advantage in terms of expense reduction for the owner of the plant. A single prosumer can freely decide to sell or auto consume the electricity produced, in the percentages that are more convenient for its specific situation.

7.5 Cash flows analysis

A cash flow analysis is fundamental to understand if this kind of business is sustainable from an economic point of view.

Considering the capacity factor of the SOFC (CF_{SOFC}) it is possible to simply calculate the operating hours of the plant in the amount of time (t) of interest:

$$Operating\ Hours = CF_{SOFC} \cdot t \tag{7.20}$$

The cash flow (CF) is simply obtained as:

$$CF = R - C \tag{7.21}$$

Where R are the revenues and C are the costs.

But it is fundamental to underline that money doesn't have the same value when the years go by, due to inflation. To consider these phenomena, a discounting factor (DF) must be considered:

$$DF = (1 + WACC)^n \tag{7.22}$$

Where WACC is the Weighted Average Cost of Capital, the average rate that a business pays to finance its assets. The figure n stands for the number of the year considered (after the investment).

It is possible to calculate the Net Present Value (NPV) of the investment as:

$$NPV = \sum_{n=1}^{N} \frac{CF}{(1 + WACC)^n} - TOC \tag{7.23}$$

Where N is the expected lifetime of the plant. In this formulation the TOC is assumed as totally occurring at the very beginning of the project (year 0). The only exception is related with the stack substitution, which is performed every 3-10 years. The highest the NPV value, the better the investment is. If the choice is between two different projects, the one with the highest NPV value is the one which is more convenient to realise.

Once the NPV is known, it is possible to find the PayBack Time (PBT), which is the first year for which the investment has paid itself.

$$PTB = 1 + n_y - \frac{n}{p} \tag{7.24}$$

Where n_y is the number of the year where the last negative cumulative cash flow occurs, n is the value of the last negative cumulative cash flow and p is the value of the first positive cash flow.

If the PBT is not reached during the lifetime of the project, that means the investment is not convenient economically.

It is also possible to consider the Internal Rate of Return (IRR), which is the value of a parameter (r) that makes the NPV value 0 at the end life of the plant, according to the following formulation:

$$NPV = \sum_{n=1}^{N} \frac{CF}{(1+r)^n} - TOC = 0 \tag{7.25}$$

The higher the value of r is, the better the investment. Exactly as said for the NPV, the projects with the highest IRR are the ones which are economically more convenient to realise. If the value of r is lower than the one of WACC, the investment is not economically convenient.

The average profitability of the investment per unit of invested capital can be calculated using the Benefit Cost Ratio (BCR):

$$BCR = \frac{\sum_{n=1}^{N} \frac{CF}{(1+WACC)^n}}{TOC} \tag{7.26}$$

Again, the higher the BCR value is, the better the investment is. A value smaller than 1 means the investment is not convenient economically.

The last economic indicator that can be useful to consider is the Levelized Cost of Electricity (LCOE), which can be calculated as:

$$LCOE = \frac{TOC_n + \sum_{n=1}^{N} \frac{OpEx_n}{(1+WACC)^n}}{\sum_{n=1}^{N} \frac{E_t}{(1+WACC)^n}} \tag{7.27}$$

Where E_t is the electricity generation [71].

Chapter VIII

8. Numerical assumptions for the techno-economic model

To compare different economic scenarios, it is possible to set some input quantities as a starting point. It was assumed to use Norit RGM-3 as sorbent material because it is the only one that guarantees good performance in the removal of all the sulphur compounds.

8.1 Assumptions for the biogas composition

Considering that Waste2Watts project is dedicated to biogas produced from agricultural wastes, it seemed reasonable to investigate the average compositions of a biogas coming from such a source. The literature on biogas compositions produced in real conditions is currently limited. A satisfying overview is provided by Calbry-Muzyka et al. [72] who visited different plants for sampling campaigns. Their results show that the sites investigated produced a biogas with a CH_4 content of 53-58% in volume. Despite the different origins of the substrate the methane content appears to be in a limited range. The same is true for CO_2, which content is in a range between 39 and 44% in all the sites investigated. Nitrogen amount is instead more variable, going from 1 to 5%. Oxygen percentage is low and its registered value is always below 1%. Generally, biogas is saturated with moisture at the temperature in which the anaerobic digestion is performed. The quantity of H_2S is also pretty variable, with values that go from only 7 ppm to even 6570 if the biogas is produced from agricultural wastes. Data on other trace compounds are unfortunately much more difficult to detect because they would require a dedicated sampling and an off-line measurement campaign.

It's clear to notice that the possibilities in terms of composition are relatively broad, this translates to the need of biogas removal techniques that can take into account significant site-to-site differences. In particular, the techno-economic multicomponent model is affected by the methane content, which determines the Lower Heating Value and consequently the inlet flow needed. Anyhow, an advantage of fuel cells is that they demonstrate to be capable of working with different concentrations of CH_4, still keeping acceptable values of efficiency [72].

In order to simplify the model, it was decided to keep the biogas composition constant in all the scenarios considered, in order to better focus on the purification aspects in equal biogas conditions. Average values were considered.

Table 8-1: Biogas assumed composition

	Biogas composition [wt%]
CH_4	55.9%
CO_2	41.3%
O_2	0.5%
N_2	2.3%
H_2O	Saturation quantity (at AD temperature)

8.2 Choice of the SOFC

Some proper assumptions were made for the Solid Oxide Fuel Cell as well. Electric power was assumed in order to produce enough electric power to guarantee significant revenues, while suitable values for efficiency and capacity factor were obtained from literature [73].

Table 8-2: SOFC main characteristics

Efficiency [%]	55
Capacity factor [%]	95
Electric Power [kW_{el}]	50

8.3 Evaluations on the adsorption capacity

The techno-economic investigation considers Norit RGM-3 as sorbent material, due to its great performances with all the sulphur compounds considered. Being also relatively cheap, is clearly one of the best choices to carry on a purification process.

Table 8-3: Resume of Norit RGM-3 adsorption capacities obtained from the experimental campaign

	Concentration [ppm]	**With water**	**No water**
H_2S	500	18.53%	5.55%
DMS	100	1.10%	1.40%
COS	30	0.083%	0.40%
CH_4S	200	No data	8.33%

For what concerns H_2S quantity, the inlet concentration tested is realistic if a real biogas is considered. Consequently, a fixed concentration inside the biogas of 500 ppm of H_2S was assumed. On the other hand, DMS, COS and CH_4S values are too high to be reasonable. The main reason is that the laboratory instrumentation used is not sensitive enough to obtain reliable results if the inlet concentration is too low.

To obtain a realistic techno-economic model, it makes sense to reduce the values related to DMS, COS and CH_4S. A value of 1 ppm was consequently chosen for each of them [22].

Theoretically, the adsorption capacity is supposed to experience a reduction if the inlet concentration of the pollutant of interest decreases. As a consequence, it is not possible to directly use the data obtained as a result if the inlet concentration is different.

COS adsorption capacity

For what concerns COS, the approach chosen is relatively easy in case of wet conditions, thanks to the sensitivities analysis performed by ENEA at a concentration of 5, 15 and 30 ppm using Norit RGM-3. The experimental results obtained allow to create a function that can predict the adsorption capacity at not tested concentration values, with a certain accuracy.

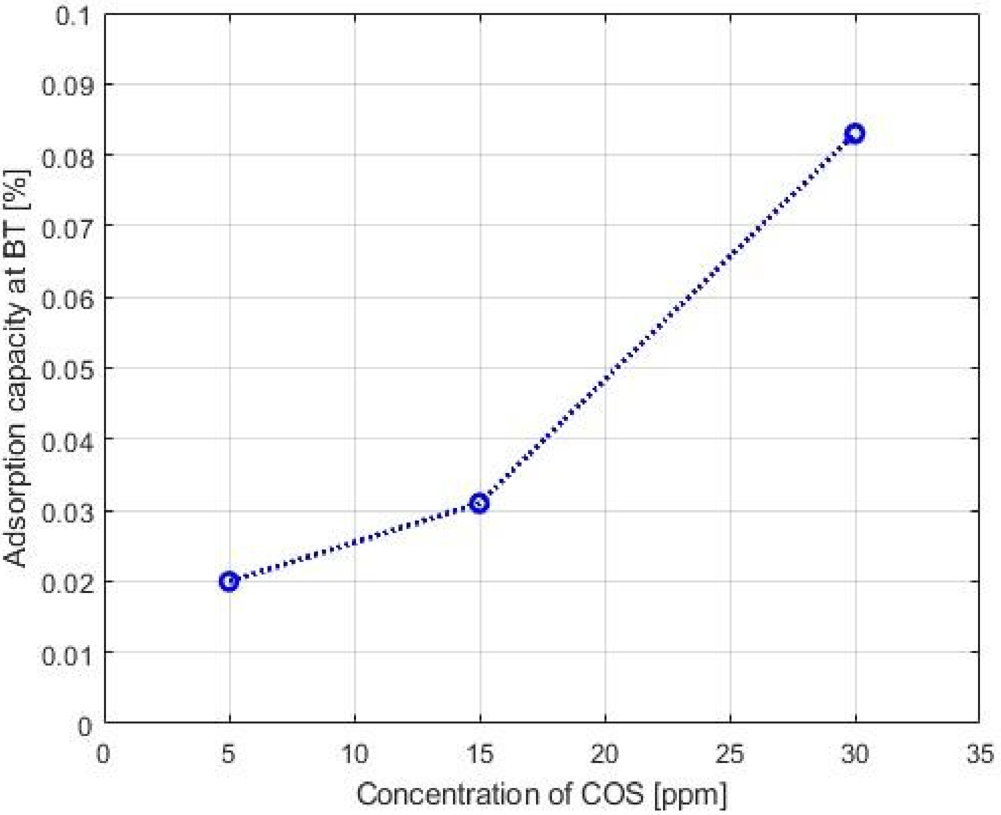

Figure 8.1: Tested adsorption capacity of Norit RGM-3 on COS removal at different concentrations

Fitting these values with a polynomial, the expression obtained is:

$$AC_{COS,wet} = 0.0001 \cdot CC_{COS}^{2} - 0.0008 \cdot CC_{COS} + 0.0216 \tag{8.1}$$

Where AC_{COS} is the adsorption capacity of Norit RGM-3 and CC_{COS} is the concentration of COS inside the biogas.

This equation can be used to find a reasonable value of adsorption capacity at 1 ppm, even though this value wasn’t tested in the experimental campaign. Performing the calculation, the result obtained is an adsorption capacity equal to 0.021% for 1 ppm.

In dry conditions it was assumed to consider the same curve, shifted so that it fits the data obtained in wet conditions (30 ppm and adsorption capacity of 0.4%). The equation consequently is:

$$AC_{COS,dry} = 0.0001 \cdot CC_{COS}^2 - 0.0008 \cdot CC_{COS} + 0.334 \tag{8.2}$$

Applying it, for 1 ppm of COS the adsorption capacity of Norit RGM-3 is 0.33%.

DMS and CH_4S adsorption capacity

For DMS and CH_4S, the situation is much more complicated, due to the lack of data available at different concentrations with respect to what was tested. Despite this difficulty, the data obtained from the experimental activity can be exploited as a starting point to obtain results that fit better the situation simulated by the techno-economic model.

In order to manipulate the data obtained, the model proposed by Papurello et al. [74] was applied. This model is able to predict the dynamic adsorption curve and the breakthrough time, depending on the characteristics of the material used. It is based on three main equations. The first one is a partial differential equation derived from a mass balance at the level of reactor, which takes into account the evolution of the pollutant concentration inside the gas:

$$\frac{\partial C_i}{\partial t} + \frac{\partial C_i u}{\partial x} + \frac{1 - \varepsilon_b}{\varepsilon_b} \frac{\partial q_i}{\partial t} - D_{ax} \frac{\partial^2 C_i}{\partial x^2} = 0 \tag{8.3}$$

The second equation is the linear driving force approximation, which concerns the gas molecules transfer between bulk gas and sorbent material at the interface:

$$\frac{\partial q_i}{\partial t} = k_i \cdot \left(q_{eq,i} - q_i\right) \tag{8.4}$$

Where q_i is the real quantity of adsorbate that the adsorbent can capture and $q_{eq,i}$ is the maximum quantity of adsorbate that the adsorbent can capture.

The third equation is the Langmuir non-linear isotherm, which considers the accumulation of the pollutant inside the porous structure of the adsorbent material:

$$q_{eq,i} = q_m \cdot \frac{K_L C_i}{1 + K_L C_i} \tag{8.5}$$

From these equations it is possible to build an algorithm that, depending on the concentration of the contaminant, calculates its adsorption capacity. It was assumed that the biogas is in dry conditions.

Applying the procedure, it is possible to obtain results for methanethiol in different concentrations.

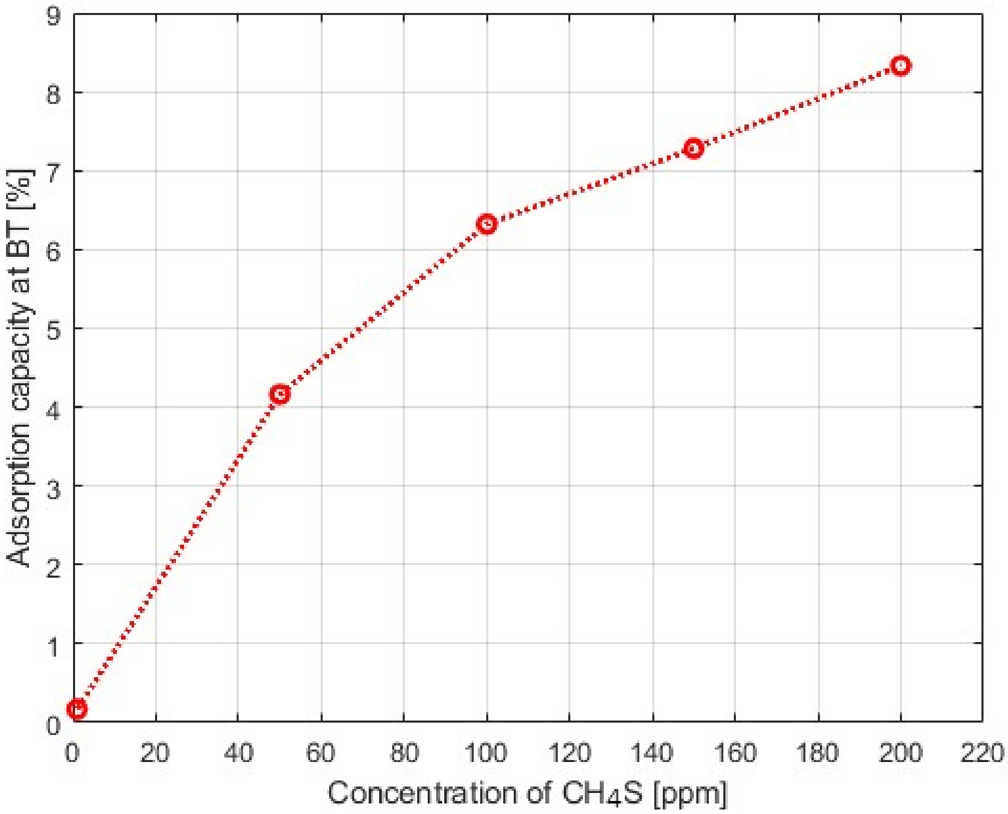

Figure 8.2: Adsorption capacity of CH_4S at different concentrations

The adsorption capacity value for 1 ppm of concentration in dry conditions is then equal to 0.17%. No data were available in wet conditions.

For what concerns DMS, the same procedure was applied.

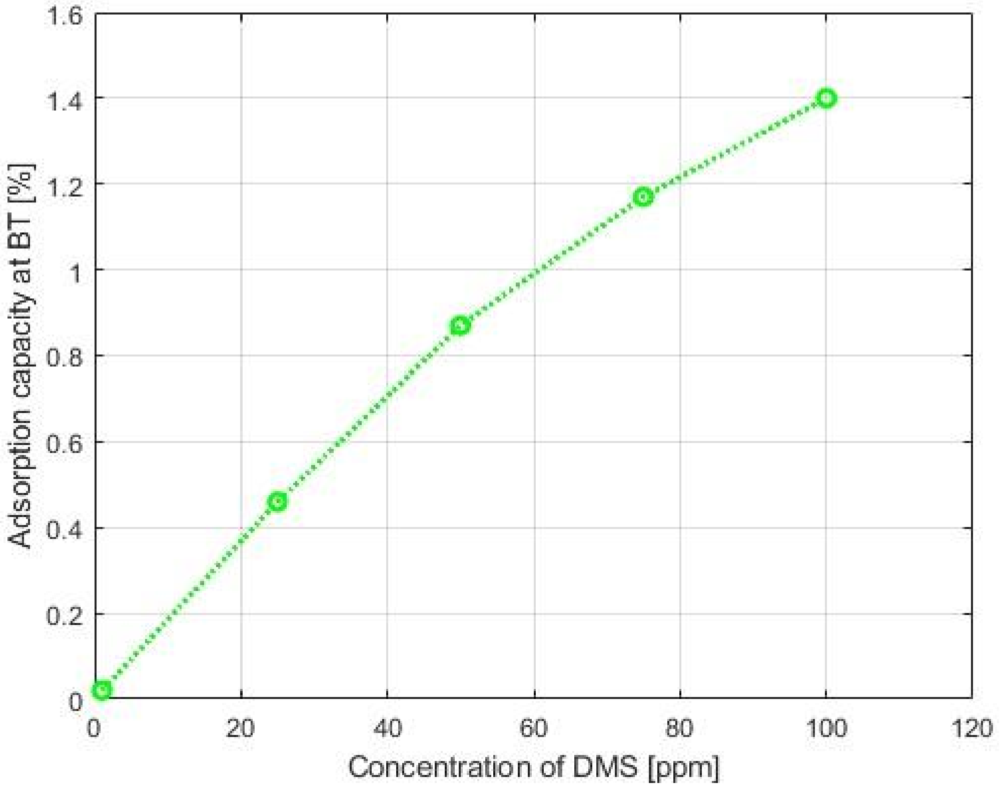

Figure 8.3: Adsorption capacity of DMS at different concentrations

In dry conditions, the adsorption capacity is consequently equal to 0.020%. To obtain a value in wet conditions, if was assumed that the curve is the same, but that it fits the experimental data registered in wet conditions. As a consequence, the adsorption capacity value in wet conditions is equal to 0.016%.

The values used for the adsorption capacity related to the chosen concentrations are then reported in the table.

Table 8-4: Adsorption capacity of Norit RGM-3 related to the pollutant concentration

	Concentration [ppm]	**With water**	**No water**
H_2S	500	18.53%	5.55%
DMS	1	0.016%	0.020%
COS	1	0.021%	0.33%
CH_4S	1	No data	0.17%

8.4 Considerations on the vessel

At this point it's possible to calculate the volume of the vessel(s), which depend on the kind of plant chosen. If there is only one vessel, it is assumed that all the components are fully removed in the same conditions and the volume dimensions is the sum of the volumes needed for the removal of each compound. In the case with two vessels, it was assumed that the H_2S is fully eliminated in the first vessel, because these are the conditions in which the process performs better. On the other hand, DMS, COS and CH_4S are assumed as fully eliminated in the second one, because they are adsorbed with better results in absence of water. Consequently, the first vessel has a volume that depends on the quantity of Norit RGM-3 needed to remove the hydrogen sulphide, while the second vessel has a volume equal to the one needed summing the quantities of material needed for each of the other sulphur compounds.

In all the cases considered, the inlet flow rate, calculated as previously described, is equal to 16.61 Nm^3/h. From the concentration it is possible to calculate the flow rate of each compound. All the other quantities will be calculated in accordance with the kind of plant investigated.

The breakthrough time is assumed to be equal to one year (8760 h), so that it is possible to calculate the amount of adsorbent material needed in a whole year of operation.

Table 8-5: Mass flow rate of the pollutant inside the biogas

Pollutant	Pollutant molar weight [g/mol]	Concentration [ppm]	Concentration [g/Nm^3]	Pollutant Mass flow [g/h]
H_2S	34.081	500	0.775	12.868
DMS	62.134	1	0.003	0.047
COS	60.075	1	0.003	0.045
CH_4S	48.107	1	0.002	0.036

8.5 Evaluation of the purchase equipment price

To calculate the purchase price of the equipment other proper assumptions were made.

First of all, the purchase equipment price obtained from the literature refers to the period between May and September 2001, when the average value of the Chemical Engineering Plant Cost Index (CEPCI) was 397 [69], while the CEPCI index in January 2022 was equal to 797.6 [75]. As a consequence, these values must be considered to obtain the actualized cost.

Then, it is fundamental to notice that for the kind of process considered in this work, the pressure is likely to be always equal to the ambient one. In this specific case, the value of the pressure factor will be then equal to 1, because the three coefficients C_1, C_2 and C_3 are all 0. This means that the pressure factor doesn't affect the costs.

For the purchase price of the vessels, it was assumed that they were vertical process ones. The correlation is true if the volume, which is the size parameter for a vessel, has a value between 0.3 and 520 m^3. This is a suitable range in the kind of process considered in this work. The coefficients values result then to be equal to:

- K_1 → 3.4974
- K_2 → 0.4485
- K_3 → 0.1074

Furthermore, it was assumed that they were made of stainless steel. As a consequence, their material factor was considered equal to 3.1.

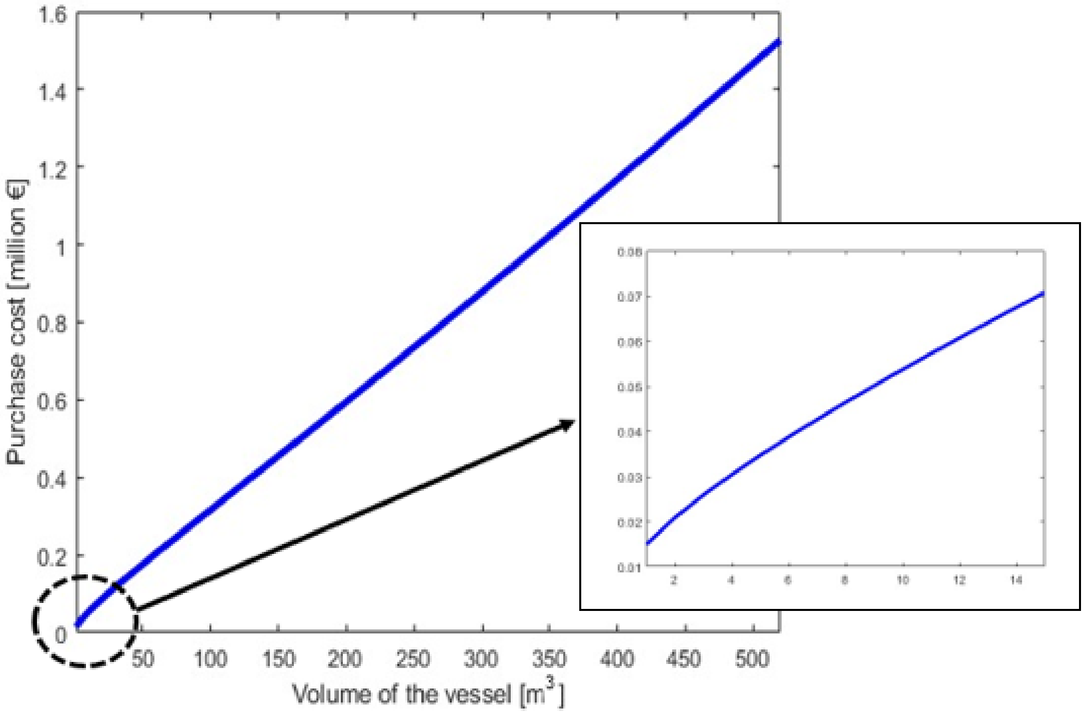

Figure 8.4: Purchase price of a vertical process vessel applying Turton cost functions

For the condenser, it was assumed that it is a multipipe heat exchanger. Its range of applicability is for area values between 10 and 100 m^2, which covers almost every possible outcome in the cases considered. The corresponding coefficient values are:

- K_1 → 2.7652
- K_2 → 0.7282
- K_3 → 0.0783

For what concerns the inlet and outlet temperatures of the condenser, it was assumed that the biogas, which is the hot stream, enters at 20 °C and exits at 5 °C, while the water, which is the cold stream, enters at 15 °C and exits at 3 °C. For the heat transfer coefficient, a value of 80 $W/m^3/K$ was chosen, considering that the heat exchange is between gas and water. For a multipipe heat exchanger, the material factor is equal to 1.

Considering that the mass flow of biogas stays constant, and all the other parameters are fixed, the area of the condenser is constant as well. In all the cases considered, the area of the condenser is then equal to 60.17 m^2 and its purchase price is 47 611 €.

8.6 Evaluation of costs and revenues

In the project, it was considered a price of 3340 €/kW for the purchase of the SOFC [76], which is a target price for the near future. It was assumed that the infrastructures, the electrical and control system account for 100 000 €. The cost of the clean-up system depends instead on the conditions and kind of plant considered.

The EPC value was assumed as 8% of the BEC, so that all home office engineering, field construction management and procurement services costs are considered. For what concerns the contingencies, their value depends on the status of the technology. Considering that small pilot plants exist for this plant, it was assumed a value equal to the 20% of the associated process capital. The owner's costs are then divided in pre-production costs, which accounts for about 2% of TPC, inventory capital, which is 0.5% of TPC, the financing cost, 2.7% of TPC, and the other owner's costs, of about 15% of TPC [70].

Table 8-6: Main contributions to the initial investment

TOC	**TPC**	**EPCM**	**BEC**	**SOFC cost**	167 000 €
				Infrastructures, electrical system and control system	100 000 €
				Clean-up system	Depend on vessel(s) volume
				EPC	8% of BEC
				Contingencies	20% of associated process capital
				Pre-production	2% of TPC
				Inventory Capital	0.5% of TPC
				Financing Cost	2.7% of TPC
				Other Owner's Costs	15% of TPC

For what concerns the OpEx, it was assumed that the substitution of the reformer catalyst occurs every year, and its cost was calculated according to the Turton cost functions. The substitution of the SOFC stack was assumed equal to the 30% of the Capex (the value of the capital expenditure was assumed as composed by the price of the SOFC and the price of the clean-up system), with a substitution every 8 years, while the general maintenance was set as equal to the 5% of CapEx [77]. Then, the labour cost was considered as equal to 30 €/h for a specialised worker that works 20 h a week during the whole year [78].

The substitution of the clean-up adsorbent, which occurs every year, depends on the quantity of sorbent needed. It was assumed a price of the sorbent material equal to 8 €/kg in a base case. On this value some sensitivity analysis could be performed because it's reasonable to assume that it will experience an increase in the future.

Table 8-7: Main OpEx contributions

Reformer catalyst substitution [€/y]	138
SOFC stack substitution [€/y]	30% of CapEx every 8 years
Labour cost [€/y]	31 200
General maintenance [€/y]	5% of CapEx every year
Substitution of clean-up adsorbent [€/y]	Depends on quantity of sorbent needed

For the electricity produced by biogas the minimum guaranteed price in 2022 was equal to 0.0963 €/kWh, according to ARERA [79], while the electric energy cost was on average 0.307 €/kWh in Italy during the period between the 1st of April and the 30th of June. This value refers to non-domestic users [80]. From the economic point of view, currently the better option is to self-consume the energy produced, due to the recent increase in purchase prices. But it is also true that if the incentives experience a significant increase, they can represent a valid option as well. Anyway, in all the scenarios considered it was assumed to self-consume 100% of the energy produced. The overall revenues are then equal to 127 743 €.

In Italy the WACC value was between 4.6 and 6% in 2019 [81]. In the further analysis, a value equal to 5% was assumed as reasonable. For what concerns the expected lifetime of the plant, it was assumed as 20 years. Considering that the capacity factor of the SOFC is set at 95%, this means the plant works for 8322 h every year.

To understand better the economic part of this system, different scenarios are consequently proposed. The goal is to underline the main differences and the investigation of the sustainability of the whole process.

Chapter IX

9. Scenarios

All the following scenarios are realized considering Norit RGM-3 as sorbent material, which is the only one, between the ones tested in the experimental campaign, that shows good performances in the removal of each of the four sulphur compounds of interest.

9.1 Monocomponent scenario

As a base case, it is possible to consider the simplest case, which is the monocomponent one. It is possible to assume that the biogas contains only one pollutant, which is exactly the condition tested in the laboratory activity. To give an overall view, it was considered singularly every sulphur compound, also to investigate which are the most critical ones in terms of costs. Of course, this case is not realistic but only theoretical: it is useful to investigate which are the most critical components to be removed.

In the case with only one vessel, all the compounds are removed in wet conditions. This is ideal for hydrogen sulphide, while the other compounds are better removed in dry conditions. The most problematic component is dimethyl sulphide, which needs a significant quantity of material in order to be removed even though its concentration is only 1 ppm, due to the extremely low adsorption capacity of Norit RGM-3 in wet conditions. The volume needed for carbonyl sulphide is also significantly high. For what concerns H_2S, the volume needed is the lowest, even though the concentration is hugely higher with respect to the other components. No tests were conducted on methanethiol removal in wet conditions, as a consequence it is not possible to examine the compound in this scenario.

The other option available for sulphur compound removal is to perform the process in dry conditions, which are the conditions advisable for COS and DMS. Even though this is not the best condition possible for H_2S removal, the adsorption capacity value is still acceptable, but the volume needed significantly increases due to the consistent inlet concentration. With respect to the wet case, the most important result is related to the mass of sorbent needed for carbonyl sulphide removal, which experiences a strong reduction. For what concerns DMS, the value is comparable with respect to the wet case, due to the slight difference between the adsorption capacity in the two different conditions. Methanethiol is removed in a satisfying way, but it is not possible to compare its performances with what registered previously.

Table 9-1: Most relevant data in a monocomponent scenario

	H_2S		**DMS**		**COS**		**CH_4S**	
	Wet	**Dry**	**Wet**	**Dry**	**Wet**	**Dry**	**Wet**	**Dry**
Mass of sorbent [kg]	608	2031	2569	2055	1892	119	No data	187
Volume of the vessel [m^3]	1.41	4.72	5.97	4.78	4.40	0.28	No data	0.44
Cost of the vessel [€]	22 965	13 934	50 635	44 265	42 151	11 930	No data	13 980

From the results obtained it is immediate to notice that the most convenient investment, as expected, is the one that allows to remove the pollutant in the best conditions tested: with water for hydrogen sulphide and without water for carbonyl sulphide. Dimethyl sulphide shows comparable value in the two cases: this is due to the little difference between the wet and dry conditions of adsorption. In its case, wet and dry conditions can eventually be both suitable for the plant.

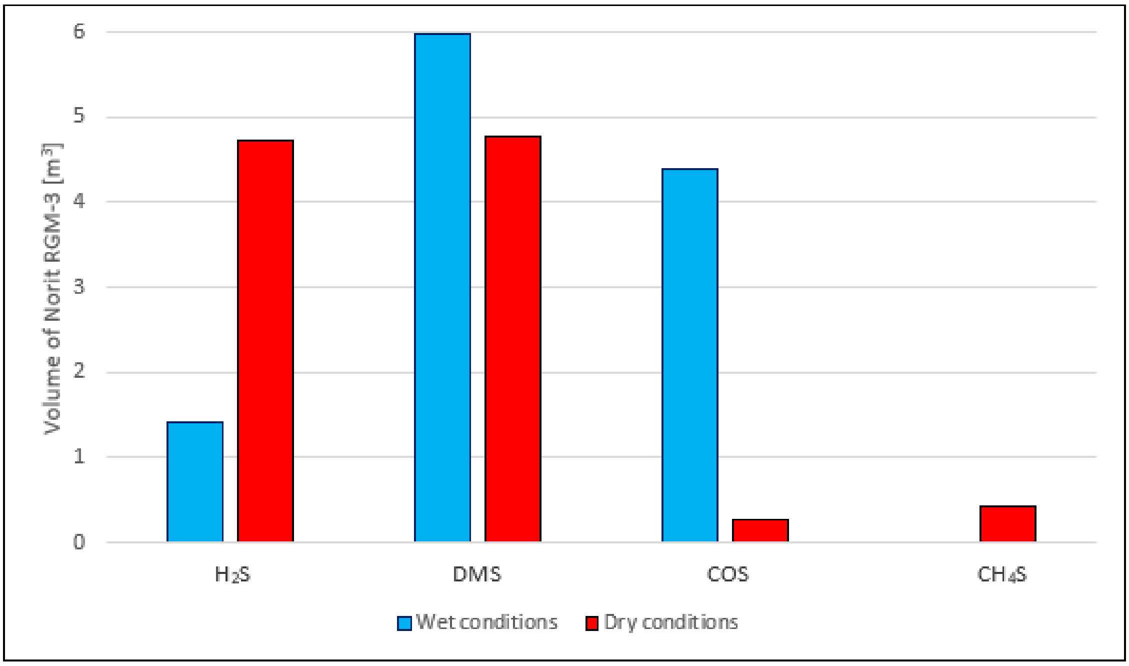

Figure 9.1: Comparison of the volume of Norit RGM-3 needed in different conditions for each component

9.2 Multicomponent scenario

In a multicomponent scenario hydrogen sulphide, dimethyl sulphide, carbonyl sulphide and methanethiol are all present inside the biogas at the same time. Due to the fact that adsorption capacity values for methanethiol are currently not available in wet conditions, it was assumed that the value is the same in both cases. This assumption can be overcome while the needed tests will be performed, but in this phase of the work allows to perform a comparison.

The amount of sorbent needed in the case with two vessels is by far the lower, and this has clearly an impact in the reduced expense for the clean-up sorbent substitution. The wet conditions plant is instead the one that requires the greatest amount of material. For what concerns the vessels, despite the greatest volume needed, the wet conditions plant appears to be the cheapest, because there is not the purchase price of the condenser, which represents about the 8% of the expense in the other two configurations. On the other hand, the option with two vessels and the condenser is the most expensive for what concerns the clean-up system, due to the fact that more equipment must be provided. The TOC is quite the same for the dry conditions and the wet and dry conditions plant (the former is slightly higher than the latter), while the wet conditions plant needs the lowest initial capital for the investment. The highest difference is related to the presence of the condenser, which significantly increases the overall expenses.

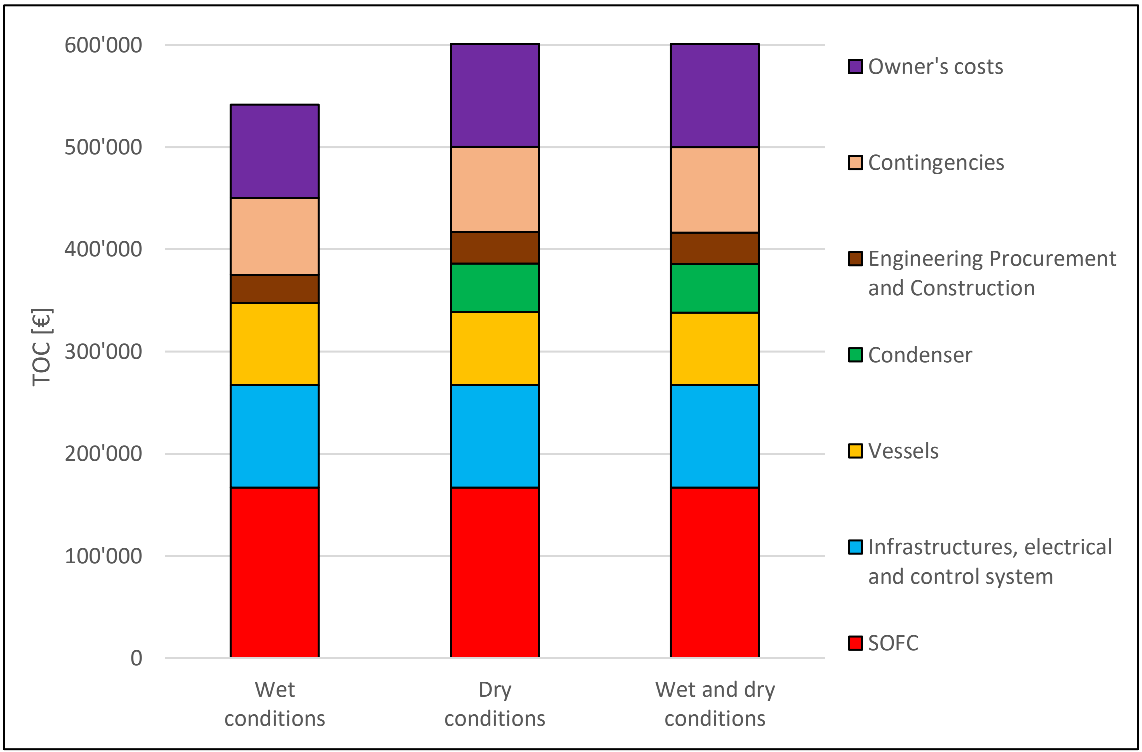

Figure 9.2: TOC shares in each of the three plants proposed

A fundamental aspect to underline is that, in general, the removal of sulphur compounds requires significant volumes in each of the models proposed. This means that, even though the economic feasibility is demonstrated, the technical feasibility can be hampered by the necessity of a dedicated area to install systems of this kind. The overall plant is in fact quite small, considering that the SOFC can produce only 50 kW at its nominal power. On the other hand, the amount of sorbent material needed as fuel is consistent. This topic could represent a major issue in the realization of a system of this kind, because limits in terms of space could make its realization unfeasible.

Table 9-2: Most relevant data in a multicomponent scenario

	Wet conditions	Dry conditions	Wet and dry conditions
Mass of sorbent [kg]	5 257	4 393	2 970
Volume of the vessel(s) [m^3]	12.23	10.22	1.42 (1st) 5.49 (2nd)
Area of the vessel(s) [m^2]	2.35	2.09	0.56 (1st) 1.38 (2nd)
Diameter of the vessel(s) [m]	1.73	1.63	0.84 (1st) 1.33 (2nd)
Length of the vessel(s) [m]	5.19	4.89	2.53 (1st) 3.98 (2nd)
Superficial gas velocity [m/s]	0.002	0.002	0.008 (1st) 0.003 (2nd)
Cost of the vessel(s)	80 602	71 417	23 002 (1st) 48 116 (2nd)
Cost of the condenser [€]	-	47 611	47 611
Cost of the clean-up system [€]	80 602	118 729	118 729
Cost for the substitution of the clean-up sorbent [€/kg]	42 054	35 141	23 759
TOC [€]	541 492	601 351	600 886
OpEx [€/y]	85 773	80 781	69 384
Revenues [€/y]	127 743	127 743	127 743

For what concerns the OpEx, the lowest value is the one connected to the plant which energetically works better thanks to its optimised design, which is the one with two vessels. In particular, it is about 15% more convenient than the dry conditions plant, which is instead the most costly from the point of view of operation. The greatest difference in operational expenditures is related to the substitution of the clean-up system, while all the other shares are comparable: the two vessels plant has almost half of the costs related to the purchase of the adsorbent material.

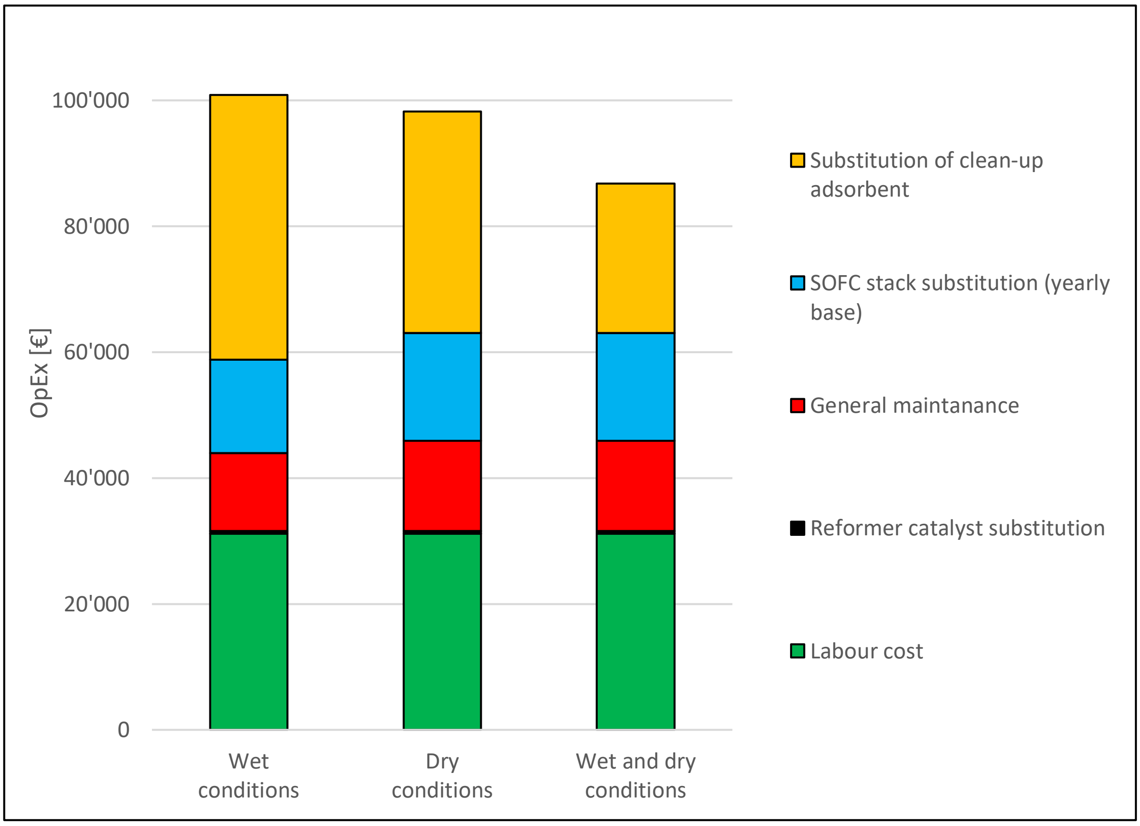

Figure 9.3: OpEx shares in each of the three plants proposed

To demonstrate that the results obtained can represent a plant economically feasible, also the economic indicators can be taken into account. For what concerns the Net Present Value, it is negative in the wet conditions plant, while slightly positive in the other two, which both are fully repaid only at the 19th year of operation on 20 years expected lifetime. The Benefit to Cost Ratio is greater than 1 in all the three plants, but only in the one that works both in wet and dry conditions the result is significantly higher. Finally, the most relevant indicator is the Levelized Cost of Electricity. Again, the plant with the best design, being an optimized option, is the cheapest option on the long run, even though the initial investment was higher. The values for the wet condition and the dry conditions plants are instead quite the same: this is possible because the former has lower TOC and higher OpEx, while the latter has higher TOC and lower OpEx. Unfortunately, these LCOE values are not particularly encouraging, because they are incredibly high when compared with other renewables. As an example, onshore wind, which is one of the most convenient, in 2019 costed only 0.052 €/kWh, while offshore wind, which is instead one of the most expensive, costed 0.110 $/kWh [82].

Table 9-3: Comparison of economic indicators in a multicomponents scenario

	Wet conditions	**Dry conditions**	**Wet and dry conditions**
Net Present Value [€]	-102 759	28 542	29 109
PayBack Time [y]	-	~19	~19
Benefit to Cost Ratio [-]	1.04	1.05	1.31
Levelized Cost of Electricity [€/kWh]	0.311	0.310	0.283

On LCOE value all the expenses related to the project have a share. In particular, in the long run what affects the most the result obtained is the substitution of the clean-up sorbent. That’s the main reason because the plant which works in wet and dry conditions, being an optimized option, represents the most indicated option.

At the end of the life cycle of a clean-up system connected to a SOFC, the costs related to the condenser and to the vessels purchase are almost irrelevant (and anyway comparable), as a consequence the initial higher investment for an energetically better plant if fully repaid. These considerations can be clearly underlined considering the initial investment and all the maintenance costs that occur during the 20 years lifetime of the plant.

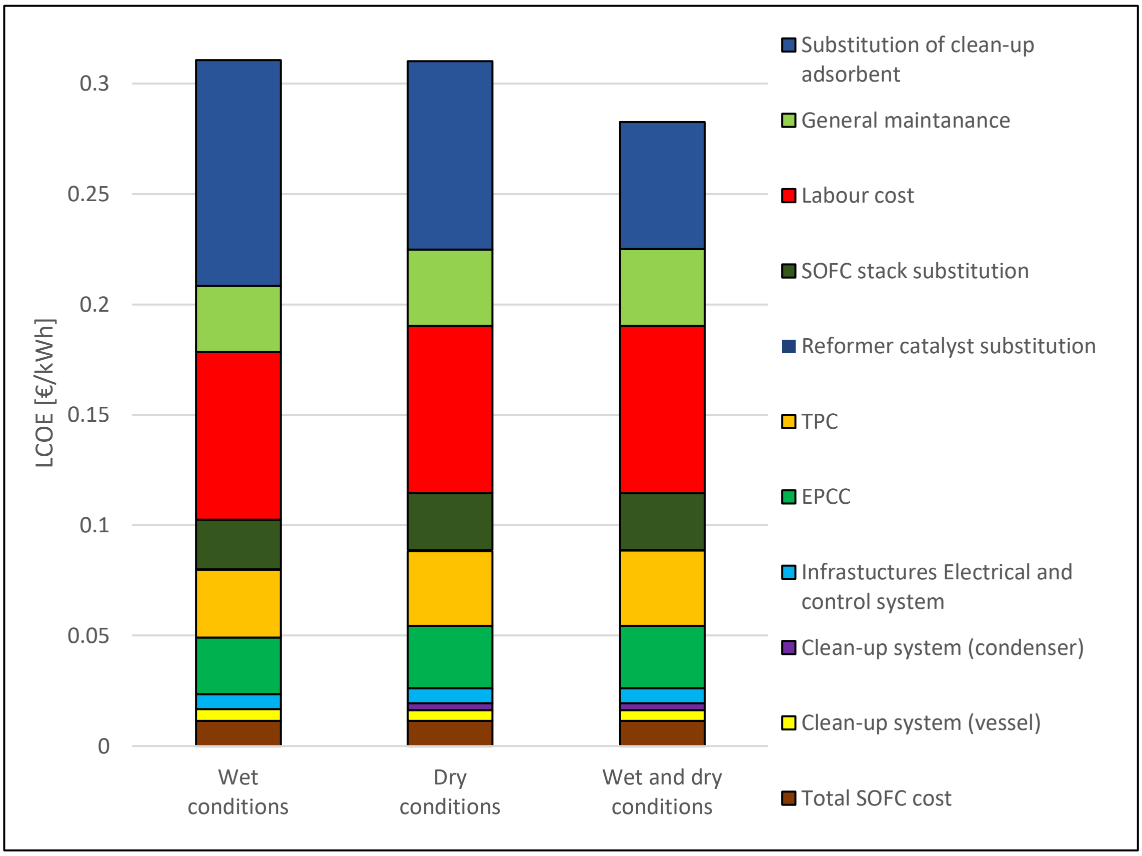

Figure 9.4: LCOE shares in each of the three plants proposed

9.3 Sensitivity analysis on cost of Norit RGM-3

The most relevant sensitivity analysis that can be performed is on the cost of the material, which is the parameter which mostly impacts on the costs and which is also the most likely to be subjected to a change in price. In particular, it is probable that in the future Norit RGM-3 will become more expensive with respect to its actual purchase price.

It was considered, as a comparison parameter, the LCOE value, which demonstrates that, if an increase of price occurs, the plant that works in both wet and dry conditions becomes even more convenient. For what concerns the other two plants, the value is approximately the same if the price of Norit RGM-3 is below about 10 €/kg, while the plant that works in dry conditions becomes more adequate with the increasing price.

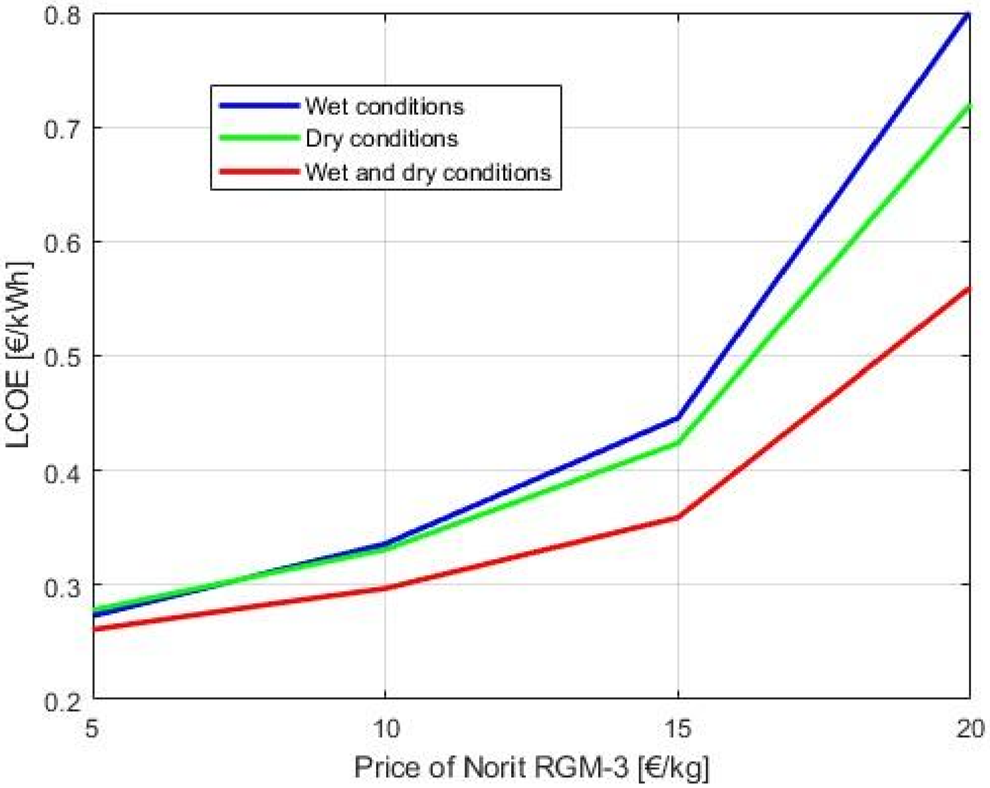

Figure 9.5: LCOE variation depending on the purchase price of Norit RGM-3

Chapter X

10. Conclusions

The experimental investigation reported in this work demonstrates that the composition of the biogas strongly affects the adsorption capacity of a sorbent material. The concentration of each pollutant has a direct effect on the adsorption capacity, furthermore the presence of water is decisive in the performances, for better and for worse. Another fundamental result is that the performances of the materials abruptly change depending on the kind of pollutant that is necessary to remove: it was demonstrated that the sulphur compounds are differently removed depending on how the process is conducted.

Consequently, it was quite difficult to find proper materials that could work effectively for each of the four molecules considered. Quite all the materials tested appears to not be suitable for a multicomponent removal, both due to the general poor performances and the specific non-compliant results obtained with specific compounds (for example, SulfaTrap R7H could have been an interesting option, but was excluded due to its transparency to COS).

The only sorbent material with which satisfying results have been obtained during the whole research activity was Norit RGM-3, an activated carbon by Cabot Corporation. This material behaves in a good way with each of the four molecules investigated, in particular with H_2S which is usually the most abundant of the four contained in a biogas. For these reasons, it was chosen in order to build a techno-economic model which simulates a multicomponent adsorption.

The goal of the model was to demonstrates that, once a suitable material is discovered, the biogas purification and its utilization in powering SOFC is a feasible option. To do so, it was built considering many parameters, coming from literature, experiments and algorithms.

For what concerns the economic point of view, the clean-up process proposed is still costly, in particular because of the relevant amount of material needed to guarantee a concentration close to zero in terms of contaminants.

Moreover, the volumes needed for the vessel(s) reactor(s) are relevant and would require dedicated spaces not always available: considering the limited electric production of the plant, probably the room that must be provided to efficiently run it could represent a major issue.

Anyway, between all the clean-up plants proposed the better option was by far the one which operates in the best conditions from the energetic point of view, allowing to remove the sulphur compounds in their best conditions. It was consequently demonstrated that the best way to perform the purification is to remove all the hydrogen sulphide in wet conditions, while eliminating carbonyl sulphide, dimethyl sulphide and methanethiol in dry conditions. In the long run, this option requires far less material, and its share of costs is therefore consistently reduced. In particular, the volumes are limited with respect to the other designs and the quantity of sorbent material needed is lower.

Acknowledgments

This work wouldn’t have been possible without the effort and dedication of many people.

I am grateful to Prof. Andrea Lanzini, Dr. Marta Gandiglio and Dr. Elena Rozzi, who guided me with kindness and patience during the realization of this work, giving me advice and help.

I’m also in debt with ENEA and PSI research teams, whose experimental activity provided some fundamental data for the building of the techno-economic model.

I would like to thank Simona Cappai, whose creativity was precious for the realization of some of the graphical representations contained in this work.

I wish to thank Matteo Ajassa, for his tireless encouragement and support.

Last but not least, I’m grateful to my family and friends, who were always by my side in every step of the road.

Bibliography

[1] IEA, “World Energy Balances (database),” 2021.

[2] I. Ionel and A. E. Cioablă, “Biogas production based on agricultural residues. From history to results and perspectives,” *WSEAS Trans. Environ. Dev.*, vol. 6, no. 8, pp. 591–603, 2010.

[3] T. Bond and M. R. Templeton, “History and future of domestic biogas plants in the developing world,” *Energy Sustain. Dev.*, vol. 15, no. 4, pp. 347–354, 2011, doi: 10.1016/j.esd.2011.09.003.

[4] Olivier Lavagne d’Ortigue, A. Whiteman, and S. Elsayed, “Renewable Energy Capacity Statistics 2015,International Renewable Energy Agency(IRENA),” p. 44, 2015, [Online]. Available: http://www.irena.org/DocumentDownloads/Publications/IRENA_RE_Capacity_Statistics_2015.pdf

[5] I. Renewable and E. Agency, *Renewable capacity statistics 2021*. 2021.

[6] “Rapporto Statistico 2020 Energia Da Fonti Rinnovabili in Italia,” 2020.

[7] P. G. Kougias and I. Angelidaki, “Biogas and its opportunities — A review Keywords,” *Front. Environ. Sci.*, vol. 12, no. June 2018, pp. 1–22, 2018.

[8] X. L. Kiros Hagos, Jianpeng Zong, Dongxue Li, Chang Liu, “Anaerobic co-digestion process for biogas production: Progress, challenges and perspectives, Renewable and Sustainable Energy Reviews,” *Renew. Sustain. Energy Rev.*, vol. 76, pp. 1485–1496, 2017.

[9] S. Rasi, J. Läntelä, and J. Rintala, “Trace compounds affecting biogas energy utilisation - A review,” *Energy Convers. Manag.*, vol. 52, no. 12, pp. 3369–3375, 2011, doi: 10.1016/j.enconman.2011.07.005.

[10] M. R. Atelge *et al.*, “A critical overview of the state-of-the-art methods for biogas purification and utilization processes,” *Sustain.*, vol. 13, no. 20, 2021, doi: 10.3390/su132011515.

[11] S. Sahota *et al.*, “Review of trends in biogas upgradation technologies and future perspectives,” *Bioresour. Technol. Reports*, vol. 1, pp. 79–88, 2018, doi: 10.1016/j.biteb.2018.01.002.

[12] N. Scarlat, J. F. Dallemand, and F. Fahl, “Biogas: Developments and perspectives in Europe,” *Renew. Energy*, vol. 129, pp. 457–472, 2018, doi: 10.1016/j.renene.2018.03.006.

[13] L. G. & G. P. Dolf Gielen, Ricardo Gorini, Nicholas Wagner, Rodrigo Leme, “Global Energy transformation: a roadmap to 2050,” *IRENA*, 2018.

[14] S. A. Saadabadi, A. Thallam Thattai, L. Fan, R. E. F. Lindeboom, H. Spanjers, and P. V. Aravind, “Solid Oxide Fuel Cells fuelled with biogas: Potential and constraints,” *Renew. Energy*, vol. 134, pp. 194–214, 2019, doi:

10.1016/j.renene.2018.11.028.

[15] J. Stern, *Measurement, Reporting, and Verification of Methane Emissions from Natural Gas and LNG Trade: creating transparent and credible frameworks*, vol. ET06, no. January. 2022.

[16] Osama Mohammed Elmardi Suleiman Khayal, “Advantages and Limitation of biogas technologies,” pp. 1–8, 2019.

[17] M. S. and M. M. L. Askari Mohammad Bagher, Golestanian Fatemeh, “Advantages and Disadvantages of Biogas Energy,” *Bull. Adv. Sci. Res.*, pp. 132–5, 2015, [Online]. Available: http://www.conserve-energy-future.com/Advantages_Disadvantages_BiomassEnergy.php

[18] E. Mulu, M. M. M’Arimi, and R. C. Ramkat, “A review of recent developments in application of low cost natural materials in purification and upgrade of biogas,” *Renew. Sustain. Energy Rev.*, vol. 145, no. April, p. 111081, 2021, doi: 10.1016/j.rser.2021.111081.

[19] O. W. Awe, Y. Zhao, A. Nzihou, D. P. Minh, and N. Lyczko, “A Review of Biogas Utilisation, Purification and Upgrading Technologies,” *Waste and Biomass Valorization*, vol. 8, no. 2, pp. 267–283, 2017, doi: 10.1007/s12649-016-9826-4.

[20] D. Andriani, A. Wresta, T. D. Atmaja, and A. Saepudin, “A review on optimization production and upgrading biogas through CO 2 removal using various techniques,” *Appl. Biochem. Biotechnol.*, vol. 172, no. 4, pp. 1909–1928, 2014, doi: 10.1007/s12010-013-0652-x.

[21] M. Arnold, *VTT RESEARCH NOTES 2496 Reduction and monitoring of biogas trace compounds*, vol. 25, no. 2496. 2006. [Online]. Available: http://www.vtt.fi/publications/index.jsp

[22] and R. K. Dionissios D. Papadias, Shabbir Ahmed, “Fuel quality issues with biogas energy - An economic analysis for a stationary fuel cell system,” *Energy 44.1*, 2012.

[23] N. N. Zulkefli, M. S. Masdar, J. Jahim, and E. H. Majlan, “Overview of H2S Removal Technologies from Biogas Production,” *Int. J. Appl. Eng. Res.*, vol. 11, no. 20, pp. 12–14, 2016.

[24] A. S. Calbry-Muzyka and T. J. Schildhauer, “Direct Methanation of Biogas—Technical Challenges and Recent Progress,” *Front. Energy Res.*, vol. 8, no. December, 2020, doi: 10.3389/fenrg.2020.570887.

[25] G. Soreanu *et al.*, “Approaches concerning siloxane removal from biogas - A review,” *Can. Biosyst. Eng. / Le Genie des Biosyst. au Canada*, vol. 53, 2011.

[26] I. Bragança, F. Sánchez-Soberón, G. F. Pantuzza, A. Alves, and N. Ratola, “Impurities in biogas: Analytical strategies, occurrence, effects and removal technologies,” *Biomass and Bioenergy*, vol. 143, no. June, 2020, doi: 10.1016/j.biombioe.2020.105878.

[27] C. T. Chiou, “Fundamentals of the Adsorption Theory,” *Partit. Adsorpt. Org. Contam. Environ. Syst.*, no. May 2003, pp. 39–52, 2003, doi:

10.1002/0471264326.ch4.

[28] K. Vivek, “Adsorption equilibra and regeneration.” 2012.

[29] O. M. A. S.D. Faust, *Adsorption Processes for Water Treatment*. 2013.

[30] M. M. Dubinin, “Modern state of the theory of gas and vapour adsorption by microporous adsorbents,” *Pure Appl. Chem.*, vol. 10, no. 4, pp. 309–322, 1965, [Online]. Available: https://doi.org/10.1351/pac196510040309

[31] S. A. Olawale, “Biosorption of Heavy Metals from Aqueous Solutions:Insight and Review,” *Arch. Ind. Eng.*, vol. 3, no. October, pp. 1–31, 2020, doi: 10.31829/2637-9252/aie2020-3(1)-113.

[32] M. D. Donohue and G. L. Aranovich, “Classification of Gibbs adsorption isotherms,” *Adv. Colloid Interface Sci.*, vol. 76–77, no. October, pp. 137–152, 1998, doi: 10.1016/S0001-8686(98)00044-X.

[33] D. Guo, Wenshan, Ayawei, Nimibofa, Ebelegi, Augustus Newton, Wankasi, “Modelling and Interpretation of Adsorption Isotherms,” *J. Chem.*, vol. 2017, 2017, doi: 10.1155/2017/3039817.

[34] D. Papurello, M. Gandiglio, J. Kafashan, and A. Lanzini, “Biogas purification: A comparison of adsorption performance in D4 siloxane removal between commercial activated carbons and waste wood- derived char using isotherm equations,” *Processes*, vol. 7, no. 10, 2019, doi: 10.3390/pr7100774.

[35] A. U. Dogan, M. Dogan, M. Omal, Y. Sarikaya, A. Aburub, and D. E. Wurster, “Baseline studies of The Clay Minerals Society source clays: Specific surface area by Brunauer Emmett Teller (BET) method,” *Clays Clay Miner.*, vol. 54, no. 1, pp. 62–66, 2006, doi: 10.1346/CCMN.2006.0540108.

[36] M. Hemant, “Factors affecting adsorption,” *https://thefactfactor.com/facts/pure_science/chemistry/physical-chemistry/factors-affecting-adsorption/11184/*, 2020.

[37] Z. Heidarinejad, M. H. Dehghani, M. Heidari, G. Javedan, I. Ali, and M. Sillanpää, “Methods for preparation and activation of activated carbon: a review,” *Environ. Chem. Lett.*, vol. 18, no. 2, pp. 393–415, 2020, doi: 10.1007/s10311-019-00955-0.

[38] L. Micoli, G. Bagnasco, and M. Turco, “H2S removal from biogas for fuelling MCFCs: New adsorbing materials,” *Int. J. Hydrogen Energy*, vol. 39, no. 4, pp. 1783–1787, 2014, doi: 10.1016/j.ijhydene.2013.10.126.

[39] S. Cimino *et al.*, “Role of H2O and O2 during the reactive adsorption of H2S on CuO-ZnO/activated carbon at low temperature,” *Microporous Mesoporous Mater.*, vol. 295, no. October 2019, p. 109949, 2020, doi: 10.1016/j.micromeso.2019.109949.

[40] H. Sawalha, M. Maghalseh, J. Qutaina, K. Junaidi, and E. R. Rene, “Removal of hydrogen sulfide from biogas using activated carbon synthesized from different locally available biomass wastes - a case study from Palestine,” *Bioengineered*, vol. 11, no. 1, pp. 607–618, 2020, doi: 10.1080/21655979.2020.1768736.

[41] T. Tuerhong and Z. Kuerban, “Preparation and characterization of cattle manure-based activated carbon for hydrogen sulfide removal at room temperature,” *J. Environ. Chem. Eng.*, vol. 10, no. 2, p. 107177, 2022, doi: 10.1016/j.jece.2022.107177.

[42] E. M. Cepollaro, D. Caputo, N. Gargiulo, F. A. Deorsola, S. Cimino, and L. Lisi, “H2S catalytic removal at low temperature over Cu- and Mg- activated carbon honeycombs,” *Catal. Today*, vol. 390–391, no. November 2021, pp. 221–229, 2022, doi: 10.1016/j.cattod.2021.11.027.

[43] A. Choudhury and S. Lansing, “Adsorption of hydrogen sulfide in biogas using a novel iron-impregnated biochar scrubbing system,” *J. Environ. Chem. Eng.*, vol. 9, no. 1, p. 104837, 2021, doi: 10.1016/j.jece.2020.104837.

[44] G. Monteleone *et al.*, “Abbattimento dell ’ H 2 S e upgrading di un biogas proveniente da digestione anaerobica degli scarti di una mensa aziendale,” p. 39, 2014.

[45] H. Jacobs, P. A., Flanigen, E. M., Jansen, J. C., & van Bekkum, *Introduction to zeolite science and practice*. 2001.

[46] A. Alonso-Vicario *et al.*, “Purification and upgrading of biogas by pressure swing adsorption on synthetic and natural zeolites,” *Microporous Mesoporous Mater.*, vol. 134, no. 1–3, pp. 100–107, 2010, doi: 10.1016/j.micromeso.2010.05.014.

[47] S. Bahraminia, M. Anbia, and E. Koohsaryan, “Hydrogen sulfide removal from biogas using ion-exchanged nanostructured NaA zeolite for fueling solid oxide fuel cells,” *Int. J. Hydrogen Energy*, vol. 45, no. 55, pp. 31027–31040, 2020, doi: 10.1016/j.ijhydene.2020.08.091.

[48] R. M. Cornell and U. Schwertman, *Corrosion Reviews*. 1997.

[49] D. M. Cristiano *et al.*, “H2S adsorption on nanostructured iron oxide at room temperature for biogas purification: Application of renewable energy,” *Renew. Energy*, vol. 154, pp. 151–160, 2020, doi: 10.1016/j.renene.2020.02.054.

[50] T. Raabe, M. Mehne, H. Rasser, H. Krause, and S. Kureti, “Study on iron-based adsorbents for alternating removal of H2S and O2 from natural gas and biogas,” *Chem. Eng. J.*, vol. 371, no. April, pp. 738–749, 2019, doi: 10.1016/j.cej.2019.04.103.

[51] C. Costa, M. Cornacchia, M. Pagliero, B. Fabiano, M. Vocciante, and A. Pietro Reverberi, “Hydrogen sulfide adsorption by iron oxides and their polymer composites: A case-study application to biogas purification,” *Materials (Basel).*, vol. 13, no. 21, pp. 1–15, 2020, doi: 10.3390/ma13214725.

[52] F. Sun *et al.*, “Solid Oxide Fuel Cells Operating on Alternative and Renewable Fuels Final Technical Report,” pp. 814–865, 2014.

[53] M. Kawase and M. Otaka, “Removal of H2S using molten carbonate at high temperature,” *Waste Manag.*, vol. 33, no. 12, pp. 2706–2712, 2013, doi: 10.1016/j.wasman.2013.08.002.

[54] A. H. Abdullah, R. Mat, A. S. A. Aziz, and F. Roslan, “Use of kaolin as adsorbent

for removal of hydrogen sulphide from biogas," *Chem. Eng. Trans.*, vol. 56, no. 2014, pp. 763–768, 2017, doi: 10.3303/CET1756128.

[55] Y. Ahn, K. Pandi, M. Lee, and J. Choi, "Removing hydrogen sulfide from a feed stream using suitable adsorbent materials," *J. Clean. Prod.*, vol. 272, p. 122849, 2020, doi: 10.1016/j.jclepro.2020.122849.

[56] L. Barelli, G. Bidini, U. Desideri, G. Discepoli, and E. Sisani, "Dimethyl sulfide adsorption from natural gas for solid oxide fuel cell applications," *Fuel Process. Technol.*, vol. 140, pp. 21–31, 2015, doi: 10.1016/j.fuproc.2015.08.012.

[57] J. Kim, J. Y. Do, N. K. Park, J. P. Hong, and M. Kang, "Adsorption/desorption behavior of carbonyl sulfide gas on Scheelite type MWO4 adsorbent," *Sep. Purif. Technol.*, vol. 207, no. April, pp. 58–67, 2018, doi: 10.1016/j.seppur.2018.06.040.

[58] A. Ryzhikov *et al.*, "Methyl mercaptan and carbonyl sulfide traces removal through adsorption and catalysis on zeolites and layered double hydroxides," *Appl. Catal. A Gen.*, vol. 397, no. 1–2, pp. 218–224, 2011, doi: 10.1016/j.apcata.2011.03.002.

[59] C. u. Bak, C. J. Lim, Y. D. Kim, and W. S. Kim, "Multi-stage adsorptive purification process for improving desulfurization performance of biogas," *Sep. Purif. Technol.*, vol. 227, no. June, p. 115702, 2019, doi: 10.1016/j.seppur.2019.115702.

[60] "https://waste2watts-project.net/description/."

[61] Tecnodelta Srl, "MANUALE DI ISTRUZIONI PER L ' USO E LA MANUTENZIONE Gas station prototipale".

[62] Waste2Watts, "Sorbent testing intermediate report, Deliverable D2.3," 2020.

[63] Thermo Fisher Scientific, "Safety Data Sheet Norit RGM-3," *Mater. Saf. Data Sheet*, vol. 4(2), no. 1, pp. 8–10, 2012, [Online]. Available: https://us.vwr.com/assetsvc/asset/en_US/id/16490607/contents

[64] "https://sulfatrap.com/sulfatrap-products/sorbents/sulfatrap-r4/."

[65] "https://sulfatrap.com/sulfatrap-products/sorbents/sulfatrap-r8/."

[66] "https://www.biocustom.it/prodotti-tecnici-materie-prime/."

[67] ProducerDataSheet, "Envirocarb ® stix ® 4mm".

[68] "https://www.desotec.com/it/carbonology/carbonology-academy/impregnated-activated-carbon."

[69] T. O. F. Content, "Cost Equations and Curves for the CAPCOST Program," no. year, pp. 3–33, 2001.

[70] USDOE/NETL, "Power Plant Cost Estimation Methodology Quality Guidelines for Energy System Studies," no. March 2010, 2011, [Online]. Available: www.netl.doe.gov

[71] IEA, *Projected Costs of Generating Electricity*. 2005. doi:

10.1787/9789264008274-en.

[72] A. Calbry-Muzyka, H. Madi, F. Rüsch-Pfund, M. Gandiglio, and S. Biollaz, "Biogas composition from agricultural sources and organic fraction of municipal solid waste," *Renew. Energy*, vol. 181, pp. 1000–1007, 2022, doi: 10.1016/j.renene.2021.09.100.

[73] M. Gandiglio, A. Lanzini, M. Santarelli, and P. Leone, "Design and optimization of a proton exchange membrane fuel cell CHP system for residential use," *Energy Build.*, vol. 69, pp. 381–393, 2014, doi: 10.1016/j.enbuild.2013.11.022.

[74] D. Papurello, M. Gandiglio, and A. Lanzini, "Experimental analysis and model validation on the performance of impregnated activated carbons for the removal of hydrogen sulfide (H2S) from sewage biogas," *Processes*, vol. 7, no. 9, 2019, doi: 10.3390/pr7090548.

[75] "https://www.chemengonline.com/site/plant-cost-index/".

[76] P. Marocco, M. Gandiglio, and M. Santarelli, "When SOFC-based cogeneration systems become convenient ? A cost-optimal analysis," *Energy Reports*, vol. 8, pp. 8709–8721, 2022, doi: 10.1016/j.egyr.2022.06.015.

[77] M. Ishaq and H. Ishaq, "Performance assessment of biogas-fed solid oxide fuel cell system for municipal solid waste treatment," *J. Clean. Prod.*, vol. 354, no. March, p. 131702, 2022, doi: 10.1016/j.jclepro.2022.131702.

[78] A. S. Mehr *et al.*, "Solar-assisted integrated biogas solid oxide fuel cell (SOFC) installation in wastewater treatment plant: Energy and economic analysis," *Appl. Energy*, vol. 191, pp. 620–638, 2017, doi: 10.1016/j.apenergy.2017.01.070.

[79] "https://www.arera.it/it/elettricita/prezziminimi.htm."

[80] "https://www.arera.it/it/prezzi.htm."

[81] AURES, "Renewable energy financing conditions in Europe: survey and impact analysis," 2021.

[82] I. R. E. Agency, *Renewable Power Generation Costs in 2019*. 2020. [Online]. Available: https://www.irena.org/-/media/Files/IRENA/Agency/Publication/2018/Jan/IRENA_2017_Power_Costs_2018.pdf